EXERGETIC ANALYSIS AND OPTIMIZATION OF A HYBRID SOLAR-BIOMASS GREENHOUSE DRYER FOR DRYING BANANA SLICES

FLORENCE GATWIRI KIBURI

DOCTOR OF PHILOSOPHY

(Agricultural Processing Engineering)

JOMO KENYATTA UNIVERSITY OF AGRICULTURE AND TECHNOLOGY

2022

Exergetic analysis and optimization of a hybrid solar-biomass greenhouse dryer for drying banana slices

Florence Gatwiri Kiburi

A Thesis Submitted in Partial Fulfilment of

the Requirements for the Degree of Doctor of Philosophy in

Agricultural Processing Engineering of the Jomo Kenyatta

University of Agriculture and Technology

2022

DECLARATION

This thesis is my original work and has not been presented for a degree in any other university.

Signature: ---------- Date: ----------

Florence Gatwiri Kiburi

We confirm that this thesis has been submitted with our approval as university supervisors.

Signature: ---------- Date: ----------

Prof. Christopher L. Kanali, PhD

JKUAT, Kenya

Signature: ---------- Date: ----------

Dr. Eng. Gareth M. Kituu, PhD

JKUAT, Kenya

Signature: ---------- Date: ----------

Dr. Patrick O. Ajwang, PhD

JKUAT, Kenya

Signature: ---------- Date: ----------

Dr. Erick K. Ronoh, PhD

JKUAT, Kenya

DEDICATION

To my family,

It is very fitting that I foremost dedicate this work to my late father Mr. Franklin Kiburi. You were a great parent and most paramount you believed in hard work. Secondly, I dedicate this work to my dear mother Mrs. Hellen Kiburi and my beloved siblings (Nicholas Ngugi, Purity Muthoni, Neema Mwende and Fridah Karendi) for making my world a better place. Further, I dedicate this work to my children Boaz Changkechir, Ephraim Kibet, Janelle Jerop and my dear husband Mr. Titus Cherutich. You all give me the reason to tighten my shoelaces and look forward to every single day in this life. May God bless you all for the roles you played in this work.

ACKNOWLEDGEMENT

I thank God Almighty for enabling me to carry out this study in good health. My appreciation to the National Research Fund (NRF) of Kenya and Jomo Kenyatta University of Agriculture and Technology (JKUAT) for funding this study. I am sincerely grateful to Prof. C. L. Kanali, Dr. Eng. G. M. Kituu, Dr. P. O. Ajwang and Dr. E. K. Ronoh for the professional guidance and mentorship they have provided me during the development of this thesis. I will forever be indebted to you all, as you have continuously tailored me to be a better-placed individual in this robust society. Special thanks to my office mates Ms. Joan, Ms. Cecilia and Ms. Hannah for all the support they offered me while developing this thesis.

Finally, I am truly indebted to everyone who provided me real love, encouragement and inspiration that enabled me to complete this work successfully. God bless you all.

TABLE OF CONTENTS

LIST OF TABLES

LIST OF FIGURES

LIST OF APPENDICES

NOTATIONS

A	Surface area of the greenhouse dryer effective in harnessing the solar energy (m^2)
a^*	Degree of redness to greenness
A_d	Duct surface area (m^2)
A_i	Area (m^2) representing the i^{th} section of the greenhouse dryer
b^*	Degree of yellowness to blueness
C_b	Intercept of a linear graph of drying air temperature against ambient temperature for biomass mode
C_d	Specific heat of bananas (kJ/kg^{o}C)
C_p	Specific heat of water (kJ/kg^{o}C)
C_{pa}	Specific heat capacity of air (J/kgK)
C_{s-b}	Intercept of a linear graph of solar radiation against drying air temperature for solar-biomass mode
d_{ic}	Internal diameter of the inner duct (m)
d_{oc}	External diameter of the inner duct (m)
$E_{u(da)}$	Useful heat gained by the drying air from the solar energy (W)
EUR	Energy utilization ratio
$Ex_{b(input)}$	Hourly exergy input from the biomass (W)
$Ex_{b(output)}$	Hourly exergy output from the biomass (W)
$Ex_{inside(da)}$	Hourly exergy potential of the drying air inside the dryer (W)
$Ex_{out(ea)}$	Hourly exergy of the exhausted air (W)
$Ex_{rad(input)}$	Hourly exergy input (W) due to solar radiation in the greenhouse dryer

$Ex_{rad(output)}$	Hourly exergy output (W) due to solar radiation in the greenhouse dryer
$Ex_{s\text{-}b(input)}$	Hourly exergy input for the solar-biomass (W)
$Ex_{s\text{-}b(output)}$	Hourly exergy output for the solar-biomass (W)
ε	Emissivity coefficient of the duct material
f	Friction factor
h	Gable height of the greenhouse (m)
H	Height of the greenhouse (m)
H_1	Initial humidity ratio of the drying air (kg)
H_2	Final humidity ratio of the drying air (kg)
h_c	Heat transfer coefficient of cold fluid (air) (W/m^2K)
h_{fg}	Latent heat of vaporization of water at 100^oC and at standard atmospheric pressure (kJ/kg)
h_h	Heat transfer coefficient of hot fluid (flue gases) (W/m^2K)
H_v	Heating value of biomass (kJ/kg)
I_i	Radiation flux incident (W/m^2) representing the i^{th} section of the greenhouse dryer
I_s	Hourly solar radiation (W/m^2)
k	Slope of a linear graph of solar radiation against drying air temperature for solar mode
k_p	Thermal conductivity of the duct material (W/mK)
$k_{s\text{-}b}$	Slope of a linear graph of solar radiation against drying air temperature for solar-biomass mode
l	Length of duct (m)

L	Length of the greenhouse (m)
L^*	Degree of lightness to darkness
m	Mass of biomass (kg)
M_1	Initial moisture content (% wet basis)
M_2	Final moisture content (% wet basis)
m_{air}	Mass of air required to achieve the desired drying (kg)
m_{exp}	Experimental values
M_i	Initial moisture content of bananas (% dry basis)
m_{pred}	Predicted values
N	Initial population
Nu	Nusselt number
PE	Percentage error
Pr	Prandtl number
Q_b	Biomass heat (kJ)
Q_{in}	Hourly amount of energy input (W)
Q_t	Total energy required (kJ/kg)
Q_{tavail}	Total heat energy available (kJ)
R^2	Coefficient of determination
R_b	Ratio of beam radiation on the tilted surface to that on the horizontal plane
Re	Reynold's number
Rh_a	Ambient air relative humidity (%)
Rh_{da}	Drying air relative humidity (%)

S_c	Biomass burning rate (kg/hr)
T_a	Ambient air temperature (K)
t_{actual}	Actual performance drying time
t_b	Drying time for biomass mode (hrs)
t_{crit}	T critical
T_{da}	Drying air temperature (K)
T_{dst}	Duct surface temperature (K)
T_{ea}	Exit air temperature (K)
t_{pred}	Predicted performance drying time
t_s	Drying time for solar mode (hrs)
T_s	Sky temperature (K)
t_{s-b}	Drying time for solar-biomass mode (hrs)
t_{stat}	T statistic
V_{air}	Volumetric flow of air (m^3/hr)
V_{gh}	Volume of the greenhouse (m^3)
VR	Ventilation rate (hrs)
W	Width of the greenhouse (m)
W_b	Moisture content wet basis (%)
W_d	Mass of bananas (kg)
W_p	Quantity of bananas to be dried (kg)
Wp	Watt peak
W_w	Amount of moisture removed (kg)
$\dot{Q}$	Heat transfer rate (kJ/s)

$\dot{m}_a$	Mass flow rate of air (kg/s)
$\dot{m}_f$	Mass flow rate of fuel (kg/s)
ΔT	Difference between temperature inside the dryer and ambient air temperature (^oC)
ΔT_{LTD}	Log mean temperature difference
Δp	Total pressure differences across the fan (Pa)
ε_f	Total system static fan efficiency
η_e	Energy efficiency
$\eta_{e(s)}$	Energy efficiency of the dryer in solar mode
η_{ex}	Exergy efficiency
η_{stove}	Biomass stove efficiency
ρ_{air}	Density of air (kg/m^3)
ρ_g	Ground reflectance factor
σ	Stefan-Boltzmann constant (W/m^2K^4)
τ_i	Solar transmissivity (W) representing the i^{th} section of the greenhouse dryer
τ	Transmittance of the glazing material

LIST OF ACRONYMS

ABED	Agricultural and Biosystems Engineering Department
AFA	Agriculture and Food Authority
ANNs	Artificial Neural Networks
ANOVA	Analysis of Variance
AOAC	Association of Official and Analytical Chemists
BP	British Pharmacopoeia
CFD	Computational Fluid Dynamics
CIE	Commission Internationale de l'Eclairage
DHT	Digital Humidity and Temperature
FAO	Food and Agriculture Organization
GA	Genetic Algorithm
GDP	Gross Domestic Product
GI	Galvanized Iron
JKUAT	Jomo Kenyatta University of Agriculture and Technology
LBM	Lattice Boltzmann Method
LDR	Light Dependent Resistor
LSD	Least Significant Difference
NRF	National Research Fund
NSGA	Non-Sorted Genetic Algorithm
PSO	Particle Swarm Optimization
PV	Photovoltaic
PWM	Pulse Width Modulation

RSM	Response Surface Methodology
SDGs	Sustainable Development Goals
Std	Standard Deviation
USD	United States Dollar
USP	United States Pharmacopoeia
UV	Ultraviolet

ABSTRACT

Bananas have high moisture content, making them highly susceptible to microbial damage and as such reducing their shelf life. Thus, the need to lowering the product moisture content is paramount. This study aimed at optimizing a hybrid solar-biomass greenhouse dryer for drying banana slices based on exergy analysis. The main components of the dryer were the greenhouse enclosure, biomass stove, double duct heat exchanger, drying trays and ventilation fans. Models were developed to simulate energy supply, drying time and dryer design parameters for the system based on dryer capacity of 240 kg banana slices. The study treatments comprised four banana varieties, peeled and unpeeled and three slice thicknesses. Three drying methods (solar, biomass and solar-biomass) were used to dry fresh banana slices in the greenhouse dryer with the open sun as the control. All measurements for the required parameters were monitored and recorded accordingly. Evaluation of the developed dryer was based on energy and exergy analyses. Optimization of the developed dryer was achieved by the use of genetic algorithm. The objective functions of optimization were to maximize exergy efficiency and drying air temperature. A comparison of colour, vitamin C content and firmness of the dried banana slices to that of fresh banana slices was made. The coefficient of determination (R^2) between the simulated and measured values for the developed model were 0.8099, 0.5393 and 0.8845 for solar, biomass and solar-biomass modes, respectively. Under no load condition, the dryer had a temperature and relative humidity difference of 16.61±6.81^{o}C and 9.77±17.89%, 8.20±1.42^{o}C and 20.60±7.44% and 16.77±5.77^{o}C and 21.48±13.94% for solar, biomass and solar-biomass modes, respectively, compared to ambient air. These conditions in the dryer indicated the potential of the drying air in holding more moisture as compared to open sun drying. During the drying period, the dryer had a temperature and relative humidity difference of 12.96±5.25^{o}C and 8.76±8.28%, 8.88±1.38^{o}C and 24.26±8.83% and 13.21±6.21^{o}C and 27.51±10.24% for solar, biomass and solar-biomass modes, respectively, compared to ambient air. The average energy utilization ratio in the greenhouse dryer was noted as 35.58±24.78, 40.60±10.52 and 33.46±13.45% for solar, biomass and solar-biomass modes, respectively. The corresponding average hourly exergy efficiency of drying air was found to be 64.60±24.78, 59.37±10.52 and 66.50±13.47%, respectively. The results of optimization showed that solar and solar-biomass modes required the same airflow rate (0.05 kg/s) indicating that at these combinations the dryer received almost equal energy input. Biomass mode trade-offs indicated that a lower flow rate (0.01 kg/s) was required for drying. Further, both solar-biomass and biomass modes required a fuel feed rate of 0.001 kg/s for maximum exergy efficiency (solar-biomass: 80.21±14.26%; biomass: 79.28±10.38%) and drying air temperature of 333 K. Performance evaluation of the optimised system demonstrated its superiority compared to the un-optimised system. Regardless of the drying method, results obtained showed that the dried products were darker, firmer and had lower vitamin C content than the corresponding fresh products. Open sun drying had the highest colour difference of 39.14±7.63 compared to 24.27±2.52, 16.53±12.81 and 21.71±2.28 for solar, biomass and solar-biomass, respectively. The highest percentage increase in firmness of banana slices after drying was found to be 317.50±8.92%, 153.19±60.54%, 233.33±26.07% and

262.50±12.62% for solar, biomass, solar-biomass and open sun drying, respectively. Biomass mode drying had the highest retention of vitamin C content of 87.19±13.97% compared to 86.90±2.84%, 85.87±2.64%, and 77.14±6.38% for solar-biomass, solar and open sun drying, respectively. However, drying of banana slices in the greenhouse dryer resulted in better conservation of quality as compared to open sun drying. Generally, drying of products in the optimized hybrid greenhouse dryer has advantages of continuous drying despite changes in weather and time, as well as protecting the product from contamination. Further research should be conducted on optimization based on extensive thermodynamic properties of the system.

CHAPTER ONE

INTRODUCTION

1.1. Background of the Study

Banana (*Musa spp*) is one of the most consumed fruits worldwide with vast economic value and socio-economic importance (Moreira *et al*., 2010). Banana accounts for about 36% of fruit produced in Kenya and 11.1% of the total value of domestic horticulture (FAO, 2014). Banana farming is a backbone to many households in rural areas as it contributes about 30 to 70% of household income (FAO, 2014). In addition, it is a way of empowering women as the majority of banana farmers are women. Along the value chain in banana production, there are several postharvest challenges such as inadequate market information, improper marketing channels, product quality deterioration and low-value addition. International Institute of Tropical Agriculture, (2010) reported postharvest losses for bananas estimated at more than 50%.

Bananas are tropical climacteric fruits with high moisture and low acid content. Depending on the harvest stage, a banana has a green life period of 20 to 30 days if properly stored at recommended temperature of 13^{o}C and relative humidity of 98%, respectively (Brat *et al*., 2019). However, maintaining these conditions is always a challenge to farmers as they require specialized facilities due to prevailing hot conditions (temperature >13^{o}C and relative humidity<98%) in most parts of the country. Thus, bananas tend to have a shorter green life period due to exogenous storage conditions that encourage accelerated ripening, which leads to product deterioration and finally loss of value (Brat *et al*., 2019). Farmers and traders do not

get a proper return for their harvest during the peak period of harvest due to low market prices and subsequent losses if the product is over-stored. Value addition to bananas can significantly add income generation to farmers and traders.

Since bananas are rich in nutrients and high in moisture content this makes them susceptible to microbial damage. This spoilage leads to poor market value and nutritive value of the fruit, either due to its unappealing appearance or the changes in the stored products of the fruits (Sawant and Gawai, 2011). Therefore, drying is necessary to reduce their water activity, prevent microbial spoilage, reduce weight, decrease packaging, handling and transportation costs (Omolola *et al*., 2015). In Kenya, open sun drying is a widely practiced technique for the preservation of agricultural products. Nonetheless, sun drying yields dried products of low value, in both the quality and quantity (Habwe *et al*., 2008). Efforts to improve on the traditional sun drying have been attempted by the use of solar dryers and hybrid dryers that use combined energy sources (Kituu *et al*., 2012; Kaddumukasa *et al*., 2005).

Several researchers have studied the application of various food dryers for different types of products in Kenya such as fish and maize (Tonui *et al*., 2014; Kituu *et al*., 2012; Ronoh *et al*., 2010). Most of the developed drying technologies for bananas and other crops have less control over drying parameters such as drying temperature and time (Ndirangu *et al*., 2018). Drying of produce in uncontrolled systems result in discolouration, loss of flavour, texture and important micronutrients (Pekke *et al*., 2013). To produce competitive products in the market, there is a need to develop

alternative banana drying technology which can ensure energy efficiency drying and high-quality products (Pekke *et al*., 2013). Additionally, proper preservation will enable the farmers to hold their produce during peak periods, for them to take advantage of the high prices prevailing during the shortage periods.

Exergy analysis is a technique that uses both conservations of mass and energy principles together with the second law of thermodynamics in analyzing, designing and improvement of drying systems (Dincer, 2002). Thus, exergy analysis comprises the use of exergy concepts, exergy balances and exergy efficiencies to assess and improve energy and other systems.

1.2. Problem Statement

Bananas just like any other horticultural crop are highly perishable and thus pose a great challenge in distribution, marketing and storage. A fully ripened banana takes about 4 to 7 days to deteriorate (Abano and Sam-Amoah, 2011). The most common preservation method for bananas in Sub-Saharan Africa is sun drying. Sun-drying is cheap but often yields poor quality as it is time consuming, exposes the products to dust, rain and wind, or even insects, birds, rodents and domestic animals while being dried (Pekke *et al*., 2013; Habwe *et al*., 2008). Efforts to introduce solar drying technologies for drying agricultural produce have been massive in the recent past both by the Government of Kenya and non-governmental organisations (FAO, 2014). Some of the drying technologies introduced include cabinet dryers, tent dryers and greenhouse dyers. However, these dryers have not been adopted by farmers due to high

costs which outweigh the expected returns (FAO, 2014). A study conducted by Ndirangu *et al*. (2018) reported that farmers experienced losses during drying due to delayed or cold weather, poor drying conditions and spillage. These losses are attributable to poor dryer design and lack of technical training for the farmers.

Other drying technologies such as freeze-drying, microwave drying and vacuum drying have been reported to be costly limiting their adoption among farmers. Most of the small-scale farmers live in rural areas where infrastructure and amenities such as electricity availability is limited (Shiundu and Oniang'o, 2007). Moreover, some of the available drying technologies require substantial capital investment and a well-developed infrastructure which is lacking in rural areas. Other than solar or sun drying, farmers also use fossil fuel burning, electrical heating and diesel engine heating systems in drying the bananas. These sources of energy though infinite, are expensive and contribute to high drying cost. Moreover, the unpredictable inflation and frequent scarcity of fossil fuel pose a great challenge to their reliability in agricultural processes such as drying.

1.3. Justification

Banana is a highly perishable and bulky fruit that requires processing into a more stable and suitable form for longer shelf-life, ease of storage and transportation to distant markets. Green bananas including the peel are a good source of dietary fibre, minerals and vitamins (Türker *et al*., 2016). Recently, green banana has been considered a new food ingredient and several studies have suggested that its consumption has a

beneficial effect on human health, since it is one of the food richest in resistant starch and a functional gluten-free product (Türker *et al*., 2016; Fuentes-Zaragoza *et al*., 2010). Processing green bananas into products that are shelf-stable, easy to handle and easy to prepare is a necessity in light of lifestyle changes. One of the options in preserving green bananas other than ripening them is drying them for future use. Drying is one of the most sort alternatives in value addition as its energy input is less when compared to freezing, canning and other sophisticated methods such as lyophilisation (Medeiros and Ramlay, 2009; Menges and Ertekin, 2006). Continuous use of fossil fuels and electricity in the drying of products is inefficient as one gets only a fraction of their energy potential which could have been used for other high-end energy-demanding industrial processes and thus saving the universe from over exploitation or degradation of natural resources (Dronachari and Shriramulu, 2019; Mathew and Venugopal, 2018; Rosen and Dincer, 2001). Moreover, the market of fossil fuels is unstable and their prices are constantly rising (Dronachari and Shriramulu, 2019; Lukas and Josef, 2014). Some of the big producers of bananas are in remote areas where there is plenty of space for drying operations, adequate sources of biomass and affordable labour.

A review by Bala and Janjai (2013) on solar drying of agricultural products recommends that one of the areas that require research on greenhouse dryers is the optimization of both product quality and dryer design. Exergy analyses have been widely used as important instruments to study and optimize various types of energy systems (Erbay and Hepbasli, 2013). Dincer (2002) reported that an exergy analysis is

a powerful tool for advancing the goal of more efficient energy-resource use and determining the locations, types and true magnitudes of energy wastes and losses in the drying systems consequently providing details on areas of improvement for optimum drying conditions. Additionally, the evaluation of the actual thermodynamic inefficiencies in any drying system is valuable for enhancing the drying operation as the process is energy demanding.

In this study, optimization of the system was realized by developing relations between drying requirements of banana slices and energy supply, performing exergy analysis of each hybrid solar-biomass greenhouse dryer component and sizing the dryer based on analysis outputs. The aim of exergy analysis for this study was an effort geared towards designing a more efficient energy system by ensuring exergy loss minimization of existing unit operations. It was also noted that exergy analysis technique provided useful information in choosing the most suitable component design and operation procedure of any given system (Tiwari *et al.*, 2009). The choice of exergy efficiency as an optimization function was due to the fact that it is a proportion to most variables in a solar drying system such as thermal efficiency, temperature, air flow rate, fuel flow rate and greenhouse properties. In addition, from the general exergy efficiency equation it was clear that optimizing exergy efficiency alone might have resulted in low drying air temperature or drying air temperature equal to ambient temperatures leading to poor drying rates of the products. Thus, there was need to consider a bi-objective optimization approach by having drying air temperature as an addition optimization function for the system. Additionally, there was need to ensure

high product quality after drying since the market prefers high quality dried products with good reconstitution properties and excellent sensory attributes (Ndayambaje *et al*., 2019; Kaddumukasa *et al*., 2005). A hybrid solar-biomass greenhouse dryer protects the products from external contamination and it can be used in adverse weather conditions and also at night time.

The study contributes in addressing specific sustainable development goals (SDGs) (i.e. SDG 1- no poverty, SDG 2- zero hunger, SDG 3- good health and well-being and SDG 9- industrial, innovation and infrastructure). In addition, the study aided in addressing three of the 'Big Four Agenda" of the Kenyan Government (food security, health, and manufacturing). These contributions were aimed towards achieving Kenya Vision 2030. The findings of this study are relevant to all parts of Kenya that grow bananas and are beneficial to the banana breeders, commercial banana handling companies, large-scale farmers, community-based groups and agricultural research institutes. The horticultural industry benefits from the study as it addresses optimum greenhouse drying conditions for maximum exergy efficiency and drying air temperatures. These outputs help the industry save on energy cost while achieving desired drying conditions in the dryer. In addition, through training, technicians could readily build suitable greenhouse dryers by adapting and replicating the pilot design.

1.4. Objectives

1.4.1. General objective

The main objective of the study was to optimize a hybrid solar-biomass greenhouse dryer for drying banana slices based on exergy analysis.

1.4.2. Specific objectives

a) To develop models relating solar and biomass energy supplies, drying of banana slices and dryer design parameters for estimating drying time.
b) To design and develop a hybrid solar-biomass greenhouse dryer for banana slices based on the determined relations.
c) To perform exergy analysis of the developed hybrid solar-biomass greenhouse dryer for drying banana slices.
d) To optimize the developed hybrid solar-biomass greenhouse dryer for drying banana slices based on the exergy analysis outputs.
e) To determine the effect of drying on nutritive and organoleptic properties of banana slices.

1.5. Hypotheses

a) H_0: It is not possible to develop a model that relates solar and biomass energy supplies, drying of banana slices and dryer design parameters for estimating drying time.

   H_1: It is possible to develop a model that relates solar and biomass energy supplies, drying of banana slices and dryer design parameters for estimating drying time.

b) H_0: Regardless of the energy mode used there is no significance difference between the average hourly drying air temperature and the average hourly ambient temperatures.

   H_1: Regardless of the energy mode used there is a significance difference between the average hourly drying air temperature and the average hourly ambient temperatures.

c) H_0: Exergy efficiency of the developed hybrid solar-biomass greenhouse dryer for drying banana slices does not significantly vary with the drying method.

   H_1: Exergy efficiency of the developed hybrid solar-biomass greenhouse dryer for drying banana slices varies with the drying method.

d) H_0: Optimization of the developed hybrid solar-biomass greenhouse dryer for drying banana slices does not improve its exergy efficiency.

   H_1: Optimization of the developed hybrid solar-biomass greenhouse dryer for drying banana slices improves its exergy efficiency.

e) H_0: Drying of banana slices in the developed hybrid solar-biomass greenhouse dryer has no effect on colour, firmness and vitamin C of the dried banana slices.

   H_1: Drying of banana slices in the developed hybrid solar-biomass greenhouse dryer has an effect on colour, firmness and vitamin C of the dried banana slices.

1.6. Scope of the Study

This study focused on the emerging knowledge on the application of exergy analysis in the optimization of solar-biomass greenhouse dryer for drying banana slices. The dryer was designed based on the weather conditions of Juja, Kenya. Four banana

varieties were selected based on their use among Kenyan farmers. The study was conducted using peeled and unpeeled banana slices. This was because of increased health awareness which encourages the use of nutritious food products such as banana peels as it contains vital nutrients. The study was limited to sliced green bananas. Three slice thicknesses were selected based on previous research recommendations. The flow rate of the drying air was kept constant based on the dryer design. For analysis of dryer performance and optimization, three energy modes (solar, biomass and solar-biomass) were used to dry the banana slices. These different drying methods were performed when the weather conditions were most appropriate for them. Thus, solar drying was conducted on a clear day and in a period when the study area experiences high solar radiation while biomass mode was performed during the night when there is no solar radiation. Solar-biomass mode was performed on a relatively cloudy day with intermittent rain so as to have the biomass energy complementing the solar energy. Optimization of the developed solar-biomass greenhouse dryer was achieved by the use of a deterministic approach commonly referred to as a genetic algorithm. Further, the study included the determination of the quality of dried banana slices based on vitamin C content, colour and firmness.

CHAPTER TWO

LITERATURE REVIEW

2.1. Theoretical Review

2.1.1. Importance and production of bananas in Kenya

The agricultural sector is the stronghold of Kenya's economy. Horticulture is the largest sector of Kenya's agriculture contributing to 33% of the agriculture GDP (AFA, 2017). A study by Food and Agriculture Organization (FAO) of the United Nations reported that bananas accounts for 36% of the fruit production in Kenya and contribute 11.1% of the total value of domestic horticulture (FAO, 2014). The banana sub-sector contributes to food security, employment and household incomes to a majority of Kenyan (FAO, 2014; Njuguna *et al*., 2008). Farmers earn about USD 148 per annum contributing to 30 to 70% of household income thus improving their livelihoods (FAO, 2014). Banana is considered to be a leading fruit in the world and ranked among the top five in terms of economic value in world trade (Aurore *et al*., 2009). In Kenya, banana is ranked the most important fruit crop among the fruit crops followed by mangoes and oranges (Kilalo *et al.*, 2009). As of 2018, banana production in Kenya was over 1.4 million metric tons with Meru, Murang'a, Kirinyaga, Taita Taveta and Tharaka Nithi counties leading by 20.4%, 11%, 8.1%, 6.6% and 5.6%, respectively (Horticultural Crops Directorate, 2018).

Fruits and vegetables play an important role in the human diet and nutrition as sources of vitamins and minerals. Green banana pulp and peel have significant benefits on human health. They are an excellent source of dietary fibre, resistant starch,

antioxidants, polyphenols, minerals and vitamins (Kumar *et al*., 2012; Fadhel *et al*., 2011). Kumar *et al*. (2012) highlighted numerous benefits derived from eating bananas. Some of the benefits listed are that bananas have medicinal qualities as the peel and pulp contain antifungal and antibiotic components which are important to the human body. Additionally, the authors reported that banana is an excellent infant food as it is easily digested and does not cause any known allergic reaction to the consumer. There are four main types of banana varieties, namely cooking, roasting, brewing and dessert bananas (Kasyoka *et al.,* 2011). The use of bananas depends on the amount of starch and sugar levels in the fruit and may vary across regions. Among the common edible subgroups of bananas are dessert (AAA- genome), East African highland bananas (AAA-EA genome) and cooking varieties (ABB- genome). Dessert is consumed when ripe, while cooking variety is consumed after cooking at various stages of maturity (Delphine *et al*., 2019). East African highland bananas can be consumed when ripe or cooked depending on community preference. Bananas from these edible sub-groups can be processed into other forms such as flour, juice, puree, or either dried or fried crisp snacks. The most consumed banana varieties in Kenya are the cooking (plantain bananas) and dessert (fruit bananas) which are grown mainly under rain-fed conditions (FAO, 2014; Kasyoka *et al.,* 2010).

2.1.2. Processing and preservation methods for bananas

Banana is a climacteric fruit and though widely consumed when ripe, it is often prone to deterioration during the maturation process. Processing of either ripe or green (unripe) bananas is necessary to curb the postharvest losses in the sub-sector and to

exploit a greater number of market options (FAO, 2014; Adeniji *et al*., 2010). Green bananas are rich in starch and thus can be used directly by cooking or processing them into other products such as flour, dried or deep-fried crisp snack (Türker *et al*., 2016; Fuentes-Zaragoza *et al*., 2010; Adeniji *et al*., 2010). Crisps or chips are hard, brittle banana products produced by deep-frying banana slices in vegetable oil. They are only consumed directly as a snack and can be stored for some time if properly packaged. However, the use of vegetable oil may reduce shelf-life due to lipid oxidation (Adeniji *et al*., 2010).

Processing green bananas into flour is a simple process as it only involves drying the product and grinding it into flour (Adeniji *et al*., 2010). During drying, the bananas may be peeled or dried together with peels. Drying bananas using the natural sun-drying method has been in practice for ages. Products processed via open sun-drying often have high variability in terms of colour, taste, odour, texture and overall acceptability (Pekke *et al*., 2013). Drying methods have continuously improved from open sun drying on the ground to raised platforms in a greenhouse, to solar dryers with trays in a closed cabinet. Hot air drying has many advantages over open sun-drying such as control of drying conditions (*viz*., drying temperature and humidity), the achievement of hygienic conditions and reduction of product loss (Dronachari and Shriramulu, 2019; Ronoh *et al*., 2010). Consequently, solar drying has evolved from being dependent on solar energy only to hybrid systems that use solar and other sources of energy such as diesel, electricity and biomass (Fudholi *et al*., 2016; Kivevele and Huan, 2014; Kaddumukasa *et al*., 2005).

2.1.3. Solar dryer design and development criteria

A solar dryer is defined as an enclosed unit, which is used to remove moisture from agricultural products by the use of air heated by solar thermal energy (Dronachari and Shriramulu, 2019). Solar dryers can be classified based on air movement mode, solar energy collectors, type of product to be dried and insulation of the assembly (Anand *et al*., 2020). Air movement classification is one of the major classifications in which the dryer operates either under natural (passive) mode or forced (active) mode. Other classifications are distinct subclasses of these two operation modes. Thus, the dryer may further be grouped as a direct, indirect, mixed-mode, or hybrid solar dryer (Dronachari and Shriramulu, 2019).

A greenhouse dryer is an enclosed structure having transparent walls and roofs, commonly made up of polycarbonate glass, fiberglass sheet, or polyethylene film used for crop drying. Prakash and Kumar (2014) have given a detailed classification of the greenhouse dryers. Based on structure, a greenhouse dryer can be of a dome shape, parabolic, hemi-cylindrical, or roof even type. The main advantage of dome shape greenhouse dryer is that there is maximum utilization of global solar radiation while the greatest merit of using roof even type is that there is proper mixing of air inside the dryer (Prakash and Kumar, 2014).

The advantage of a greenhouse dryer over other indirect solar dryers is that the dryer combines the plenum chamber (heater) and drying chamber as a single unit. Like a heater, the size and effective heat capacity of the greenhouse enclosure are larger than

those of comparable indirect solar dryers (Olutoye and Uthamalingam, 2012). Greenhouse dryers are reported to be two to five fold more efficient compared to open sun drying (Koyuncu, 2006). Janjai (2012) observed that a parabolic greenhouse solar dryer covered with polycarbonate sheet operated under forced convection mode took 2 to 3 days shorter to dry tomatoes as compared to natural sun drying with the dryer temperature varying from 35 to 60^{o}C. Kassem *et al*. (2011) reported that a gable-even-span greenhouse to be the most thermally efficient and convenient type of greenhouse when compared to four sides pyramid and hemispherical shape dryers in the drying of onion flakes. Almuhanna (2012) researched on the utilization of a gable even span greenhouse for drying dates in active mode. The author reported that the drying air in the greenhouse dryer had a temperature gain of 14.1^{o}C compared to ambient air and the dryer had an average thermal efficiency of 57.2%.

The design principles of the conventional greenhouse for crop growth are the same as those of a greenhouse dryer except that the emphasis on the dryer design is on heat entrapment to facilitate the drying process (Olutoye and Uthamalingam, 2012). Parameters used in evaluating the performance of a solar dryer can be divided according to the physical features of the dryer, thermal performance and quality of the dried product (Dronachari and Shriramulu, 2019). To design and develop an effective dryer these parameters must be put into consideration to curb losses due to poor drying conditions (Ndirangu *et al*., 2018). The physical parameters indicate dryer type, size, shape, loading density, capacity and the number of batches per given time.

The thermal energy required for drying is governed by the initial moisture content, desired final moisture content, specific heat capacity of the crop, latent heat of vaporization of water, drying times, production capacity, drying air temperature and relative humidity, air flow rate in the dryer and the efficiency of the drying equipment (Nwakuba *et al*., 2018; Adefemi and Ilesanmi, 2018). Thermal performance parameters can be simulated based on the selected physical parameters and validated experimentally (Nwakuba *et al*., 2018). These parameters indicate the performance of the developed dryer in terms of drying rate, achieved drying temperature and relative humidity and dryer efficiency (Anand *et al*., 2020). It is also important to consider the location of the dryer, availability and cost of dryer construction materials as well operation and maintenance cost of the dryer.

2.2. Empirical Review

2.2.1. Importance of simulation models in drying systems

Simulation is the imitation of the operation of a real world process or system over time. It is always important to simulate the drying process before the actual system development to identify areas that can be optimized in the design. The drying simulation model provides information about the influence of various important parameters on the drying phenomenon (Nwakuba *et al*., 2018). For the developed models to be acknowledged to represent the system they must be validated using the experimental results. Recently, there have been various attempts to develop models for predicting the drying rate or drying time and energy requirements of various commodities. In a review of energy requirements for drying, Nwakuba *et al*. (2016)

highlighted some of the scholars who have developed various mathematical models for predicting heat requirements in the drying of selected agricultural products.

The most common models used in drying are the empirical or semi-empirical thin layer drying models which are derived from Newton's law of cooling and Fick's law of diffusion (Erbay and Icier, 2010). These models determine the drying rate of a product by expressing the moisture ratio as a function of drying time. Empirical models can only be customized for a specified drying condition by curve fitting using non-linear regression in a statistical computer software based on the non-linear optimization to determine the respective constants in any given empirical model (Querikiol and Taboada, 2018). The limiting factor about thin layer drying models is that the selected models have to be subjected to curve fitting in which the best fitting models are selected to represent the drying kinetics of the product. Other models that are useful in drying predictions are fundamental models such as those based on heat and mass transfer within and out of the product (Feng, 2012).

The time required to reduce the moisture content of a fresh product in a solar-biomass dryer to safe levels for storage depends on several factors. These factors mainly include product properties, weather conditions and dryer properties. Whereas dryer properties are constant during drying, weather conditions are highly variable and result in variations of drying time. The estimation of drying time is therefore necessary for designing batch drying systems. Drying agricultural products for domestic or commercial use requires one to be equipped with relevant knowledge such as final

moisture content for safe storage and optimum drying conditions to retain nutrients in the dried product (Nwakuba *et al*., 2016). A poor estimate of drying time and excess supply of supplemental heat energy may cause irreplaceable damage to the dried products. Consequences of over-drying include increased production cost due to additional fuel used and product weight loss. Conversely, not drying the product to safe storage may lead to spoilage of the product due to microbial activity causing decay (Nwakuba *et al*., 2018). It is thus important for one to be able to make a subjective judgment when it comes to trying to make reasonable cost-benefit.

2.2.2. Hybrid solar-biomass greenhouse dryer

Solar drying is one of the recommended methods of fruit and vegetable preservation. Solar energy is freely available, the world's most plentiful, permanent and environmentally-friendly form of energy (Fudholi *et al*., 2016; Bennamoun, 2012). Solar drying has several advantages compared to traditional open sun drying. These include protecting the product from re-wetting, attack by insects, pests and dust (Dronachari and Shriramulu, 2019). However, the solar drying method just like traditional sun drying is severely affected by intermittent weather conditions such as low solar intensity and is not feasible for night time drying (Fudholi *et al*., 2016; Oyero *et al*., 2007). A hybrid solar drying system is an alternative to a solar drying system. Hybrid drying systems allow continuous drying due to supplemental heat supplied to the system from alternative energy sources and stored energy.

Electricity is a clean source of energy and easier to use. Unfortunately, in most developing countries like Kenya, its cost remains relatively high and it is not readily available in rural areas where most of the farming activities take place. Fossil fuel, on the other hand, may still be an alternative energy source which, however, is not a renewable source and is faced with several challenges (Dronachari and Shriramulu, 2019; Mathew and Venugopal, 2018). Biomass remains an alternative energy source for drying, not only because it is readily available in many forms, but it is also a renewable source of energy (Dronachari and Shriramulu, 2019; Mugo and Gathui, 2010; Omiti *et al.*, 2007).

Recently, there have been increased studies on the use of biomass fuels such as agro-waste in biomass combustion processes (Lukas and Josef, 2014). Biomass can be used as a form of renewable energy, for both heat and power generation through thermochemical treatments, such as combustion and gasification. However, the most preferred method of producing energy from biomass is conventional combustion (Kocer *et al*., 2014). There is increasing demand for cheaper, cleaner and more efficient ways of utilizing biomass as a source of energy hence the growing production of biomass briquettes in Kenya. Briquettes are cleaner and easier to use compared to loose biomass material such as rice husks, straws and banana leaves (Efomah and Gbabo, 2015). According to Lukas and Josef (2014), moisture content, chemical composition, particle size, energy content as well as the energy density of the feedstock are the major factors that are considered in the selection and evaluation of a desirable type of biomass for briquette production. The raw material varies from an unlimited

number of agricultural residues and wastes to industrial waste such as charcoal dust, coal dust and other forestry products.

Although hybrid solar dryers have been studied enormously, most of these studies have been limited to convectional solar-biomass dryers with fewer studies reported on solar-biomass greenhouse dryer (Yuwana and Sidebang, 2017). Barnwal and Tiwari (2008) developed and studied a hybrid photovoltaic integrated greenhouse under natural and forced mode without load. They reported that the thermal loss efficiency under forced mode was high for crop drying. Lokeswaran and Eswaramoorthy (2013) studied a natural convection greenhouse dryer integrated with a biomass back-up unit for drying coconut. The study showed that the moisture content of coconut reduced from 53.4% to 9.2% within 26, 30 and 44 hours for solar-biomass mode, biomass mode and solar mode, respectively. The dryer had an overall thermal efficiency of 19%. Arun *et al*. (2014) developed a convection solar tunnel greenhouse dryer coupled with a biomass heater for drying coconut and compared it to a solar tunnel greenhouse dryer without biomass heater. Their study demonstrated that the use of biomass heater reduced drying time as it took 44 hours to reduce the moisture content from 53.84% to 7.00% and 56 hours for reducing the moisture content to the same level without the heater.

2.2.3. Exergy analysis of a solar-biomass greenhouse dryer

Exergy of a system is a property of system and environment combination and is defined as the maximum amount of useful work that can be obtained from the system at a given state as it is brought to equilibrium with a reference environment at constant

conditions (Hepbasli *et al*., 2010). Wall (2010) refers to exergy as work potential, i.e., ordered motion or ability to do useful work. It is important to note that everything that happens involves conversion of energy and consumption of exergy. Exergy analysis is a universal method of evaluating the rational use of energy. According to Dincer (2002), exergy analysis is based on both the conservation of mass and conversion of energy principles together with the second law of thermodynamics for analysis, design and improvement of energy and other systems. Exergy analysis is a measure of quality of energy form and helps in identifying the nature of energy degradations, where they are occurring in the system and their magnitudes. Thus, exergy analysis also aids in understanding the energy conversion in complex systems (Tsatsaronis and Cziesla, 2009).

To reduce energy consumption and optimally utilize the available energy in a system, the efficiency of the system must be improved. In the past years, exergy analysis has been used to evaluate the performance of various systems and improve their efficiencies (Ahamed *et al*., 2011). The exergy of a system or process is maximized when exergy loss is minimized and exergy efficiency is maximized. Exergy efficiency is the ratio of output exergy to the input exergy of the system. Exergy analyses of food drying were performed by several researchers. Lingayat *et al*. (2019) developed an indirect type natural convection solar dryer for drying banana slices in India. They performed drying experiments using 2000 g of fresh ripe sliced bananas to study energy and exergy analysis of the system. They reported the average efficiency of the collector and drying chamber to be 38.2% and 17.73%, respectively. Additionally, the

dryer exergy efficiency was found to vary from 7.4 to 46.58% with an average of 21.57%.

Barki *et al*. (2019) developed a solar dryer with a back-up incinerator for drying chili pepper. They conducted experiments on a clear and cloudy day using 1000 g of chili pepper to determine the exergy efficiency of the developed dryer. They reported the exergy efficiency of the hybrid dryer increased with increase in drying time (i.e. from 8.00 am to 2.00 pm the exergy efficiency increased from 83.1 to 92.4%) and then decreased during the latter drying hours to 73.4% by 6.00 pm. They attributed the observed trend to the dependency of exergy efficiency on the solar intensity. Subramani *et al*. (2020) evaluated the performance of a simple low-cost greenhouse dryer using energy and exergy analysis. They conducted drying experiments using an ultra-violet (UV) stabilized polyethylene sheet and drip lock glazing material under passive and active modes to dry Ivy gourd (*coccinia grandis*) and Turkey berry (*solanum torvum*). Thermal efficiencies were reported to be up to 30.64% and exergy efficiency values were between 0.001 to 0.09% and the maximum value of exergy efficiency of 0.09% was obtained during the drying of ivy gourd with the drip lock sheet under active mode. Additionally, the authors reported a reduction in exergy values compared to thermal efficiency values of the system which they attributed to the exergy destruction due to irreversibility in the system.

Fudholi *et al*. (2016) performed energy and exergy analysis of a hybrid solar dryer for drying salted Malaysian silver jewfish. The dryer was of the forced convection indirect

type with a rotating rack drying chamber and used a diesel burner to provide supplemental heat for drying. They stated that the collector and dryer efficiencies were 41 and 23%, respectively. Additionally, the exergy efficiency was found to range between 17 and 44% with an average of 31%. Panwar *et al*. (2013) investigated thermal modelling, energy and exergy analysis of a walk-in-type solar tunnel dryer for drying 600 kg of surgical cotton in India. The experimental and predicted values for the energy efficiency of the drying process were found to vary from 1.051–1.793% and 1.298–2.224%, respectively. The values of exergy efficiency were found to vary from 0.039–0.072% and 0.030–0.058%, respectively.

2.2.4. Selection of optimization technique

Optimization of a system or process helps in obtaining the best set of values that gives the best results (Joshi *et al*., 2019). The goal of optimizing a drying system is to increase its workability, increasing accuracy and reducing drying time and cost investments. Sunil *et al*. (2013) stated that before using any drying systems on large-scale, optimization techniques must be applied to find the optimum set of different parameters that affect the performance of the drying systems. For a system or process to be optimized, one needs to identify the optimization problem. It is also important to define initial and final parameters of the system or product, as well as decision variables for which the optimal values will be sought (Poświata and Szwast, 2012). There are various optimization techniques applied in the drying of agricultural products such as artificial neural networks (ANNs), genetic algorithm (GA), response surface method (RSM), particle swarm optimization (PSO), fuzzy logic,

computational fluid dynamics (CFD) and Taguchi technique (Bansal *et al*., 2020; Joshi *et al*., 2019; Sunil *et al*., 2013). The ANNs is commonly applied in complex, nonlinear agricultural systems (Mortaza *et al*., 2015). Several neural network topologies are available and therefore proper selection of neural network is critical for model accuracy and simplicity.

Optimization of a system or process can be achieved by the use of a deterministic approach commonly referred to as a GA. A GA is a global search algorithm that is designed to imitate the principles of biological evolution in natural genetic systems. GA is commonly applied when the relationships between inputs and outputs of a drying process are known or can be developed using mathematical, statistical, numerical and analytical techniques (Dhumne *et al*, 2016; Lapczynska-Kordon *et al*., 2013; Kituu *et al*., 2012). Using selection, crossover and mutation, the algorithm can generate a new population that yields optimum objective functions (Dhumne *et al*., 2016). The GA is suitable when the search space is very large or too complex for analytic treatments. Dhumne *et al*. (2016) used a GA approach to optimize the solar tunnel dryer for drying red chilies. The reported that optimization results using GA showed good performance indicating that the technique can be used in the drying process successfully.

The ANNs is often applied when the analytical form of the relations to be optimized is unknown and is coupled with other techniques for Pareto optimal development (Winiczenko *et al*, 2018). A drawback with the ANNs is that it is time consuming as

the models require extensive training to obtain reliable results. However, it is an easier way to correlate data in case a complex nonlinear relationship exists. For example, Winiczenko *et al*. (2018) combined ANNs and GA in the optimization of convective drying of apple cubes. They studied the parameters to be optimized experimentally and then used an ANNs to develop the objective functions. Later, the objective functions were optimized using an elitist non-dominated sorting genetic algorithm (NSGA II).

RSM is a collection of mathematical and statistical techniques that are useful for the modelling and analysis of programs in which a response of interest is influenced by several variables and the objective is to optimize this response (Bradley, 2007). According to Bradley (2007), response surface method is used to approximate the dependent variable when treatments are from a continuous range of values and the relationship between the dependent variable and independent variables is not known. Adefemi and Ilesanmi (2018) optimized drying parameters for a low-cost hybrid solar dryer for drying cassava and tomatoes using the response surface method. The authors optimized the system based on energy efficiency to reduce on drying time of the respective products.

Taguchi method which is based on orthogonal array experiments helps optimization by reducing the number of trial experiments to be performed (Ghani *et al*., 2004). Orthogonal arrays stipulate the way of conducting the least number of experiments which could give the necessary information of all the factors that affect the dependent variable. The basis of the orthogonal arrays method lies in choosing the level

combinations of the input design variables for each experiment. Although the Taguchi method lies in the minimization of trial experiments, fewer studies on its application have been published (Sunil *et al*., 2013). Joshi *et al*. (2019) used the Taguchi technique to obtain the optimum combination of air velocity, airflow and humidity required to dry potatoes in a conventional solar dryer. Majdi and Esfahani (2018) used a combination of the Taguchi method and Lattice Boltzmann method (LBM) to optimize a convective dryer by minimizing drying time and energy consumption. Remarkable works have been carried out on the optimization of various drying systems using these optimization techniques mainly to optimize the system design (Kituu *et al*., 2012). The most widely used optimization techniques in drying processes are ANNs and GAs according to Sunil *et al*. (2013).

In this study, GA was adopted as the optimization technique to be used due to its suitability for optimisation when the relationships are known or can be determined.

2.2.5. Effect of drying on nutritive and organoleptic properties of bananas

The nutritional value of food refers to all the constituents of the given food and its contribution to the consumers' nutrition and energy requirement expressed as per quantity, range and energy content, vitamins, minerals and phytochemicals that are found in the food (Singh and Medina, 2012). Green bananas are rich in resistant starch while ripe bananas have high levels of digestible starch and protein. The organoleptic qualities of food are those qualities that involve the use of sensory organs such as taste, texture, flavour, appearance and colour (Muchoki *et al.,* 2007). Previous studies have

shown that drying may cause discolouration, poor flavour and loss of nutrients (Taiwo and Adeyemi, 2009). For instance, the loss in vitamin C has been reported to be higher where the fruits have been subjected to pre-treatment such as washing and blanching, as vitamin C is water soluble (Santos and Silva, 2008). Additionally, Kumar *et al*. (2019) reported darkening of green banana samples during drying which affected the final colour of flour obtained.

It is known that starch content is responsible for low drying rates when drying fresh banana slices, and this is exacerbated when fruit is dried using open sun drying. Prolonged drying period increases the toughness in bananas and may cause impairment to colour, flavour and nutrient (Amankwah *et al*., 2019). An increase in drying temperature increases moisture removal rate from the dried material and vice versa (Kiburi *et al*., 2014; Taiwo and Adeyemi, 2009). When drying tropical fruits, drying temperature should be in the range of 37 and 71^{o}C to prevent the growth of microorganisms and at the same time, avoiding cooking of the product being dried (Abano, 2010). However, Abano (2010) noted that the drying temperature should be high (about 60^{o}C) to drive moisture out of the product as quickly as possible to avoid adversely affecting flavour, texture and colour. High drying temperature and low humidity during drying cause the dried banana slices to harden on the surface, while low drying temperatures in the beginning may lead to microbial growth before complete dehydration is achieved (Abano and Sam-Amoah, 2011).

Although hybrid solar dryers have been studied enormously, there are limited studies reporting the quality attributes of dried green bananas. Several studies on quality of dried ripe bananas have been reported (Amer *et al.*, 2009; Intawee and Janjai, 2011; Hegde *et al.*, 2015) with fewer studies regarding the quality of dried green banana slices (Barroca and Guiné, 2013). Amankwah *et al*. (2019) studied the effects of different drying methods (solar adsorption drying, solar drying and open sun drying) on vitamin C, colour and composition of yams. They observed that composition was not affected by drying method but did affect vitamin C content and colour. Additionally, application of solar greenhouse dryer with biomass back-up has been studied and reported by Arun *et al*. (2014) as earlier reported. Their study reported that the quality of the coconuts dried in the greenhouse dryer with biomass heater was superior to that of coconuts dried in a greenhouse dryer without a biomass heater. There is limited knowledge on the effects of different drying methods using a single solar greenhouse set up with biomass back-up on local banana varieties available in Kenya. It is vital to evaluate the effects of any drying method on product quality before adopting it for commercial application.

Conversely, several studies on the quality of blended green banana flour exist (Ndayambaje *et al*., 2019; Islam *et al*., 2012). Often, for dried fruits and vegetables, vitamin C, colour and texture are considered as the quality indicators of the dried product (Swasdisevi *et al*., 2007; Santos and Silva, 2008; Barroca and Guiné, 2013; Kadam *et al*., 2015). The texture of food is composed of so many variables. However, just few selected properties with the greatest influence on consumer acceptance are

measured. For example, Swasdisevi *et al*. (2007) considered the product hardness to represent texture. Physical characteristics of the product vary depending on the mode of drying (Amankwah *et al*. 2019; Piotr and Grzegorz, 2003). The dried banana slices can be processed into flour for baking, and cooking of gluten free products (Kumar *et al*. 2019). Vitamin C was selected as one of the quality indicator of the dried product as it is least resistant to external factors such as exposure to heat, light and oxygen. The firmness of dried product was evaluated as it determines the energy required unit operation such as grinding. Additionally, colour of the dried product greatly influences consumer acceptance and thus colour was evaluated to determine the total colour change of the dried banana slices.

2.3. Summary of Literature and Research Gaps

The following specific conclusions and research gaps were drawn from the literature review:

a) There exist a number of empirical and semi-empirical models for estimating moisture ratio and drying energy requirement in thin layer drying of agricultural products. However, fewer studies exist on predicting drying time of product in solar drying system. It was also noted that a simulation model requires to be product, system and condition specific.

b) Different types of hybrid solar dryers have been reviewed in this study. These dryers differ in construction materials used, shape, product dried, methods of performance evaluation, source of supplemental energy and location. Although hybrid solar dryers have been studied enormously, most of these studies have been

limited to convectional solar-biomass dryers with fewer studies reported on performance of a solar-biomass greenhouse dryer under Kenyan conditions.

c) Many studies have been carried out on energy and exergy analysis of drying system while drying different products. Fewer studies have been carried out on energy and exergy analysis of solar-biomass greenhouse dryer operated using different energy modes (solar, biomass and solar-biomass modes). It is also necessary to evaluate the performance of the developed dryer under local conditions.

d) GA is commonly applied when the relationships between inputs and outputs of a drying process are known or can be developed using mathematical, statistical, numerical and analytical techniques. Studies have been carried out using GA to optimize drying processes based on exergy, but none on solar-biomass greenhouse dryer operated using solar, biomass and solar-biomass modes, respectively. It is therefore necessary to carry out research to determine the best combination of process parameters that would result in the optimum performance of such dryer.

e) The most common and notable quality attributes of the products that changes during processing include Vitamin C content, colour and firmness. Various studies have been conducted to study the changes that occur to product during drying using different solar dryers. However, there is limited knowledge on the effects of different drying methods using a single solar greenhouse set up with biomass back-up on local banana varieties available in Kenya. It is also necessary to evaluate the effects of any drying method on product quality before adopting it for commercial application.

2.4. Conceptual Framework

The conceptual framework shown in Figure 2.1 presents the relationship between independent and dependent variables in this study.

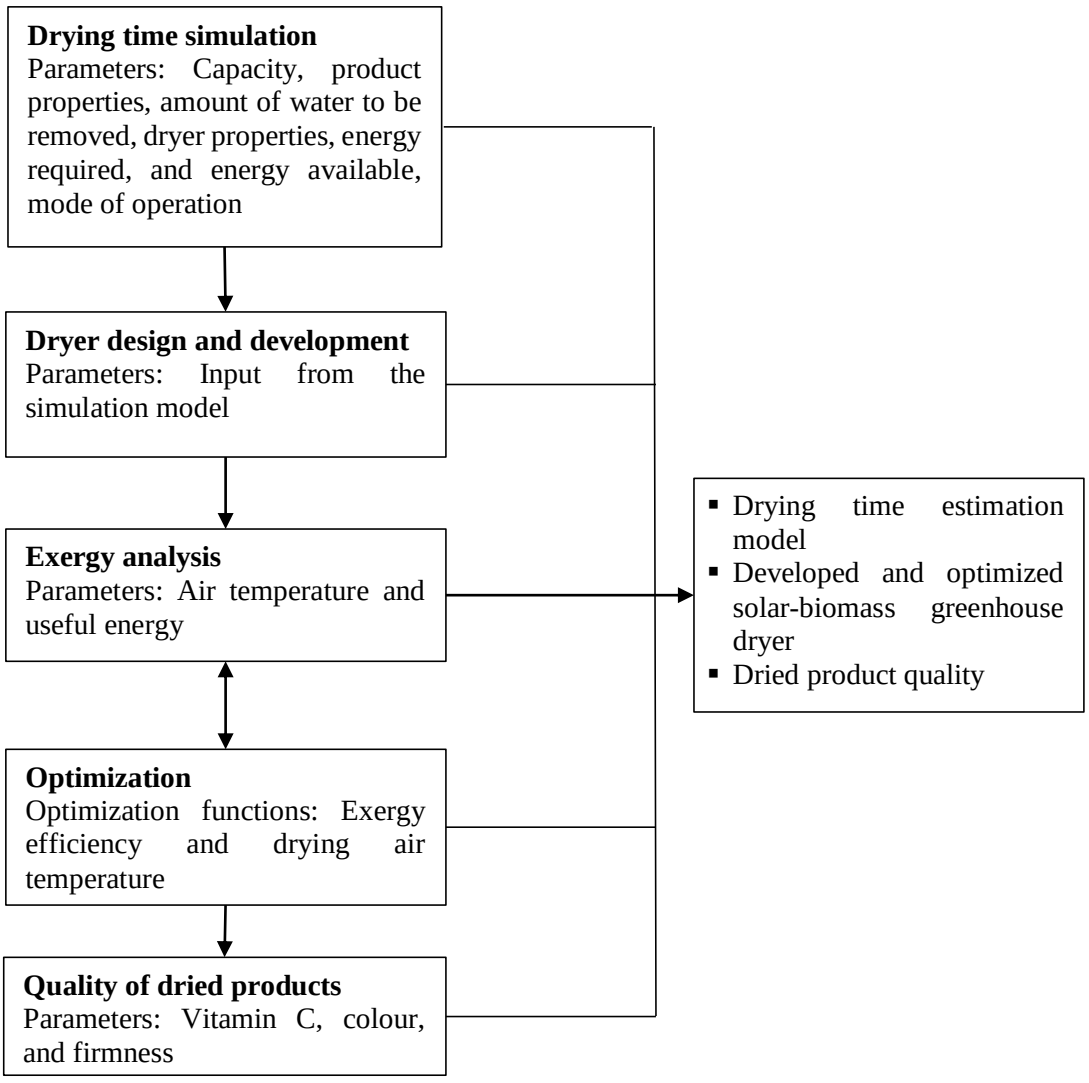

Figure 2.1: Conceptual model for the study.

CHAPTER THREE

MATERIALS AND METHODS

3.1. Empirical Models for Estimating Drying Time in a Solar-Biomass Greenhouse Dryer Operated Using Different Energy Modes

3.1.1. Determination of energy required in drying

Before the development of simulation models, there was need to determine various relations that would be used in calculating the drying time. The amount of moisture removed from the banana slices was determined according to Equation (3.1) (Sangamithra *et al.*, 2014; Seveda, 2012). In the equation, (W_w) is the amount of moisture removed (kg), where W_p is the quantity of bananas to be dried (kg), M_1 is the initial moisture content (% wet basis) and M_2 is the final moisture content (% wet basis).

$$W_w = \frac{W_p(M_1 - M_2)}{(100 - M_2)} \tag{3.1}$$

The quantity of heat energy required per unit weight of banana slices dried under atmospheric pressure was determined by Equation (3.2) (Sangamithra *et al.*, 2014). In this equation, Q_t is the total energy required (kJ/kg), W_d is the dry mass of bananas (kg), C_d is the specific heat of bananas (kJ/kg^{o}C), ΔT is the difference between temperature inside the dryer and ambient air temperature (^{o}C), M_i is the initial moisture content of bananas (% dry basis), C_p is the specific heat of water (kJ/kg^{o}C), W_w is the moisture removed (kg) and h_{fg} is the latent heat of vaporization of water at 100^{o}C and standard atmospheric pressure (kJ/kg).

$$Q_t = W_d C_d \Delta T + M_i C_p \Delta T + W_w h_{fg} \quad (3.2)$$

The total solar radiation harnessed by the greenhouse dryer depends on various aspects, such as the transmissivity and surface area of the glazing material as well as the orientation of the greenhouse dryer. In general, the hourly amount of energy input, in the greenhouse dryer was calculated using Equation (3.3) (Panwar *et al*., 2013). In the equation, Q_{in} is the hourly amount of energy input (W), I_s is the average hourly solar radiation (W/m^2), A is the surface area of the greenhouse dryer effective in harnessing the solar energy (m^2) and τ is the transmittance of the glazing material.

$$Q_{in} = I_s \times \tau \times A \quad (3.3)$$

The average hourly solar radiation I_s absorbed by a greenhouse solar collector per unit area of absorber surface was given by the Equation (3.4) (Dragicevic, 2011). In the equation, *(1+cosβ)/2* and *(1-cosβ)/2* represents the view factors from the solar collector to the sky and from the collector to the ground, respectively; in addition, subscripts *b* and *d* represent beam and diffuse respectively, R_b is the ratio of beam radiation on the tilted surface to that on the horizontal plane, I is the solar radiation (J/m^2) and ρ_g is the ground reflectance factor.

$$I_s = I_b R_b + I_d\left(1 + \frac{\cos\beta}{2}\right) + I\rho_g\left(1 - \frac{\cos\beta}{2}\right) \quad (3.4)$$

The hourly solar radiation I_s incident on different inclined and vertical surfaces of the greenhouse dryer on hourly basis was obtained as the total sum of solar radiation

falling on different surfaces (i.e., each wall and roof) of the greenhouse dryer. Hence, the solar radiation through different surfaces was estimated separately based on the orientation of the surfaces. Considering an east-west orientation, the total solar radiation available on the greenhouse dryer was computed using Equation (3.5). In the equation, τ_i, A_i and I_i are the solar transmissivity, area (m^2) and radiation flux incident (W/m^2) representing the i^{th} section of the greenhouse dryer, respectively. Assuming the total energy required for drying to be equal to heat energy gained from solar radiation, drying time for solar mode, t_s (hrs) was computed using Equation (3.6).

$$Q_{in} = \tau A I_s = \sum_{i}^{6} \tau_i A_i I_i \tag{3.5}$$

$$t_s = \frac{Q_t}{Q_{in}} \tag{3.6}$$

For the biomass only mode, it was assumed that the total energy required for drying to be equal to heat obtained from biomass combustion as given by Equation (3.7) (Okoroigwe *et al*., 2013). In this equation, Q_b is the biomass heat (kJ), m is the mass of biomass (kg), H_v, is the heating value of biomass (kJ/kg) and η_{stove} is the biomass stove efficiency. Drying time, t_b (hrs) for the biomass mode was determined using Equation (3.8), where S_c is the biomass burning rate (kg/hr).

$$Q_b = \eta_{stove} m H_v \tag{3.7}$$

$$t_b = \frac{m}{S_c} \tag{3.8}$$

During the solar-biomass energy mode, total heat energy available (Q_{tavail}) to dry the banana slices to the required moisture content was obtained as the sum of heat energy from biomass (Q_b) and heat output of the greenhouse solar collector (Q_{in}) as shown in Equation (3.9). For this mode, the biomass stove was set to operate at its design biomass burning rates hence, it was assumed that the heat from biomass combustion would meet half of the drying heat energy demand. Drying time, $t_{s\text{-}b}$ (hrs) was thus determined using Equation (3.10).

$$Q_{tavail} = Q_b + Q_{in} \tag{3.9}$$

$$t_{s-b} = 0.5 \times (\frac{Q_t}{Q_{in}}) \tag{3.10}$$

A flow chart of the algorithm for predicting drying time for the solar-biomass hybrid greenhouse dryer is represented in Figure 3.1. The code for the developed program is presented in Appendix I.

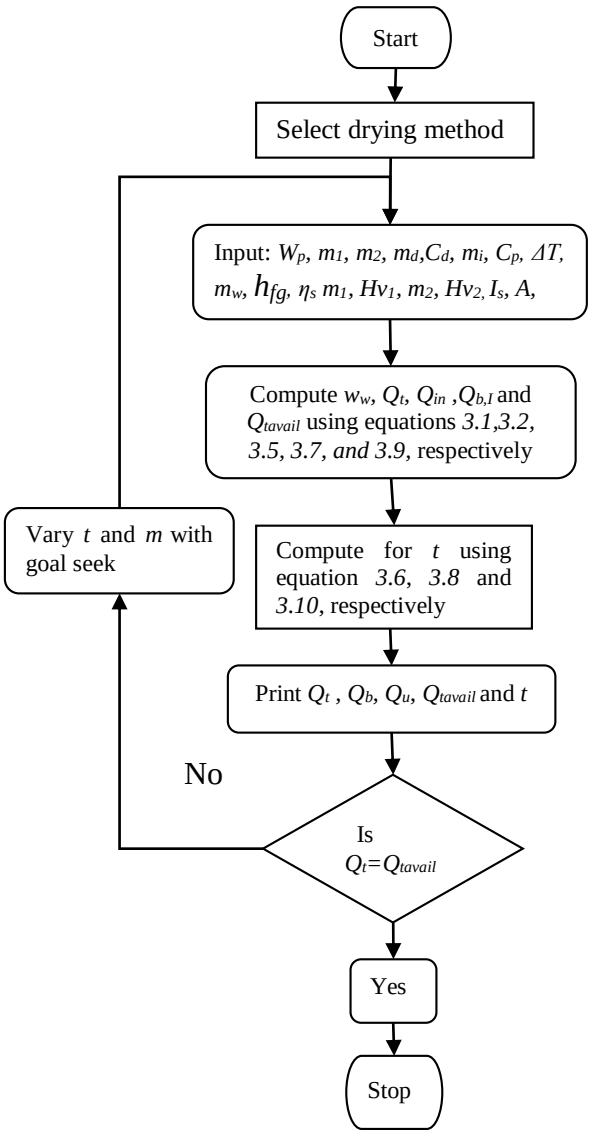

Figure 3.1: A flow chart of the algorithm for predicting drying time for the hybrid solar-biomass greenhouse dryer.

3.1.2. Acquisition of models input parameters and models validation

To make the predictions on drying time, the model required two sets of data which included constant model input data and variable input data. Constant parameters consisted of those variables that were considered to have negligible change throughout

the drying process and were selected with a conservative approach. Table 3.1 shows the constant parameters and their respective values as used in the model.

Table 3.1: Constant input values for simulation of drying time in the hybrid solar-biomass greenhouse.

Parameter	Value
Specific heat of bananas	3.45 kJ/kg^{o}C
Specific heat of water	4.2 kJ/kg^{o}C
Latent heat of water	2264.76 kJ/kg
Heating value of charcoal dust briquettes	18000 kJ/kg
Biomass stove thermal efficiency	35%
Surface area of greenhouse	102.2 m^2
Transmittance of glazing cover	50%

Variable input data included ambient air temperature, initial moisture content of the product, initial weight of the product, expected final moisture content, drying air temperature and solar radiation. These model variable data were acquired during the drying experiments detailed in Section 3.3.2. Visualization of the comparison between predicted and actual data was done using scatter plots. The values of coefficient of determination (R^2) and the resulting regression equations were also reported. The model results were further analyzed using one sample Student's *t*-test. The level of adequacy of the actual experimental values against the predicted values was

determined using Equation (3.11) (Kituu *et al*., 2010). In the equation, *PE* is the percentage error, m_{exp} and m_{pred} were experimental and predicted values, respectively.

$$PE = \left(\frac{m_{exp} - m_{pred}}{m_{exp}}\right) \times 100 \quad (3.11)$$

3.2. Design and Development of the Hybrid Solar-Biomass Greenhouse Dryer

3.2.1. Study site

The solar-biomass hybrid greenhouse dryer was developed at the Department of Agricultural and Biosystems Engineering, Jomo Kenyatta University of Agriculture and Technology (JKUAT). The study site is approximately 10 km West of Thika town and 36 km North-East of Nairobi, Kenya. The institution is located on latitude 1.0891^{o} South, longitude 37.0105^{o} East and 1460 m above sea level.

3.2.2. Experimental set up

Figure 3.2 shows the schematic of the developed solar-biomass greenhouse dryer used for this study. The greenhouse dryer measured 8 m long, 4 m wide and 3.6 m high. The dryer frame was fabricated using 38.1 mm GI round pipes and was glazed with ultra-violet (UV) stabilized polythene film of 200 µ (0.2 mm) thickness fixed by zig-zag profile. Foundation pipes were placed by digging holes of depth 0.5 m and pouring cement concrete mixture of a ratio of 1:3:6. The floor base was made of layered 101.6 mm thick gravel compacted to a depth of 0.3 m and a wire mesh of 6 mm wires used for concrete reinforcement. The dryer was of standard peak even span positioned in an east-west orientation to maximize available solar energy throughout the year (Kassem

et al., 2011; Dragicevic, 2011). A door was provided on the east face of the dryer with a 1.0 m width and 1.75 m height for access. The drying trays had a total effective area of 24 m^2 with a banana loading capacity of 240 kg. Each drying tray measured 7 m by 1 m with a spacing between the two levels being 0.3 m.

The biomass stove was used to provide supplemental heat during drying. The stove had dimensions of 0.48 m length, 0.4 m width and 0.4 m height and was fabricated using a 1.29 mm plain aluminium sheet and lagged with fibreglass of 25.4 mm thickness. The study used briquettes made from charcoal dust as a source of fuel. The biomass stove was coupled to a double duct heat exchanger such that the inner duct conveyed the flue gases and the outer ducts had the drying air. The double duct heat exchanger runs across the centre of the greenhouse dryer with the flue gases exhausted via a chimney provided at the end of the west side. The drying air was redirected to the drying trays through ducts that had outlet holes designed to discharge the drying air direct to the product. To maintain a steady flow of air in the duct, a blower (Fengda, FDA250E2/ST, China) of 2500/2600 rpm with an air flow rate of 2378 to 2551 m^3/hour was mounted on the biomass heater. Humid air from the dryer was exhausted to the outside using a fan (Fengda, FDA250SL, China) of 2500/2600 rpm with an air flow rate of 1868 to 2803 m^3/hour mounted on the west roof of the dryer. The exhaust fan was controlled using a speed regulator (Orient fans, India) to achieve the desired air flow rate. The fans were powered using a solar power system consisting of a 125 Wp, 24 V PV module (TPS-105S-125W, China) recharging a 100 AH, 24 V solar battery. A 20 A pulse width modulation (PWM) solar charge controller was used to

protect the battery. In addition, a 350 W direct current to alternating current converter (HT-M-350-12, Taiwan) was used for current conversion. The floor of the dryer was painted black to help increase the effectiveness of heat absorption and radiation inside the greenhouse dryer.

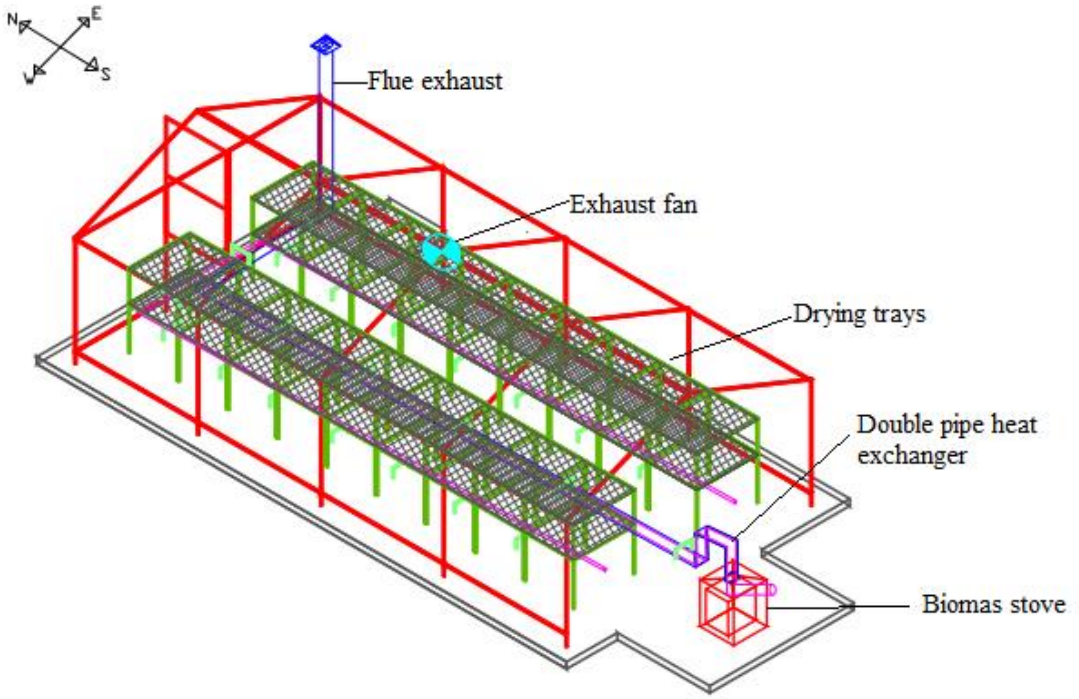

Figure 3.2: A schematic representation of the hybrid solar-biomass greenhouse dryer.

3.2.3. General dryer design considerations and assumptions

A gable, even-span greenhouse dryer was designed to meet the target capacity (240 kg) of banana slices per batch under thin layer drying. According to Kassem *et al*. (2011), a gable even-span greenhouse possess a higher solar heat gain and drying efficiency as compared to the pyramid and hemispherical greenhouses. The design factored in environmental conditions such as ambient air temperature of 25^{o}C, average

relative humidity of 50%. Air velocity of 0.8 m/s and drying air temperatures of 60ºC were used for the study. These parameters represented the safe drying conditions of agricultural materials as reported by other scholars (Alagbe *et al.*, 2020; Aduewa *et al*., 2014; Abano, 2010; Nguyen and Price, 2007). The banana slices were assumed to have an initial moisture content of 80% (wet basis) dried down to a moisture content of 15% (wet basis) (Sahdev *et al*., 2016).

The initial and final humidity ratios of the drying air were determined using the psychrometric chart, i.e., H_1 (25ºC and 50% relative humidity) and H_2 for dryer temperature of 60ºC, respectively. The mass of air required to achieve the desired drying was determined using Equation (3.12) (Seveda, 2012; Ehiem *et al*., 2009). In the equation, m_{air} is the mass of air required (kg) and W_w was as earlier defined.

$$m_{air} = \frac{W_w}{H_1 - H_2} \tag{3.12}$$

The volume of air required for the drying process was computed as shown in Equation (3.13) (Ehiem *et al*., 2009). In the equation, V_{air} is the volumetric flow of air (m^3/hr), t is time for drying (hrs) and ρ_{air} is the density of air (kg/m^3). The ventilation rate is the time it takes to replenish the volume of air in the greenhouse calculated using Equation (3.14) (Olutoye and Uthamalingam, 2012). In the equation, VR is the ventilation rate (hrs) and V_{gh} is the volume of the greenhouse (m^3).

$$V_{air} = \frac{m_{air}}{\rho_{air} \times t} \tag{3.13}$$

$$VR = \frac{V_{gh}}{V_{air}} \quad (3.14)$$

The study considered a rectangular greenhouse floor area whose length was twice the width. The volume of the greenhouse (V_{gh}) was determined according to Equation (3.15). In the equation, L is the length (m), h is the gable height (m), W is the width (m) and H is the height of the greenhouse (m).

$$V_{gh} = L((0.5 \times h \times W) + (H \times W)) \quad (3.15)$$

The drying trays were movable and the greenhouse dryer had a hinged door on the East side to facilitate loading and unloading of bananas. The height of the drying trays was ergonomically designed based on the consideration of the normal working height of an average person (Hrovatin *et al*., 2015). The loading capacity of banana slices of approximately 10 kg/m^2 with a walk-through area of 1 m across the centre of the greenhouse dryer and an inspection space of 0.5 m wide around the entire effective drying.

3.2.4. Fan and PV system design

Due to the curved nature of the heat exchanger, air flow by convection alone would not be sufficient to effectively operate the dryer. Thus, a suction fan was used to blow in ambient air which was heated by the heat exchanger. An exhaust fan was used to expel moist air from the dryer and create negative pressure for steady flow of air through the heat exchanger. The volumetric capacity of the fans was determined based on the volume of the greenhouse dryer and the maximum number of air changes

required per hour. The power requirement of the fans was calculated using Equation (3.16) (Aduewa *et al*., 2014). In the equation, V_{air} is as earlier defined, Δp is the total pressure differences across the fan (Pa) and ε_f is the total system static fan efficiency.

$$Fan\,power(w) = \frac{V_{air} \times \Delta p}{60 \times \varepsilon_f} \tag{3.16}$$

The power consumption of the fans and the data acquisition instruments were considered as the consumption demand for PV system sizing.

3.2.5. Biomass stove and heat exchanger design

The design of the biomass stove was based on the following assumptions; no mixing of flue gases with the drying air, continuous combustion of biomass will be maintained and thus handling hours will be reduced. The design basis calculations were performed depending on the amount of biomass required to generate the required amount of energy as earlier determined using Equation (3.7). The simplicity of the biomass stove was considered for easiness of fabrication and thus a square base of 400 mm by 400 mm with a height of 480 mm was selected. The biomass unit was made of clay double walls supported with a wire mesh framework for strength. The spacing between the walls was 160 mm while the outside walls had a thickness of 100 mm. The combustion compartment floor comprised of a perforated grate made of cast iron to provide a platform for fuel and ash fall in ash pit. The dimensions of the grate were 260 mm by 180 mm fitted with stands of 35 mm height. Provision for ash collection was made below the grate with an ash tray measuring 250 mm by 170 mm and a shutter fixed to enable ash removal. Moreover, the shutter enabled air flow into the combustion

compartment. A provision of 180 mm diameter for double duct heat exchanger coupling was provided on the unit as shown in Figure 3.3. Fibreglass insulation of 0.2 m thickness with aluminium cladding was used on the outer surface of the biomass heater unit and the exposed heat exchanger section to minimize heat loss to the surrounding.

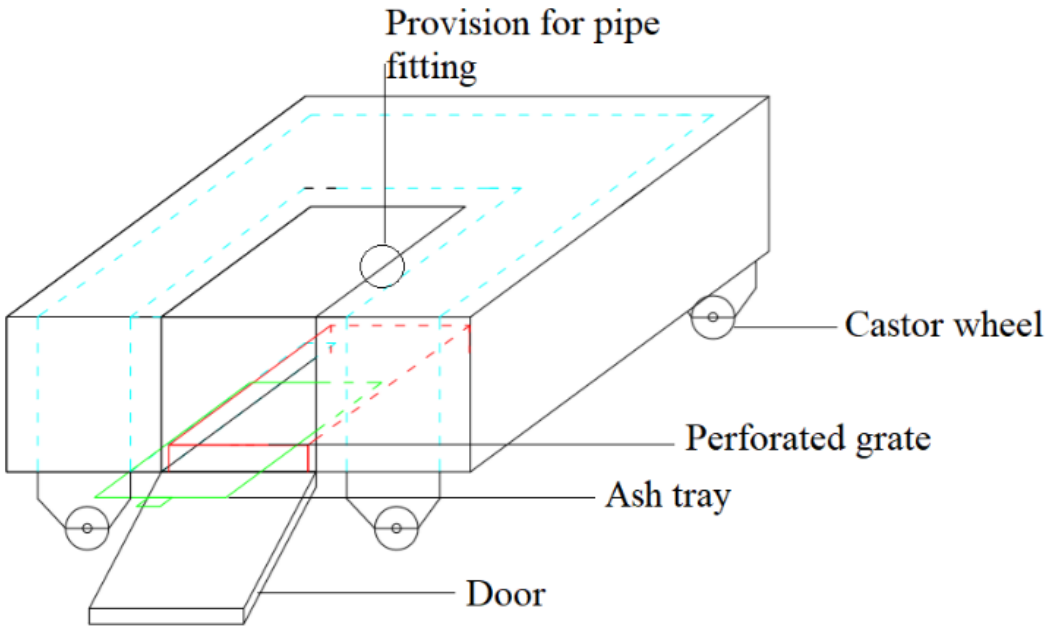

Figure 3.3: Schematic representation of the developed biomass unit.

A double duct heat exchanger was used to allow transfer of heat from the flue gases to the drying air. Figure 3.4 shows the schematic representation of the double duct heat exchanger. Some of the assumptions that were made during the design included: steady operations were maintained during drying operation, proper insulation was made and the heat loss to the surrounding was negligible, changes in kinetic and potential energies of drying air and flue gases were negligible, no fouling would occur and

drying air and flue properties would remain constant. The design of the double duct heat exchanger was guided by Equations (3.17) to (3.21) (Dependra and Jagrit, 2014).

In Equation (3.17), $\dot{Q}$ is heat transfer rate, $\dot{m}$ is mass flow rate and ΔT is change in temperature calculated from the inlet and outlet temperatures of both fluids. In Equation (3.18), ΔT_{LTD} referred to the log mean temperature difference. For Equations (3.19) and (3.20), *Nu* is the Nusselt number, *Re* is the Reynold's number, *Pr* is the Prandtl number and *f* is the friction factor. The parameters in Equation (3.21) are defined as follows: d_{ic} referred to the internal diameter of the inner duct, d_{oc} is the external diameter of the inner duct, k_p is the thermal conductivity of the duct material, h_c is the heat transfer coefficient of cold fluid (air), h_h is heat transfer coefficient of hot fluid (flue gases) and *l* is the length of duct.

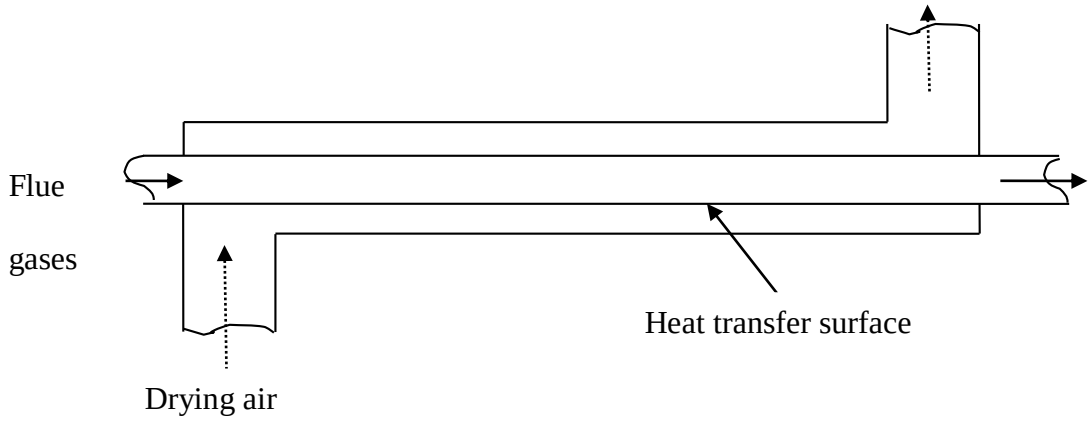

Figure 3.4: Schematic representation of the double duct heat exchanger.

$$\dot{Q} = \dot{m}\, Cp \Delta T \qquad (3.17)$$

$$\Delta T_{LTD} = \frac{\Delta T_{in} - \Delta T_{out}}{\ln(\frac{\Delta T_{in}}{\Delta T_{out}})} \tag{3.18}$$

$$Nu = \frac{\frac{f}{2}(\mathrm{Re}-1000)\,\mathrm{Pr}}{1+12.7(f/2)^{0.5}(\mathrm{Pr}^{\frac{2}{3}}-1)} \tag{3.19}$$

$$f = (1.58\ln(\mathrm{Re}) - 3.28)^{-2} \tag{3.20}$$

$$l = \frac{Qd_{ic}h_c k_p + Qd_{oc}h_h k_p + \pi Qd_{ic}d_{oc}h_c h_h \ln((\frac{d_{oc}}{d_{ic}})^{\frac{1}{2\pi}})}{\pi \Delta T_{LTD} d_{ic} d_{oc} h_c h_h k_p} \tag{3.21}$$

The length, log mean temperature difference, overall heat transfer coefficient and heat transfer were computed using MS Excel 2016™. Using goal seek function, the desired length of the heat exchanger was chosen as 10.44 m. Outlet holes on the ducts conveying drying air to the trays were designed to discharge air at velocities such that the air stream reaches the trays. The holes were spaced so that the boundaries of the adjacent air jets meet just before reaching the trays. This technique helped in reducing cold air pockets hence allowing uniform removal of moisture from the products. Positioning the holes on the upper side of the duct also allowed air flow to be directed to the drying products.

3.2.6. Performance of the developed dryer under no load

The no-load experiments were performed in November 2018. Solar and biomass modes were performed on 11th November 2018 day and night, respectively. Solar-biomass mode was performed on 19th November 2019. The hourly temperature and

relative humidity inside and outside the dryer were measured using DHT22 sensors. The DHT22 sensors are laboratory calibrated with a measurement range of 0-100% (±5percentage) for humidity and -40-125 ^{o}C (±0.2) for temperature (Tastan and Gökozan, 2019). The DHT22 sensors were placed at the ends and middle of each drying bed. Ambient temperature and humidity monitoring DHT22 sensor was securely placed 2.6 m above the ground as guided by the sensor data sheet (Mouser, 2018). Additionally, the sensor was mounted with an improvised weather shield to avoid direct exposure to sunlight. The weather shield was serrated to allow adequate flow of air around the sensor. A mercury glass thermometer was used for temperature and reading re-calibration for all the sensors. The hourly out door solar radiation and transmitted radiation in the greenhouse was measured using LDR sensors which were calibrated using an LI-200R pyrometer and placed strategically inside and outside the dryer at 2.6 m above ground level. The reading from the sensors was logged to an Arduino Mega (AT mega 2560) microcontroller which was equipped with an 8 GB storage disk. With the no load condition for solar-biomass mode, 18 kg of biomass were used to compliment the solar energy available for drying while for biomass mode, 26 kg of biomass was used. Graphs relating inside and outside solar radiation, air temperature and relative humidity for the respective modes were plotted. The average hourly temperature gain for the different energy modes was statistically compared using one- way ANOVA. The Least Significant Difference (*LSD*) value was used to determine significant differences between means and to separate means at $p \leq 0.05$. An independent-samples Student's *t*-test was performed to compare the drying air

temperature and ambient air temperature for each energy mode. These analyses were carried out using MS Excel 2016™.

3.3. Exergy Analysis of the Developed Solar-Biomass Greenhouse Dryer

3.3.1. Experimental design

Mature green bananas at stage 1 of ripening (all green) of four varieties namely Apple Banana (*Musa sapientum*) (Sweet banana), Gros Michel AAA (*Musa acuminata*) (AAA Group) (Kampala), Kiganda AAA (*Musa acuminata* (AAA-EA)) and Muraru AAA (*Musa AA* "*Muraru*") were used in this study. These bananas were selected based on their uses and availability. They were obtained from identified banana farmers in Kiambu and Murang'a Counties, Kenya. Identification of farmers from these counties ensured that the bananas were sourced from matching locations sharing similar agro-climatic zone (UM2) and cultural practices, thus it was assumed that the bananas were subjected to similar cultivation practices (Kabubo and Mulwa, 2019; Narayana *et al.*, 2017). The study considered peeled and unpeeled bananas as the sub-plots. Sub-sub-plots included three different banana slice thicknesses (2, 3 and 4 mm). The thicknesses were selected to be in a range of optimum slice thickness recommended for thin layer drying (Krishnan and Sivaraman, 2017; Wakjira *et al.*, 2011, Swasdisevi *et al*., 2007). The drying was conducted using three different modes of energy sources for the greenhouse dryer (solar, biomass and solar-biomass). The control for the study was drying the product under the open sun. The experimental research design for each of the modes used in the study comprised of 4×2×3 factorial experiment under a

randomized complete block design. The simplified experimental research design was as shown in Table 3.2. For each treatment data collected was in quadruplicate.

Table 3.2: Experimental research design.

Banana variety	Peeling	Thickness	Source of energy			
			Combined	Biomass	Solar	Control
Apple Banana	Peeled	2.0				
		3.0				
		4.0				
	Unpeeled	2.0				
		3.0				
		4.0				
Gros Michel (AAA)	Peeled	2.0				
		3.0				
		4.0				
	Unpeeled	2.0				
		3.0				
		4.0				
Kiganda AAA	Peeled	2.0				
		3.0				
		4.0				
	Unpeeled	2.0				
		3.0				
		4.0				
Muraru AAA	Peeled	2.0				
		3.0				
		4.0				
	Unpeeled	2.0				
		3.0				
		4.0				

3.3.2. Sample procurement and preparation

The bananas were harvested and transported to the experimental site with great care to minimize any mechanical injuries. On reception, the bananas were inspected for any physical damage and only healthy ones were selected and washed in clean water to remove any dirt on them. For the pulp drying, bananas samples were hand peeled using a clean stainless steel kitchen knife and sliced into the required thickness using a hand-

held mechanical slicer. For unpeeled treatments, the bananas were also sliced as for the above procedure, without peeling. During slicing, the samples were dipped in pre-treated water which constituted 0.5% (w/v) sodium meta-bisulphite and 0.5% (w/v) salt solution for 5 minutes. This treatment was necessary for both peeled and unpeeled banana samples to reduce enzymatic browning and microbial growth (Islam *et al*., 2012). The sodium meta-bisulphite was food grade and conformed to BP and USP standards. The samples were removed from the treating water using a colander and were allowed to freely drain as much water as possible. Excess moisture on the surface of the banana slices was drained using paper towels. The prepared samples were then weighed in lots of 500 g using a high precision balance (HZT-A 200, China) with a precision of ±0.01 g. These samples were immediately loaded on the drying trays in a thin layer for drying. Each drying tray was divided into 24 equal parts and each part randomly held one treatment. The parts were labelled with the respective treatment before placing the samples on them.

3.3.3. Data collection procedure

The experiments in the greenhouse dryer were spread from November 2018 to February 2019. Solar drying and open sun drying (control) were performed on 31st January 2019 from 8.00 am to 6.00 pm. Biomass mode only was performed during the night of 6th February 2019 from 8.00 pm to 6.00 am when there was no solar radiation. The experiment for combined solar-biomass mode was performed on a relatively overcast day that experienced intermittent rain (20th November, 2018) from 8.00 am to 6.00 pm. A 10-hour drying period was considered appropriate for purposes of

analysis as carrying on with biomass mode on two consecutive nights was not feasible. The limit was preserving the large quantities of samples involved. Samples dried using solar and solar-biomass modes were monitored in the consecutive day for all the parameters. To ensure continuity of the data collection, the fans were switched off and the door secured from 6.00 pm to 8.00 am the following day. Weight reduction was monitored using a high precision balance (HZT-A 200, China) with a precision of ±0.01 g. Hourly temperature and humidity readings were collected as described in Section 3.2.6. Duct surface temperature for the heat exchanger was recorded using ASSTech professional series high-temperature infra-red thermometer (ST677, South Africa). Before the start of the experiment a hot wire anemometer (TES 1340, Taiwan) with a precision of ±3%+ 0.20 m/s was used for air flow calibration. All data collection commenced immediately the samples were loaded in the dryer.

The initial and final moisture content of the banana slices for both peeled and unpeeled was determined using the constant temperature oven method set at 105^{o}C for 24 hours as described by the Association of Official Analytical Chemists (AOAC) (2010). During drying, the weight of the banana slices was recorded at a three-hour interval using an electronic balance (HZT-A 200, China) with a precision of ±0.01 g. For the biomass mode, the biomass stove was initially loaded with 4 kg of briquettes and later on topped up at an average rate of 1.8 kg per hour. The hourly instantaneous moisture content was determined using Equation (3.1). The drying rate of banana slices for each mode was determined according to Equation (3.22). In the equation, *DR* is the drying rate of banana slices (g/gdm/hour), W_w is the amount of moisture removed (g), W_p is

the quantity of product (bananas) to be dried (g), W_{dm} is the total bone dry weight of a sample (g), T is the time of drying (hours) and M_o is the initial moisture content (% wb).

$$DR = \frac{W_p(M_o - M)}{TW_{dm}(100 - M)} \tag{3.22}$$

Graphs relating inside and outside solar radiation, air temperature and relative humidity for the respective modes were plotted. Additionally, a graph relating drying rate and time for the different energy modes was also plotted.

3.3.4. Energy and exergy analysis

The hourly energy input in the solar-biomass hybrid dryer for solar, biomass and solar-biomass modes was determined using previous Equations (3.5), (3.7) and (3.9), respectively. The useful heat gained by the drying air from the solar radiation was determined according to Equation (3.23) (Panwar *et al*., 2013). In the equation, $E_{u(da)}$ is useful heat gain (W), m_a is the mass flow rate of drying air (kg/s), C_{pa} is the specific heat capacity of air (J/kgK), T_a and T_{da} are ambient and drying air temperatures, respectively (K).

$$E_{u(da)} = \dot{m}_a C_{pa}(T_{da} - T_a) \tag{3.23}$$

Energy efficiency (η_e) was computed according to Equation (3.24) (Panwar *et al*., 2013). In addition, the energy utilization ratio (*EUR*) of the dryer which is given as a ratio of magnitudes of heat utilization by the system to useful heat gained was

evaluated according to Equation (3.25). In the equation, T_{ea} is the exit air temperature (K), which was determined using the psychometric chart.

$$\eta_e = (\frac{Useful\ enegy}{energy input}) \times 100 \quad (3.24)$$

$$EUR = \frac{\dot{m}_a C_{pa}(T_{da} - T_{ea})}{\dot{m}_a C_{pa}(T_{da} - T_a)} \quad (3.25)$$

Exergy analysis is based on the second law of thermodynamics and represents a measure of useful work performed by a thermodynamic system. Exergy is thus considered as the total energy minus the corresponding entropy multiplied by the absolute temperature of ambient air (Michel, 2019). The exergy input in a system represents the maximum useful energy supplied to the system that results into a change of the thermodynamic properties of the system or material within the surrounding system. Thus, hourly exergy input, $Ex_{rad(input)}$ and output, $Ex_{rad(output)}$ (W) due to solar radiation in the greenhouse dryer was determined using Equations (3.26) and (3.27), respectively. In the equation, T_s is the sky temperature (K) adopted from literature (Panwar *et al.*, 2013).

$$Ex_{rad(input)} = E_{in(s)}[1 - \frac{4}{3} \times (\frac{T_a}{T_s}) + \frac{1}{3} \times (\frac{T_a}{T_s})^4] \quad (3.26)$$

$$Ex_{rad(output)} = E_{u(s)}[1 - (\frac{T_a}{T_{da}})] \quad (3.27)$$

The hourly exergy input for the biomass mode, $Ex_{b(input)}$, (W) and exergy transfer accompanying heat transfer for biomass mode, $Ex_{b(output)}$ (W) were determined using

Equations (3.28) and (3.29), respectively (Sethi and Dhiman, 2020; Kazanci *et al.*, 2016). In the equation, ε is the emissivity coefficient of the duct material, σ is the Stefan-Boltzmann constant (W/m^{2}K^4), A_d is the duct surface area (m^2) and T_{dst} denotes the duct surface temperature (K).

$$Ex_{b(input)} = \varepsilon\sigma A_d (T_{dst}{}^4 - T_{da}{}^4)(1 - (\frac{T_{da}}{T_{dst}}) + \dot{m}_{da} C_{pa} (T_{dad} - T_{da}) - T_a \ln(\frac{T_{dad}}{T_{da}}) \quad (3.28)$$

$$Ex_{b(output)} = E_{u(b)} (1 - (\frac{T_a}{T_{da}})) \quad (3.29)$$

The exergy input for combined solar-biomass mode, $Ex_{s\text{-}b(input)}$ (W) and exergy output, $Ex_{s\text{-}b(output)}$ (W) were determined according to Equations (3.30) and (3.31), respectively (Panwar *et al.*, 2013).

$$Ex_{s-b(input)} = Ex_{rad(input)} + Ex_{b(input)} \quad (3.30)$$

$$Ex_{s-b(output)} = Ex_{rad(output)} + Ex_{b(output)} \quad (3.31)$$

The hourly exergy potential of the drying air inside the dryer, $Ex_{inside(da)}$ (W) and hourly exergy of the exhausted air $Ex_{out(ea)}$ (W) were determined according to Equations (3.32) and (3.33), respectively (Abhay *et al.*, 2019).

$$Ex_{inside(da)} = \dot{m}_a C_{pa} ((T_{da} - T_a) - T_a \ln(\frac{T_{da}}{T_a})) \quad (3.32)$$

$$Ex_{out(ea)} = \dot{m}_a C_{pa} ((T_{ea} - T_a) - T_a \ln(\frac{T_{ea}}{T_a})) \quad (3.33)$$

The general form of exergy efficiency (η_{ex}) was adopted for all energy modes given in Equation (3.34).

$$\eta_{ex} = \frac{Exergy\,output}{Exergy\,input} \times 100 \tag{3.34}$$

Graphs of energy efficiency, energy utilization and exergy efficiency against time were plotted in MS Excel 2016™. Energy and exergy flow diagrams were used to further visualize the results. ANOVA was used to determine whether there was any statistical difference between the exergy efficiency for the three energy modes.

3.4. Optimization of the Developed Solar-Biomass Greenhouse Dryer

3.4.1. Development of optimization functions

To develop comprehensive relationships for objective functions for each drying mode, the system was linearized around drying air and exit air temperatures. This is because linear functions help in understanding the models and are usually faster and easier to solve than non-linear equations. The coefficients of linearity for each energy mode were identified by reformulating the energy and exergy equations outlined in Section 3.3.4. Similarly, other scholars have adopted the concept of linearizing the system around its operating points in their study (Zoukit *et al*., 2018). Additionally, writing the linear functions helps in understanding the models and implement them efficiently in a high-level programming language.

Solar radiation was the main input parameter influencing the drying air temperature for solar mode drying. Thus, a linear relationship between solar radiation, I_s (W/m^2)

and drying air temperature, T_{da} (K) was obtained as shown in Equation (3.35), where k represents the slope of a linear graph given by Equation (3.36). In the equation, $\eta_{e(s)}$ is energy efficiency of the dryer in solar mode. Other researchers (Manyumbu *et al*., 2014; Condori and Saravia, 2003) generated a similar simplified relationship.

$$T_{da} = kI_s + T_a \tag{3.35}$$

$$k = \frac{\eta_{e(s)} \tau A}{\dot{m}_a C_{pa}} \tag{3.36}$$

To determine output relation for solar mode, exhaust air temperature T_{ea} (K) was expressed as a function of drying air temperature (T_{da}) as given in Equation (3.37). The equation shows a linear relationship relating T_{ea} to T_{da} with a slope of unity.

$$T_{ea} = T_{da} - EUR \times (T_{da} - T_a) \tag{3.37}$$

Substituting Equations (3.35) to (3.37) into Equations (3.32) and (3.33) then Equation (3.34) can be rearranged to yield Equation (3.38).

$$\eta_{ex(s)} = \frac{k_s I_s (1 - EUR) - T_a \ln(\frac{k_s I_s (1 - EUR) + T_a}{T_a})}{k_s I_s - T_a \ln(\frac{k_s I_s + T_a}{T_a})} \tag{3.38}$$

During biomass mode (night hours), the main input parameter influencing the drying air temperature was the ambient air temperature. Variation in ambient air temperature during the night influences the heating requirement in the dryer (Sethi and Dhiman 2020). Therefore, the drying air temperature, T_{da} (K) was expressed as a function of

ambient air T_a (K) as shown in Equation (3.39). The intercept, C_b of the linear graph of given by Equation (3.39) is further expressed as shown in Equation (3.40). Exhaust air temperature, T_{ea} was expressed as shown by Equation (3.41).

$$T_{da} = T_a + C_b \tag{3.39}$$

$$C_b = \frac{\dot{m}_f \, \eta_{e(b)} H_v \eta_{stove}}{\dot{m}_a \, C_{pa}} \tag{3.40}$$

$$T_{ea} = T_a + C_b - (C_b \times EUR) \tag{3.41}$$

Substituting Equations (3.39) to (3.41) into Equations (3.32) and (3.33) then Equation (3.34) can be rearranged to yield Equation (3.42).

$$\eta_{ex(b)} = \frac{(C_b(1-EUR)) - T_a \ln(\frac{T_a + C_b(1-EUR)}{T_a})}{C_b - T_a \ln(\frac{T_a + C_b}{T_a})} \tag{3.42}$$

During solar-biomass mode, the main input parameters influencing the drying ambient air temperature were the solar radiation, ambient air temperature and biomass heat supply. Equation (3.43) show the linear relation as a result of this combination. In the equation, k_s and $C_{s\text{-}b}$ are constants representing slope and intercept of the plot, given by Equations (3.44) and (3.45), respectively.

$$T_{da} = k_s I_s + C_{s-b} \tag{3.43}$$

$$k_s = \frac{\eta_{e(s-b)} \tau A}{\dot{m}_a C_{pa}} \tag{3.44}$$

$$C_{s-b} = \left(\frac{\dot{m}_f \eta_{e(s-b)} H_v \eta_{stove}}{\dot{m}_a C_{pa}}\right) + T_a \tag{3.45}$$

To get all the variables from the linearization of Equation (3.43), part of the equation was further simplified as shown in Equation (3.46). In the equation, k_s represents the slope of a linear graph of ΔT against I_s.

$$\Delta T = k_s I_s + C_b \tag{3.46}$$

To determine output relation for solar-biomass mode, exhaust air temperature T_{ea} (K) was expressed as given in Equation (3.47).

$$T_{ea} = (1 - EUR)(k_s I_s + C_b) + T_a \tag{3.47}$$

Substituting Equations (3.43) to (3.467 into Equations (3.32) and (3.33) then Equation (3.34) can be rearranged to yield Equation (3.48).

$$\eta_{ex(s)} = \frac{(k_s I_s + c_b)(1 - EUR) - T_a \ln\left(\frac{(k_s I_s + c_b)(1 - EUR) + T_a}{T_a}\right)}{(k_s I_s + c_b) - T_a \ln\left(\frac{k_s I_s + c_{sb}}{T_a}\right)} \tag{3.48}$$

The constants of each linear model were determined using experimental data analysed in Section 3.3 and plotting the graphs in MS Excel 2016^{TM}. The developed exergy efficiency functions suitability in the relations were verified by comparing their values with computed values of the thermodynamic properties of the greenhouse dryer.

3.4.2. Optimization of the dryer using genetic algorithm

The Pareto front for the optimization problem for each drying mode was generated using an elitist non-dominated sorting genetic algorithm (NSGA II) implemented in jMetal Development Suite (jMetal 5.7). This jMetal software is a Java-based framework for multi-objective optimization using metaheuristics. To use jMetal suite, coding was achieved by the use of Eclipse Mars 2 installed with jdk8u221 and by setting properly the algorithms by modifying the available code (Durillo and Nebro, 2011). The flowchart for NSGA-II is shown in Figure 3.5. NSGA II requires a start with a given initial population (N) using random number generator within the specified constraints then algorithm applies genetic operators' tournament selection, crossover and mutation to obtain a new population (offspring). The old and new populations are combined and sorting is done using a non-dominance criterion. The ranks and crowding distance (density of individuals surrounding a particular one) are used to guide the selection (Florea *et al*., 2016). The population size was 100 solutions with a distribution index of 20 and a crossover probability of 0.9. The method implements a polynomial mutation operator with a distribution index of 20 and a mutation probability of 1/number of decision variables. The selection process used a binary tournament selection method. A stopping criteria was also specified at 500 generations if the optimizer failed to converge.

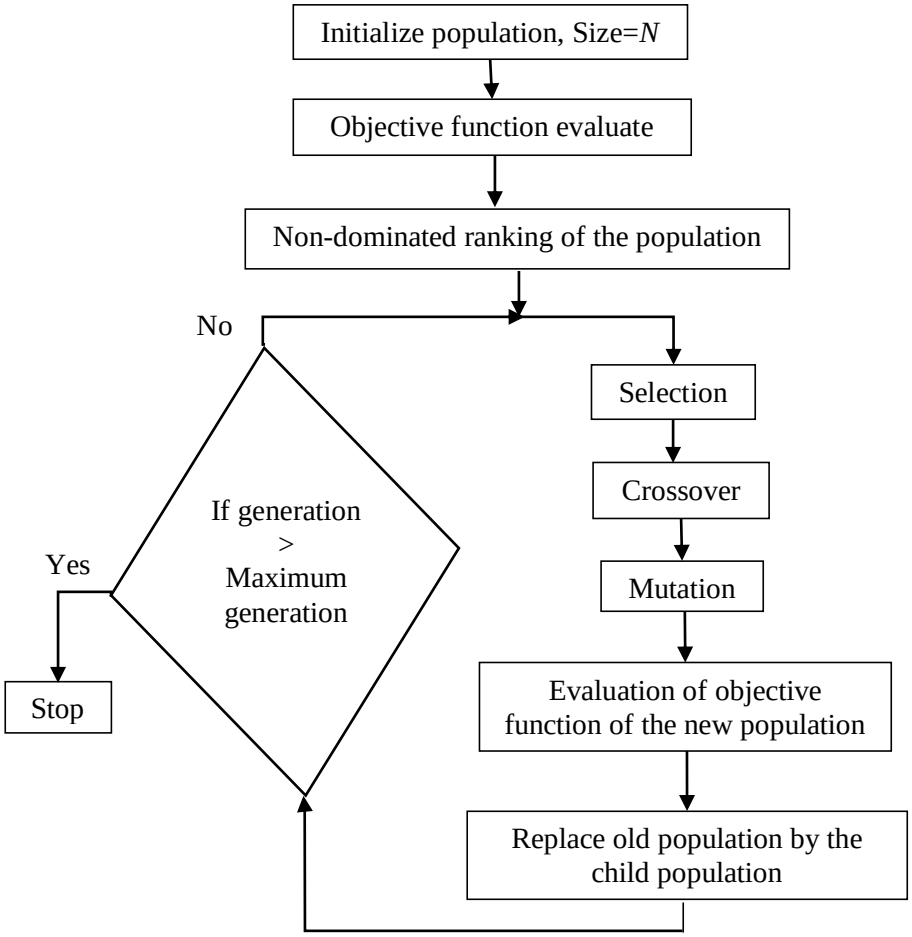

Figure 3.5: Flow diagram for NSGA II.

Adapted from Buditjahjanto *et al*. (2011).

To achieve the objective of maximizing exergy efficiency for solar mode, the drying air temperature, ambient air temperature and mass flow rate of drying air were used as decision variables. Additionally, other variables in the equation were assigned optimal values. The objective functions were to maximize T_{da} and η_{ex} in Equations (3.34) and (3.37), respectively. The area of the dryer, A, and cover optic properties, τ, was kept constant during optimization. However, solar radiation, I_s, was assigned a value of 300 W/m^2 for any feasible drying to occur by solar drying. Rani and Tripathy (2020)

recognized that solar radiation of below 350 W/m^2 led to lower moisture removal hence one cannot exclusively rely on solar drying. The upper limit for the drying air temperature (333 K) corresponded with the recommended safe drying temperature for banana slices (Alagbe *et al*., 2020; Aduewa *et al*., 2014). An assumption made was that at the start of drying, air temperature inside the greenhouse was equal to ambient air temperature due to thermal equilibrium. Thus, a lower limit for the drying air temperature corresponded with the minimum ambient temperature values determined for each energy mode. Other parameter boundaries and constraints were obtained from the linearized graphs described in Section 3.4.1. Additionally, ambient air temperature was adjusted to match the weather conditions for each energy mode without temperature overlap. The solar mode was assigned an ambient temperature boundary that heating demand could be met through solar energy. Solar-biomass was assigned ambient temperature range that heating demand required supplementation from biomass heat. Likewise, biomass mode was assigned a minimum value that represented the least temperature reading recorded during the study. Thus, the optimization functions, boundaries and constraints for the solar energy mode were as shown in Equations (3.49) to (3.52).

$$Maximize\ objective\ function = (3.35)\ and\ (3.38)$$

$$Such\ that = \begin{bmatrix} 305 \le T_{da} \le 333 \\ 305 \le T_a \le 313 \\ 0.01 \le \dot{m}_a \le 0.05 \\ 0.5 \le EUR \le 1.0 \\ 0 \le \eta_{ex(s)} \le 1.0 \end{bmatrix} \tag{3.49}$$

And;

$$g_1 = \frac{\eta_{e(s)} \tau A}{\dot{m}_a C_{pa}} - 0.027 \geq 0 \tag{3.50}$$

$$g_2 = T_{da} - T_a - 12.69 \geq 0 \tag{3.51}$$

$$g_3 = \eta_{ex(s)} - 1.0 \geq 0 \tag{3.52}$$

For biomass mode, the optimization functions, boundaries and constraints were as shown in Equations (3.53) and (3.54).

$$Maximize\ objective\ function = (3.39)\ and\ (3.42)$$

$$Sucht\ that = \begin{bmatrix} 284 \leq T_a \leq 305 \\ 0.001 \leq \dot{m}_f \leq 0.0006 \\ 0.01 \leq \dot{m}_a \leq 0.05 \\ 0.5 \leq EUR \leq 1.0 \\ 0 \leq \eta_{ex(b)} \leq 1.0 \end{bmatrix} \tag{3.53}$$

And;

$$g_1 = 333 - (T_a + C_b) \geq 0 \tag{3.54}$$

During the combined solar-biomass mode optimization, the maximum available solar radiation was assumed to be 300 W/m^2. The optimization functions, boundaries and constraints were as shown in Equations (3.55) to (3.58).

$$Maximize\ objective\ function = (3.43)\ and\ (3.48)$$

$$Such\ that = \begin{bmatrix} 295 \le T_a \le 305 \\ 295 \le T_{da} \le 333 \\ 0.001 \le \dot{m}_f \le 0.0006 \\ 0.01 \le \dot{m}_a \le 0.05 \\ 0 \le I_{s-b} \le 300 \\ 0 \le \eta_{ex(b)} \le 1.0 \end{bmatrix} \tag{3.55}$$

And;

$$g_1 = \frac{\eta_{e(s)} \tau A}{\dot{m}_a C_{pa}} - 0.027 \ge 0 \tag{3.56}$$

$$g_2 = T_{da} - T_a - 38 \le 0 \tag{3.57}$$

$$g_3 = C_b - 5.56 \ge 0 \tag{3.58}$$

3.4.3. Performance of the developed solar-biomass greenhouse dryer after optimization

Experiments for each mode were performed with the chosen optimized parameters. Before the experiment, the greenhouse cladding was meticulously cleaned to minimize the effect of dirt and dust accumulation on the transmittance of the cladding material. Cleaning the dirt and dust accumulation is acknowledged to restore the solar radiation transmissivity of cladding films by up to 99% (Sangpradit, 2014). Additionally, the floor was repainted black to enhance heat absorption and radiation inside the greenhouse dryer. The data collected from independent experiments were computed as in section 3.3.2. The optimum parameters from the GA were compared with the

experimental data in tabular format. The level of adequacy of the actual data against the model parameters was determined using Equation (3.11) as presented in Section 3.1.2. In addition, the data obtained from the study was compared to the un-optimized data in Section 3.3.4 statistically using one-way ANOVA. The *LSD* value was used to determine significant differences between means and to separate means at $p \leq 0.05$. These analyses were carried out using MS Excel 2016™.

3.5. Effect of Drying on Nutritive and Organoleptic Properties of Bananas Slices

3.5.1. Data collection procedure

During the procedure described in Section 3.3.3, measurements of colour, firmness and vitamin C were determined on fresh and dried banana slices. During the experiments after optimization, changes in colour, firmness and vitamin C content were also determined for comparison. The data obtained from the study were statistically subjected to a one-way analysis of variance (ANOVA). The *LSD* value was used to determine significant differences between means and to separate means at $p \leq 0.05$. These analyses were carried out using MS Excel 2016™.

3.5.2. Determination of colour change in banana slices during drying

A colourimeter (BCM-200, BIOBASE, Shandong, China Mainland) with a measuring aperture of diameter 8 mm and D65 light source was used for colour measurements. The colourimeter was set in CIE L*a*b* colour space display mode to determine the values of *L*, a* and b**. The parameters *L*, a* and b** represented the degree of

lightness to darkness, degree of redness to greenness and degree of yellowness to blueness, respectively. The colourimeter was calibrated using a white base provided with the instrument before the actual measurements were taken. During measurement, care was taken so as not to leak the light thrown from the colourimeter. For consistency in colour monitoring, the same samples were monitored throughout the drying process.

The values of *L*, a* and b** for the banana slices during drying were presented in tabular form. The total colour difference of the dried banana slices (ΔE^*) was determined by comparing the colour of dried banana slices to the fresh slices as presented in Equation (3.59) (Wrolstad and Smith, 2017). In the equation, L_0^*, a_0^* *and* b_0^* are the values of fresh banana slices (Amankwah *et al.*, 2019).

$$\Delta E^* = \sqrt{(L_0^* - L^*)^2 + (a_0^* - a^*)^2 + (b_0^* - b^*)^2}^2 \quad (3.59)$$

The hue angle (h^*) is a colour attribute that is associated with the dominant wavelength in a mixture of wavelengths hence representing the dominant colour as perceived by the human eye. Thus in the 360^o colour space 90^o is yellow, 180^o is green, 270^o is blue and 0^o is red. The hue angle was computed according to Equation (3.60) and consideration of the quadrant the readings were (Wrolstad and Smith, 2017).

$$h^* = tan^{-1}(\frac{b*}{a*}) \quad (3.60)$$

3.5.3. Determination of firmness in banana slices during drying

The firmness of fresh and dried banana slices was determined using a penetrometer (Compact-100, Sun Scientific Co. LTD, Japan) with an operation mode of maximum force of 10 kg at a distance of 1.5 mm and a constant head speed of 5 mm/s (Maina *et al.*, 2019). The probe was allowed to penetrate the sample to a depth of 3 mm and the corresponding force required to penetrate this depth was determined. The firmness value was expressed by force in Newtons (N).

The average and standard deviation for the firmness values for the banana slices during drying were also presented in tabular form. An increase in firmness of banana slices as a result of drying was computed using Equation (3.61). In the equation, ΔF is the increase in firmness, F_f is the firmness of fresh banana slice (N) and F_d is the firmness of dried banana slice (N).

$$\Delta F(\%) = \frac{F_d - F_f}{F_f} \times 100 \tag{3.61}$$

3.5.4. Determination of vitamin C in banana slices during drying

Vitamin C content of fresh and dried banana slices was determined by indophenol titration procedure defined by AOAC (2010) method. The titration was performed in triplicate and the average value of the titre recorded. The amount of vitamin C content (mg/100g) was determined using Equation (3.62) as described by the vitamin C testing procedure (AOAC, 2010). In the equation, T is the titre value (ml), c is the dye factor,

v is the volume made (ml), *l* is the volume of sample aliquot titrated (ml) and *s* is the sample weight (g).

$$Vitamin\ C\ (mg/100\ g) = (\frac{T \times c \times v}{l \times s}) \times 100 \quad (3.62)$$

The percentage retention of vitamin C during drying of banana slices was computed by Equation (3.63). In the equation, C_f is the vitamin C content of fresh banana slice (mg/100g) and C_d is the vitamin C content of dried banana slice (mg/100g) (Sanusi *et al.*, 2018).

$$Retention\ of\ vitamin\ C\ (\%) = \frac{C_d}{C_f} \times 100 \quad (3.63)$$

CHAPTER FOUR

RESULTS AND DISCUSSION

4.1. Empirical Models for Estimating Drying Time in a Solar-Biomass Greenhouse Dryer Operated using Different Energy Modes

4.1.1. The developed simulation models

A computer model was developed using Java to empirically simulate the drying heat available, estimated drying time, drying temperature and existing ambient conditions using different energy modes considered in the study as detailed in Section 3.1.1. A free and open source software, Eclipse Kepler (4.3) installed with a Java Platform SE binary (jdk-8u202-windows-x64) from Oracle corporation was used to develop the models.

Figure 4.1 shows a graphical user interface for the developed computer simulation model for computing drying time using the different energy modes. In this figure, input parameters were entered into the model in their corresponding check boxes and the output parameters were computed as guided by Equations (3.1) to (3.10), respectively, by selecting the respective mode and clicking the compute button.

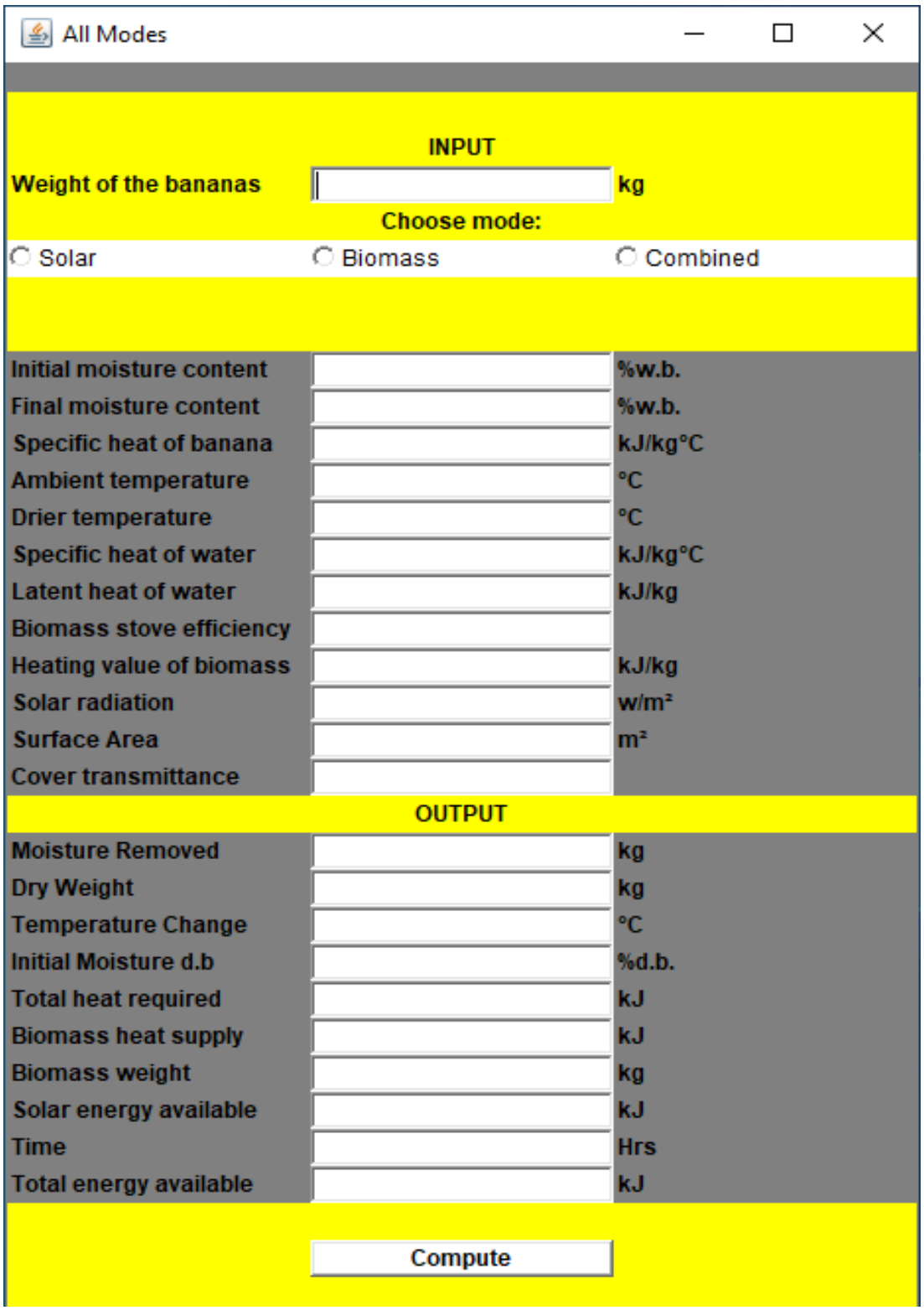

Figure 4.1: Graphical user interface of the developed models showing the input and output parameters.

4.1.2. Validation of the developed simulation models

The code for the simulation model and variable data used in model validation for different energy modes are given in Appendix I. Figures 4.2 to 4.4 present scatter diagram of predicted drying time against actual drying time for the three energy modes. The figures show that the predicted drying time increased as the actual drying time increased. In addition, the figures show that the relationship between the simulated and actual data is linear. The linear regression equations comparing actual data to predicted data had a coefficient of determination (R^2) of 0.8099, 0.5393 and 0.8845 for solar, biomass and solar-biomass modes, respectively. The value of R^2 was high for solar and solar-biomass mode indicating a strong correlation between the predicted data and actual data in these two modes. This is consistent with the observation of Kituu *et al*. (2010) and Butts *et al*. (2004). The results of Student's *t*-test did not show existence of any significance difference (t_{stat} = 0.66; $t_{crit,\ 5\%}$ = 2.04 and t_{stat} = 0.21; $t_{crit,\ 5\%}$ = 2.02) between predicted and actual data for solar and solar-biomass mode respectively, rejecting null hypothesis (a) on basis of solar and solar-biomass modes. However, the results of the Student's *t*-test for biomass mode (t_{stat} = 7.83; $t_{crit,\ 5\%}$ = 2.02) showed a significant difference between the predicted and actual data challenging the null hypothesis (a) on basis of biomass mode. These results suggested that the models prediction of drying time was good for solar and solar-biomass mode and performed dismally in biomass mode. This was attributed to the design assumptions made for biomass mode. During the drying using solar and solar-biomass modes the heating of ambient air was cumulative whereas, for biomass mode the cooling effect was cumulative.

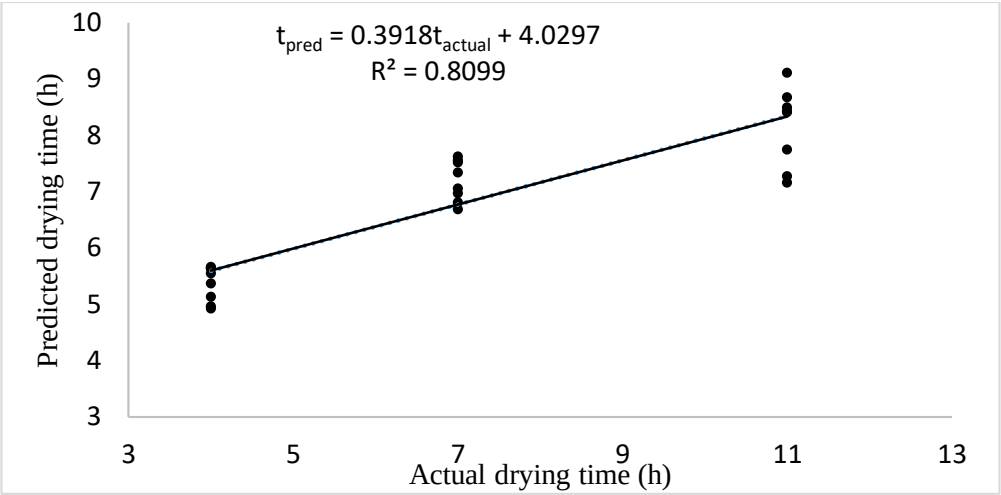

Figure 4.2: Scatter plot of model simulated drying time versus actual drying time for solar mode.

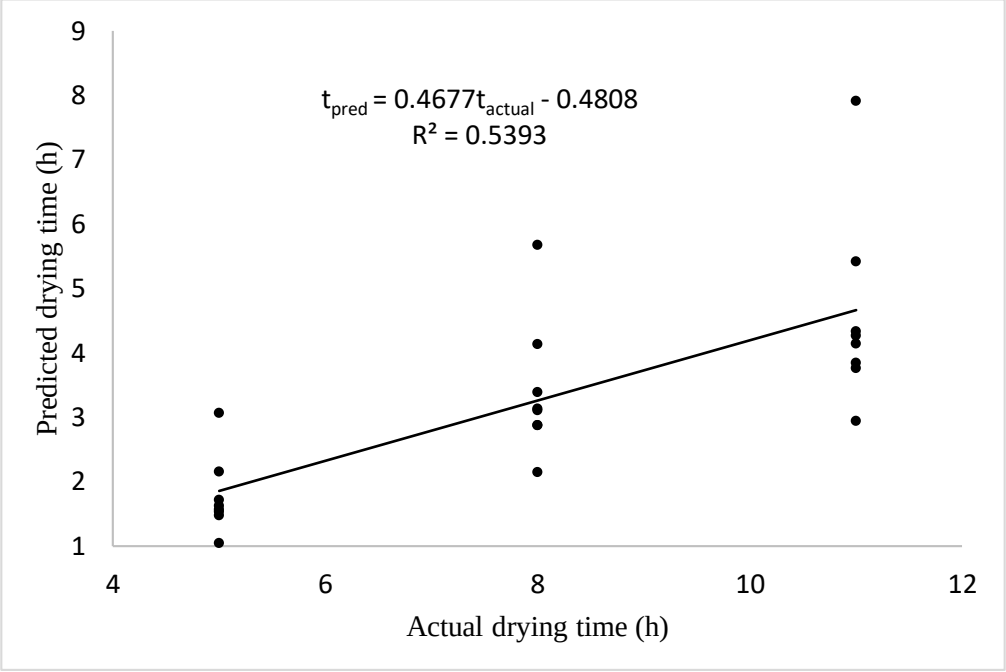

Figure 4.3: Scatter plot of model simulated drying time versus actual drying time for biomass mode.

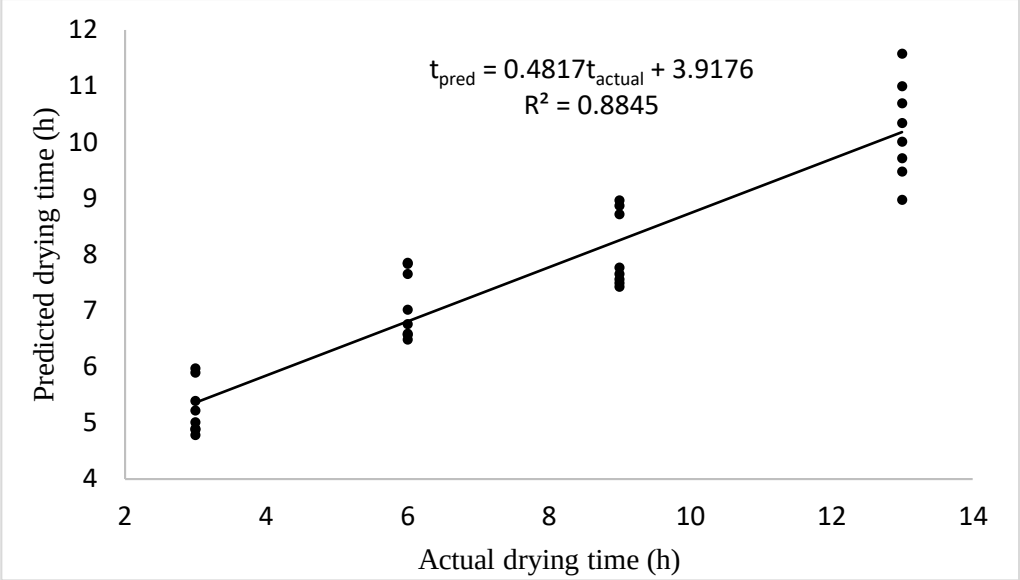

Figure 4.4: Scatter plot of model simulated drying time versus actual drying time for solar-biomass mode.

Percentage error between the predicted and actual drying time for solar only, biomass only and solar-biomass was found to be 9.09, 45.45 and 3.22%, respectively. At night, there is no solar radiation hence the temperature of ambient air decreases and relative humidity increases. Thus, biomass mode may have performed poorly due to high heat losses due to conduction, convection, thermal radiation and air exchange at night. Moreover, infiltration load was high due to wind pressure outside the greenhouse, which forces air to infiltrate through and around the door. The cold air that rushes through the door due to opening and closing during data monitoring also increased the heating requirement. Mesmoudi *et al.* (2010) observed a similar phenomenon that the temperature difference between inside and outside air in a greenhouse decreases with increasing wind speed in a nonlinear relationship. The authors further noted that the

influence of wind speed on the temperature difference between inside and outside air is countered by solar radiation on a sunny day under similar conditions. In general, these analyses indicate that reasonable estimates of drying time can be achieved by using the developed models.

4.2. The Developed Hybrid Solar-Biomass Greenhouse Dryer

Figure 4.5 (a) and (b) show the developed dyer and inside view of the dryer, respectively. More figures of the developed solar-biomass dryer are given in Appendix II. The economic analysis of the dryer was performed and reported in Kiburi *et al*. (2020). The capital cost of the dryer was found to be 600,000 Kenya shillings. Additionally, the payback period of the dryer was found to be less than 1 year which is lower than the life span of the dryer (4 years).

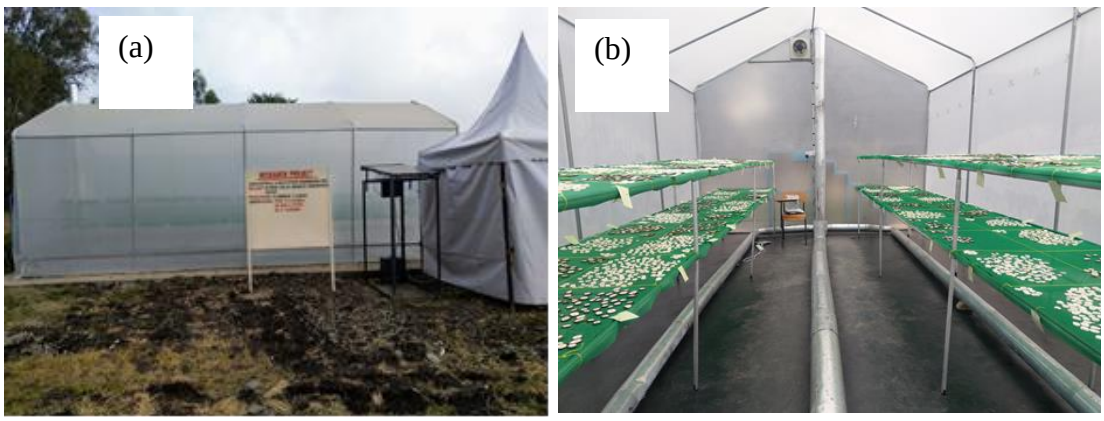

Figure 4.5: (a) The developed hybrid solar-biomass greenhouse dryer and (b) inside view of the greenhouse dryer with the drying banana slices.

Figure 4.6 shows the variation of temperature, relative humidity and solar radiation for the solar mode with the no load conditions. The experiment was selected to be performed during dry season on a clear sky when the study site experiences high solar radiation so as to have ideal conditions for solar mode drying. The average hourly ambient temperature increased with increasing solar radiation and then decreased in the evening as the solar radiation decreased. Additionally, the average hourly relative humidity of ambient air decreased with an increase in time due to increased solar radiation. After 5.00 pm the relative humidity started increasing due to low solar radiation. Similar behaviour was observed with inside relative humidity. However, inside relative humidity was lower than outside as a result of temperature rise in the greenhouse. Additionally, outside solar radiation was higher than recorded inside radiation. This was attributed to the optic properties of the glazing material used. These observations are in agreement with observations made by Yassen *et al.* (2014) and Almuhanna (2012). The maximum solar radiation was recorded between 12.00 and 3.00 pm with a correspondingly high value of 728.48 W/m^2. The trend observed with solar radiation was comparable to what is expected on a clear sky day in the tropics. The average hourly solar radiation from 8.00 am to 6.00 pm was 406.11±265.10 W/m^2 and the dryer had an average inside temperature of 48.97±12.24^{o}C with a corresponding ambient temperature average of 32.36±6.98^{o}C. It was clear that solar radiation greatly influenced drying air temperature and relative humidity as increase in solar radiation (8.00 am to 3.00 pm) resulted in an increase drying air temperature and decrease in relative humidity. After 3.00 pm the solar radiation started decreasing as it approached sunset and thus the drying air temperature decreased while relative

humidity increased. Observations of similar magnitudes were made by other scholars (Ayyappan, 2018; Yassen *et al.*, 2014; Almuhanna, 2012).

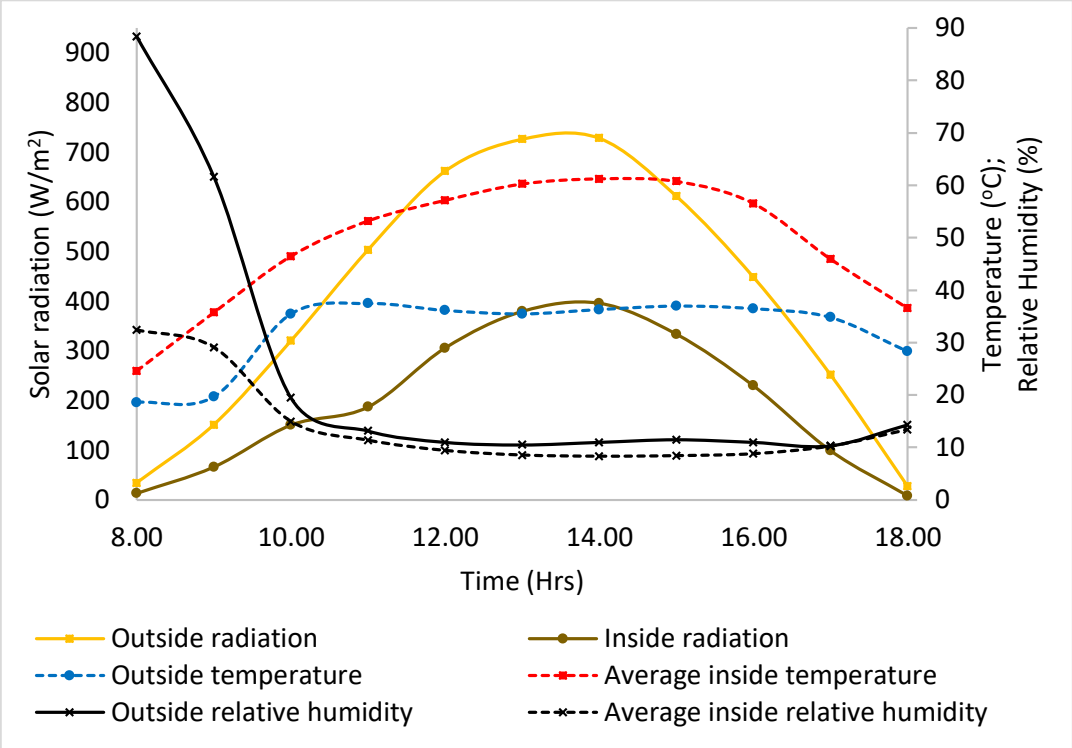

Figure 4.6: Variation of temperature, relative humidity and solar radiation with time of the day for no-load solar mode.

Comparison of inside and outside relative humidity and temperature during the biomass mode (night drying) with the no load conditions are as shown in Figure 4.7. The ambient air temperature reduced as the relative humidity of air increased as the night progressed. This is because the cooling was cumulative and lowest temperature and highest relative humidity were experienced at around 5. 00 am. The cumulative cooling effect resulted in high energy requirement to raise the temperature of drying air. Thus, the drying air had a similar pattern to that of ambient air. During this test

period, the dryer had an average inside temperature of 23.63±3.71ºC with a corresponding ambient temperature average of 15.42±3.77ºC. In addition, average hourly inside and outside relative humidity was found to be 56.31±14.66 and 76.91±18.26%, respectively. Arun *et al.* (2014) observed that a greenhouse dryer with a biomass back-up had a temperature difference of 5-7ºC compared to that without biomass back-up for daytime experiment.

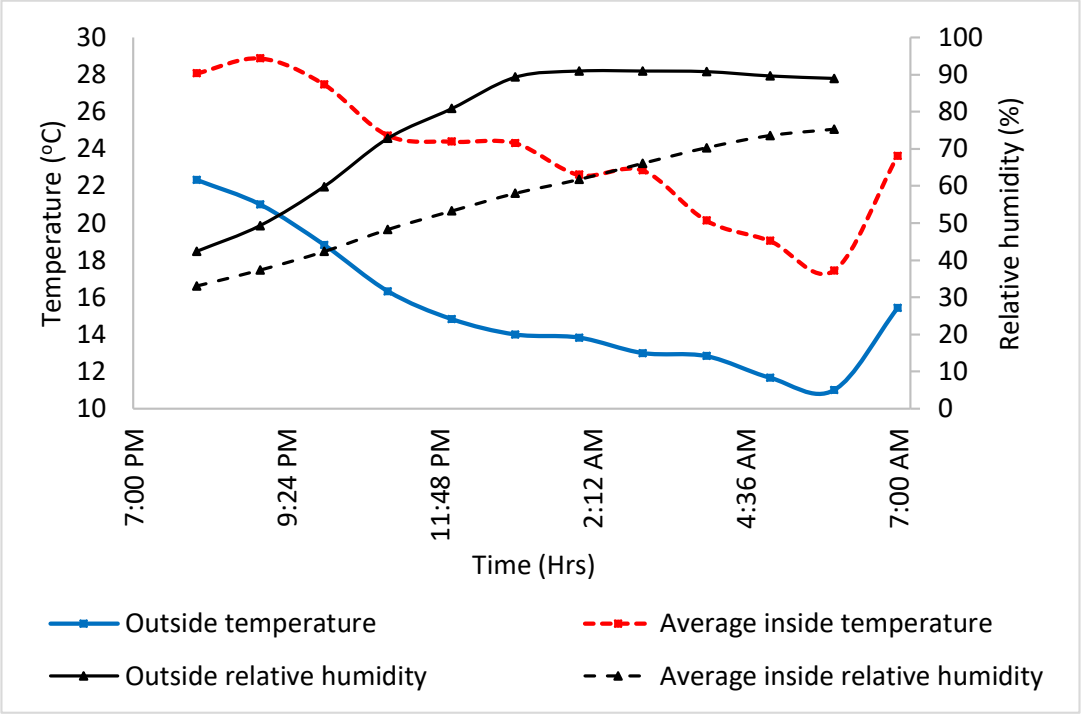

Figure 4.7: Variation of temperature and relative humidity with time of the day for no-load biomass mode.

The variation of solar radiation, temperature and relative humidity versus time of the day for the solar-biomass mode is shown in Figure 4.8. The experiment was selected to be performed during a cloudy day with intermittent rain so as to have ideal

conditions for complimenting solar energy. As a result of low solar radiation and intermittent rain during the drying period, the average hourly ambient temperatures were low while the average hourly ambient relative humidity were high compared to those reported in this study when using solar mode. The average drying air temperature was found to be 43.06±10.67^{o}C with an average corresponding ambient temperature of 26.29±7.07^{o}C and average solar radiation of 255.81±172.61 W/m^{2}.

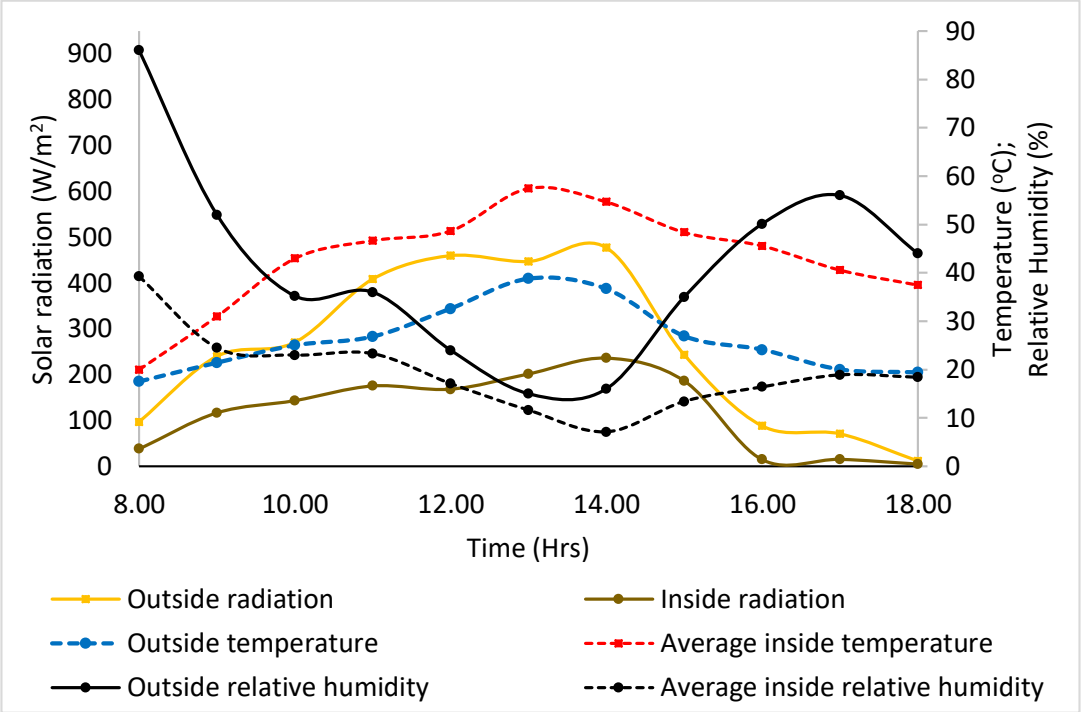

Figure 4.8: Variation of temperature, relative humidity and solar radiation with time of the day for no-load solar-biomass mode.

Figures 4.9 and 4.10 show the temperature and relative humidity difference between the outside and inside the greenhouse dryer for each of the energy modes used. Variations in temperature and relative humidity difference were caused by the

variations in solar radiation with time of the day as earlier explained. During the drying period the dryer had an average hourly temperature and relative humidity difference of 16.61±6.81^{o}C and 9.77±17.89%, 8.20±1.42^{o}C and 20.60±7.44% and 16.77±5.77^{o}C and 21.48±13.94% for solar, biomass and solar-biomass modes, respectively. Regardless of the low solar radiation during the solar-biomass mode, the combination of solar and biomass had an advantage of achieving average drying temperature relatable to those experienced during the solar mode drying. Similarly, Mondru *et al*. (2017) reported low solar radiation values of 291.84 - 562.13 W/m^2 that resulted in an increase in greenhouse dryer temperature of 6.3 - 13.2°C compared to ambient air at no load conditions.

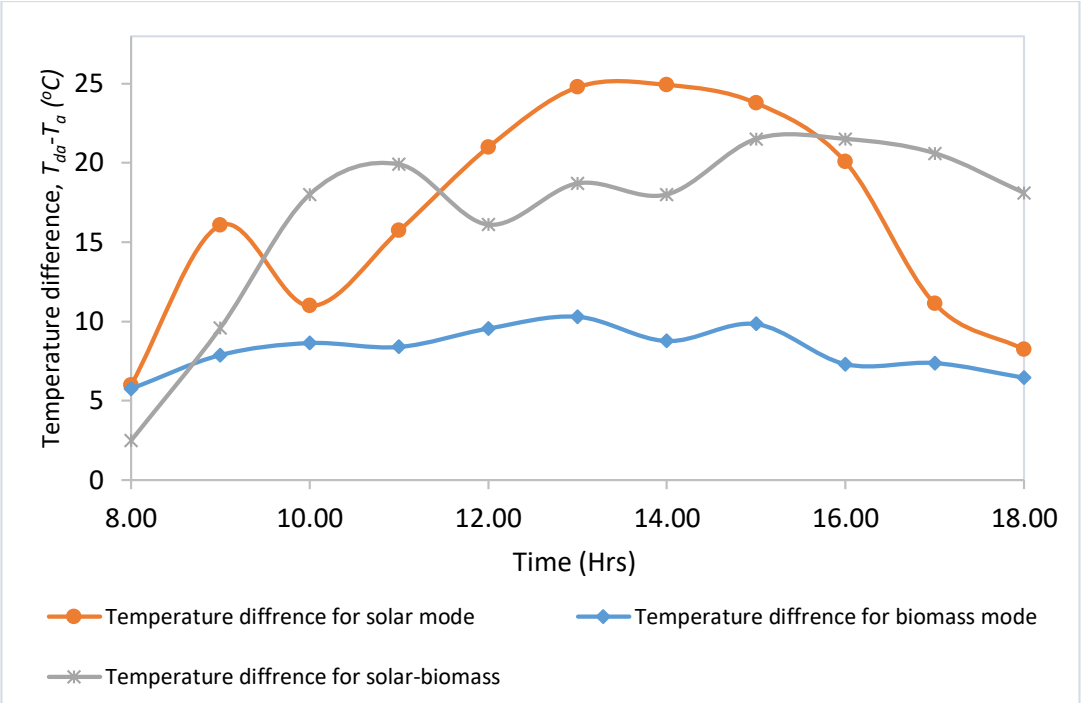

Figure 4.9: Temperature difference between drying air and ambient air for each of the energy mode.

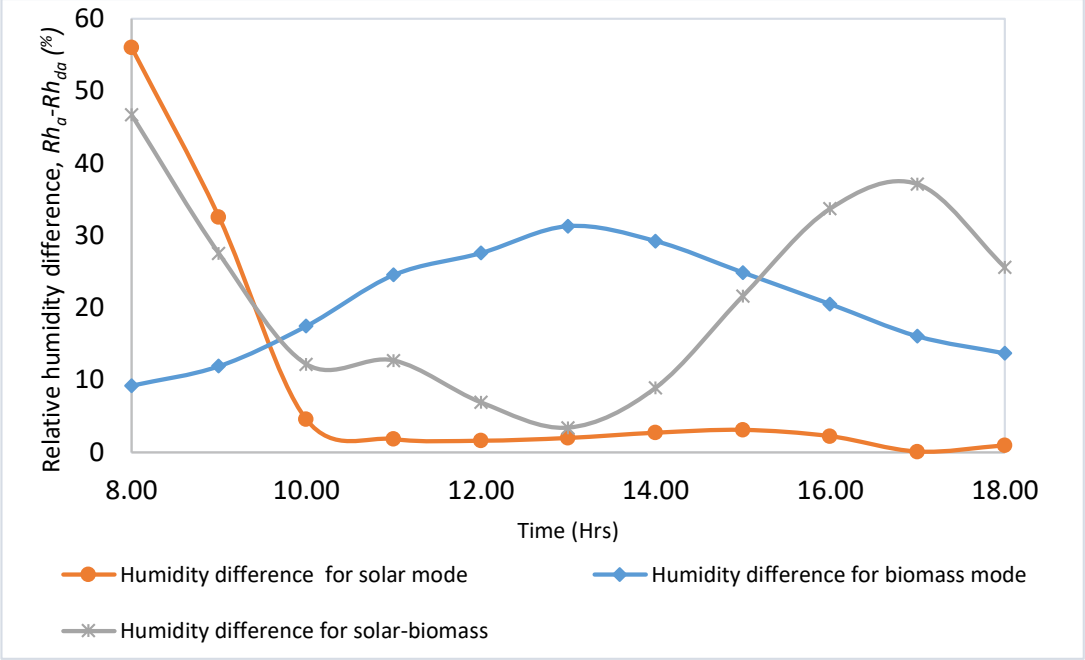

Figure 4.10: Relative humidity difference between drying air and ambient air for each of the energy mode.

The no load experiments aided in determining the expected drying air conditions inside the dryer for each energy mode. The temperature gains in the drying air and lower relative humidity compared to ambient air indicated the potential of the drying air in holding more water as compared to open sun drying. The results of a one-way ANOVA indicated there was significant difference between the average hourly temperature gain for the three energy modes used (F_{calc}, = *9.70*, $F_{crit,0.95}$ = *3.32*, $F_{crit,0.99}$ =*5.39* and $p \leq$ 0.05). Further separation of means using *LSD* showed that there was no significant difference between the average hourly temperature gain for solar and solar-biomass modes. There was significance difference in the average hourly drying air temperature and average hourly ambient air temperature t (20) = 3.91, p = 0.00087; t (20) = 5.14,

p = 0.00005 and t (20) = 4.35, p = 0.00031 for solar, biomass and solar-biomass modes, respectively and hence rejecting the null hypothesis in (b). These results indicated that each energy mode had an effect on the drying air temperatures. Specifically, the results suggested that each energy mode increased potential of the drying air in holding more water as compared to ambient air. Thus, the dryer has a greater drying potential compared to open sun drying

4.3. Exergy Analysis of the Developed Hybrid Solar-Biomass Greenhouse Dryer

4.3.1. Performance of the solar-biomass greenhouse dryer with load

Figure 4.11 shows the variation of temperature, relative humidity and solar radiation for the solar mode with load. Similar to solar mode conditions with no load, the experiment was performed on a clear sky day and a season when the area experiences high solar radiation during the year. Solar radiation, temperature and relative humidity had similar behaviour as dryer with no load conditions. Maximum solar radiation was recorded between 12.00 and 3.00 pm in the day with a corresponding high value of 896.29 W/m^2. The average hourly solar radiation from 8.00 am to 6.00 pm recorded was 494.01±337.35 W/m^2. The dryer had an average inside temperature of 45.23±9.58^{o}C with a correspondingly ambient temperature average of 32.89±5.27^{o}C. These observations are comparable to those made on no-load for solar drying mode. The dryer generated drying air temperature of 12.96±5.25^{o}C higher than ambient air temperature and had drying air relative humidity 8.76±8.28% lower than ambient relative humidity. The temperature gain reported in this study was higher than the

temperature gains of the solar-biomass dryer (10.6^{o}C) reported by Yuwana and Sidebang (2017). Almuhanna (2012) reported a higher temperature gain (14.1^{o}C) for a gable even span greenhouse dryer. The difference in design, locations, year seasons and prevailing weather conditions could be the reason for the difference in these temperature gains (Rani and Tripathy, 2020; Adefemi and Ilesanmi, 2018).

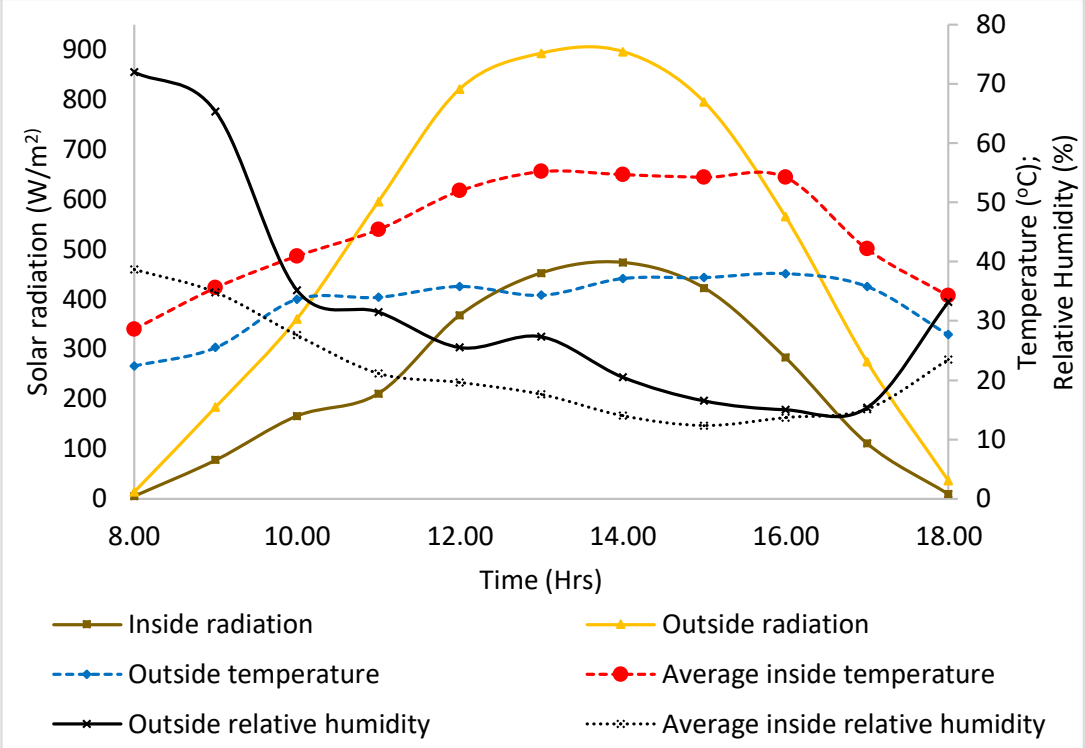

Figure 4.11: Variation of temperature, relative humidity and solar radiation with time of the day for solar mode.

Comparison of inside and outside relative humidity and temperature during the biomass mode only experiments are as shown in Figure 4.12. The behaviour of ambient air temperature and relative humidity was similar to that of no load condition. During this test period, the dryer had an average inside temperature of 26.22±4.09^{o}C

with a corresponding ambient temperature average of 17.26±2.67ºC. The corresponding average hourly temperature difference between the outside and inside of the greenhouse dryer was found to be 8.88±1.38ºC. In addition, average hourly inside and outside relative humidity was found to be 68.37±7.26 and 92.57±1.38%, respectively. The corresponding average hourly relative humidity difference between the outside and inside of the greenhouse dryer was found to be 24.26±8.83%. The observations on temperature and relative humidity trends are comparable to those reported during the no-load biomass mode experiment and agree with observations made by Zaineb *et al*. (2020) for a solar greenhouse dryer with paraffin wax as phase change material.

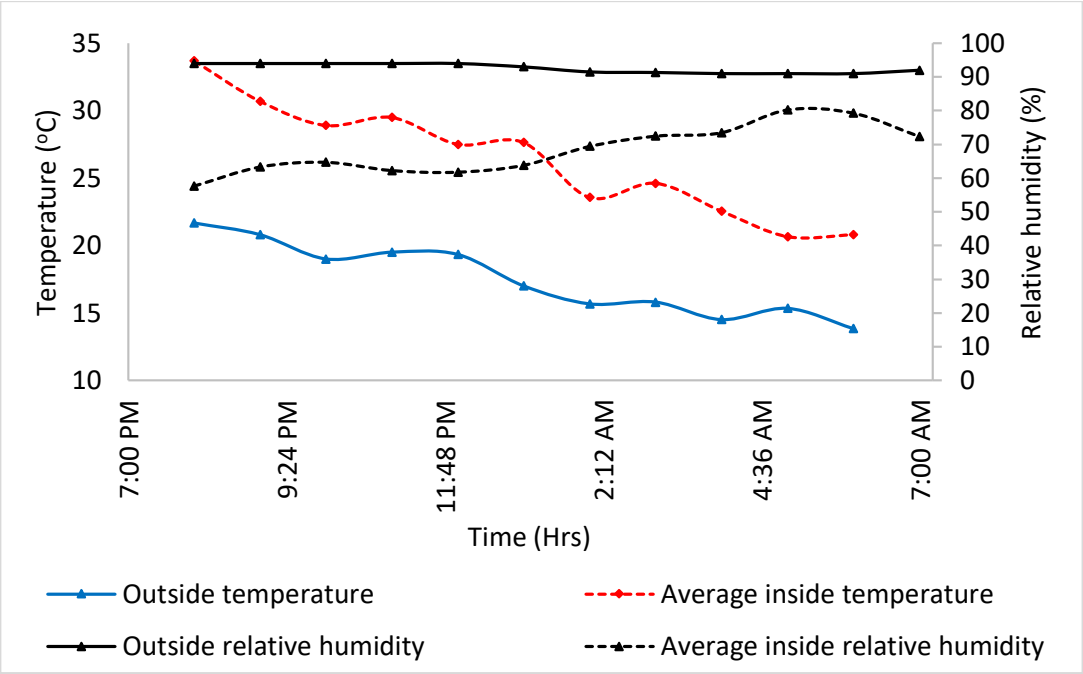

Figure 4.12: Variation of temperature and relative humidity with time of the day for biomass mode.

The variation of solar radiation, temperature and relative humidity versus time of the day for the solar-biomass mode is shown in Figure 4.13. The drying period was dominated with cloudy sky and low solar radiation. The average inside temperature was found to be 34.97±6.59ºC with an average corresponding ambient temperature of 21.76±1.99ºC and average solar radiation of 192.43±168.80 W/m^2. In addition, the average hourly temperature and relative humidity difference between the outside and inside of the greenhouse dryer were 13.21±6.21ºC and 27.51±10.24%, respectively. The dryer maintained average drying temperatures comparable to solar mode drying despite the low solar radiation experienced. There was a notable drop in solar radiation at 12.00 pm which did not result in a drop in drying air temperature as biomass heat complimented the energy required. These observations are in comparable to those made on no-load solar-biomass mode experiment and are in agreement with the findings of Mondru *et al*. (2017) who reported solar radiation values of 291.84 - 562.13 W/m^2 during December in Bapatla, India. With these variations in solar radiation, Mondru *et al*. (2017) also reported an increase in greenhouse dryer temperature of 6.3 to 13.2°C compared to ambient air at no load conditions.

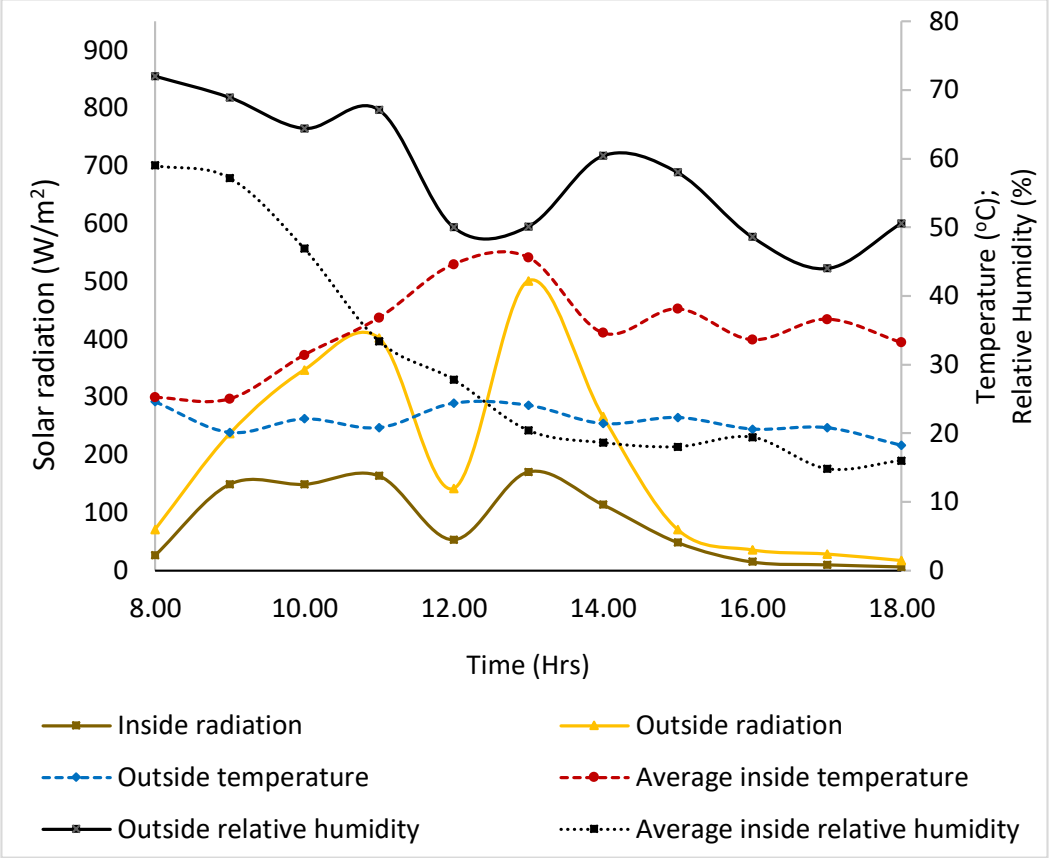

Figure 4.13: Variation of temperature, relative humidity and solar radiation with time of the day for solar-biomass mode.

The initial moisture content of bananas was found to be 74.1±4.9, 78.3±3.9 and 73.0±5.3% during the solar, biomass and solar-biomass mode experiments, respectively. After a drying period of 10 hours, the moisture content was reduced to 33.52±10.15, 62.4±6.2 and 40.27±9.12% for solar, biomass and solar-biomass modes, respectively. The control samples (open sun drying) dried from 74.1±4.9 to 44.49±6.71% after the same drying period. The 10-hour period was considered for purposes of analysis as carrying on with biomass mode on two consecutive nights was not feasible. The limit was preserving the large quantities of samples involved. Similar

drying period was considered by Genobiagon Jr. and Alagao (2019) when experimenting on drying of green bananas using a cabinet dryer. The authors noted that after drying sliced green bananas for 10 hours the moisture content reduced from 78.6 to 33.3% on a clear sunny day when using a solar cabinet dryer with a heat exchanger. In addition, the moisture content reduced from 78.6 to 38% on a cloudy day. In both experiments, the maximum solar radiation recorded was 1043 W/m^2.

The drying rate for the 10-hour drying period of banana slices for the three energy modes was compared as shown in Figure 4.14. The computed average drying rates were found to be 0.28±0.02, 0.21±0.03 and 0.24±0.06 g/gdm/hour for solar, biomass and solar-biomass modes, respectively. The high drying rate experienced in the first two hours of drying for all the modes was due to easiness of evaporation of free moisture from the banana slices. The drying rate observed was a falling rate period as free moisture reduced and bound moisture was evaporated. Bound moisture is controlled by diffusion of the moisture from the interior of the solids to the surface hence difficult to evaporate as compared to free moisture. The fluctuations in solar radiation during the solar-biomass mode could be the reason for the peak experienced in drying rate experienced at 14.00 pm. These observations are comparable to those noted by Genobiagon Jr. and Alagao (2019). They reported drying of banana slices occurred in the falling rate period at rate of 0.27 and 0.32 g/gdm/hour for clear sunny day and cloudy day, respectively.

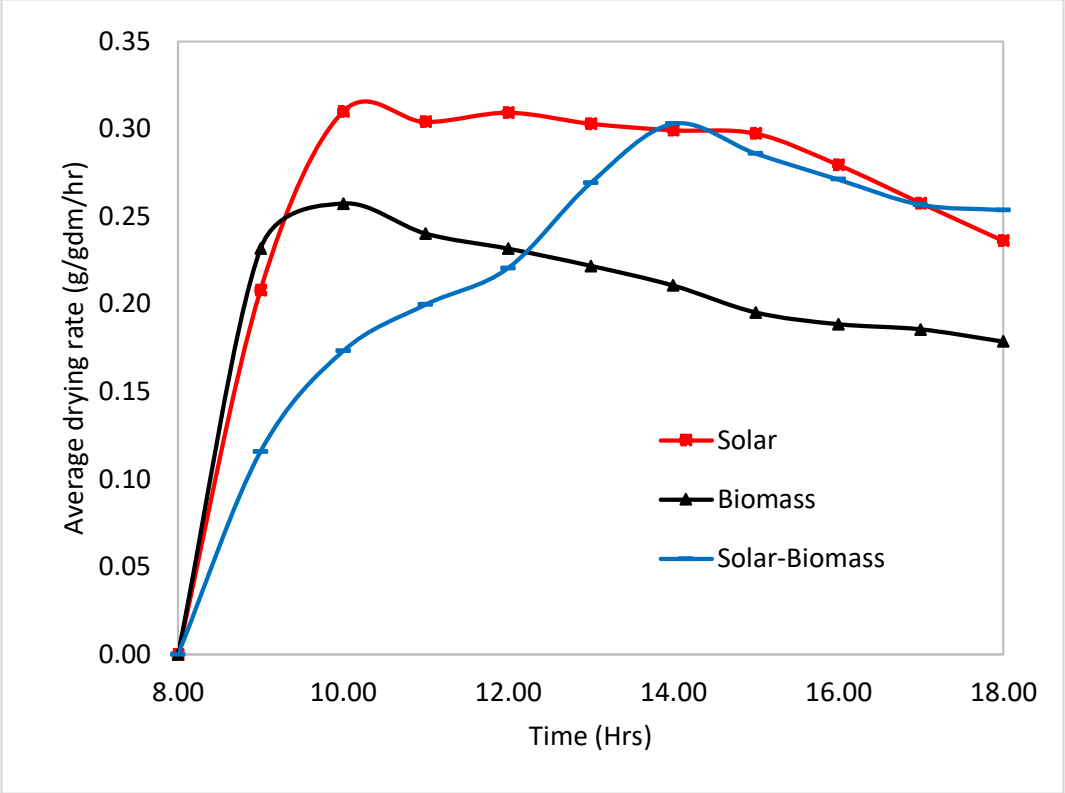

Figure 4.14: Variation of drying rate of banana slices with drying time for the three energy modes.

Further drying of the product was done for solar and solar-biomass modes and the moisture content achieved after 11 and 13 hours was 16.2±3.6 and 11.4±5.5%, respectively which are good ranges for safe storage. The control samples after 11 hours of drying had a moisture content of 32.81± 3.91%. Other studies have reported longer drying periods of bananas as noted by Ndirangu *et al*. (2018). In their review of the analysis of designs and performance of existing greenhouse solar dryers in Kenya, the

authors noted the average drying time for bananas was 56 hours with most of the drying occurring in the first 48 hours.

4.3.2. Energy analysis for the dryer

Figure 4.15 shows a graph of energy efficiency against time for the three energy modes used in this study. On the horizontal axis is the time for solar and solar-biomass, from 8.00 am to 6.00 pm while the biomass experiment ran from 8.00 pm to 6.00 am. From the figure, the solar mode exhibited the least energy efficiency as compared to the biomass and solar-biomass especially during the higher solar radiation hours. The average hourly energy efficiencies were found to be 2.07±3.58, 3.07±0.65 and 7.23±4.30% for solar, biomass and solar-biomass modes, respectively. The energy efficiency for solar was lowest because during high solar radiation hours, the amount of solar energy available was higher than the energy gained in the greenhouse dryer. This is because the whole greenhouse dryer was considered a large solar collector area and the heat gain was low. Alike observations were made by Panwar *et al.* (2013). Greenhouse dryers capture more energy than indirect solar dryers as they absorb energy directly from the sun and they usually have a larger enclosure (Olutoye and Uthamalingam, 2012). However, the magnitude of thermal losses is higher as losses are directly proportional to the enclosure size. This explains the resultant lower energy efficiency as compared to indirect solar dryers (Fudholi *et al*. 2016). The advantage of a greenhouse dryer lies in the simplicity of construction and high capacity as compared to indirect solar dryers.

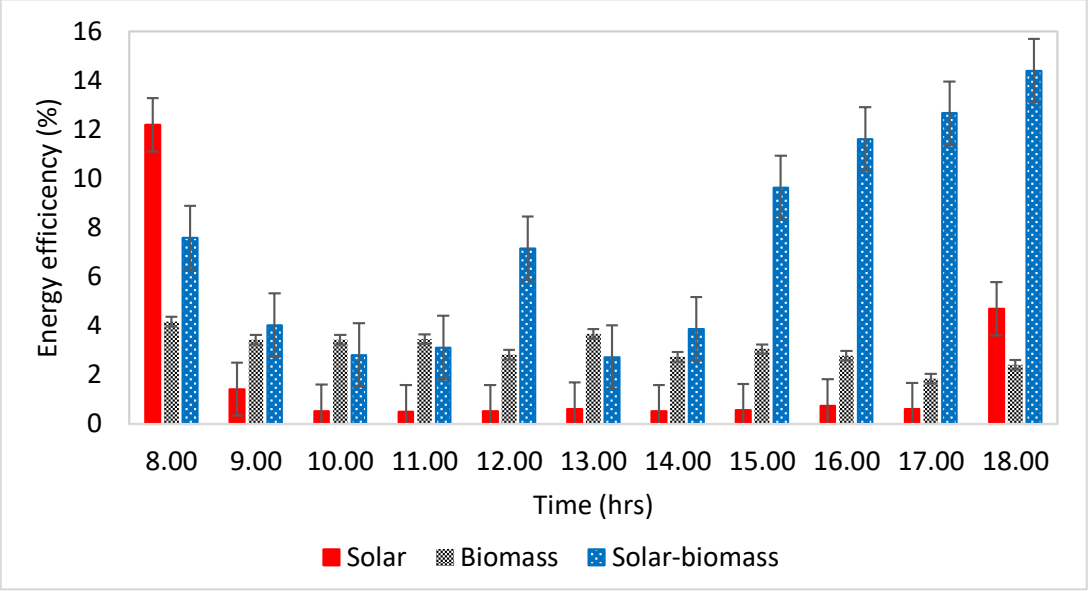

Figure 4.15: Energy efficiency of the greenhouse dryer for the three energy modes used.

The energy utilization ratio (EUR) is a function of drying air temperature as expressed in Equation (3.25). Figure 4.16 shows the variation of EUR against time for the three mode. From the figure, it was observed that EUR generally decreased with an increase in drying time for solar and biomass modes. However, for the solar-biomass mode there were fluctuations observed due to variations in solar radiation experienced during the drying period. In addition, the average hourly EUR was noted as 35.58±24.78, 40.60±10.52 and 33.46±13.45% for solar, biomass and solar-biomass modes, respectively. A similar observation was made while experimenting on a solar cabinet dryer where values of EUR varied from 41.56 to 8.57% (Akpinar, 2011).

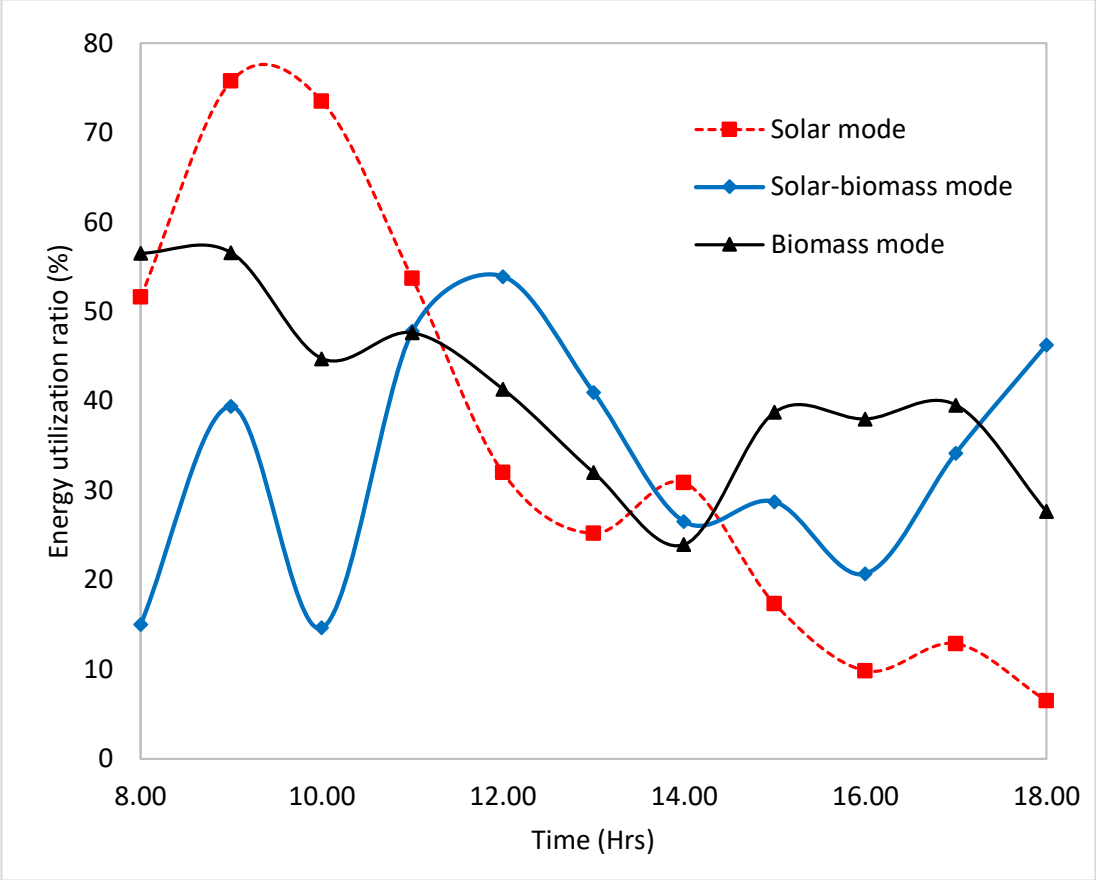

Figure 4.16: Variation of energy utilization ratio of drying air against time for the three energy modes.

The energy flow diagram given in Figure 4.17 shows that not all solar energy harnessed by the dryer is transferred to the drying air as useful energy because losses occur due to thermal heat losses of the system. For biomass and solar-biomass modes additional losses occur due to sensible heat of the flue gas discharged to the environment and heat loss through hot ash removal. Further, energy utilized in drying the product is less than useful energy due to energy exhausted with the hot humid air to the environment. Almuhanna (2012) made similar observations while investigating

the utilization of a solar greenhouse as a solar dryer for drying dates under the climatic conditions of Eastern Province of Saudi Arabia.

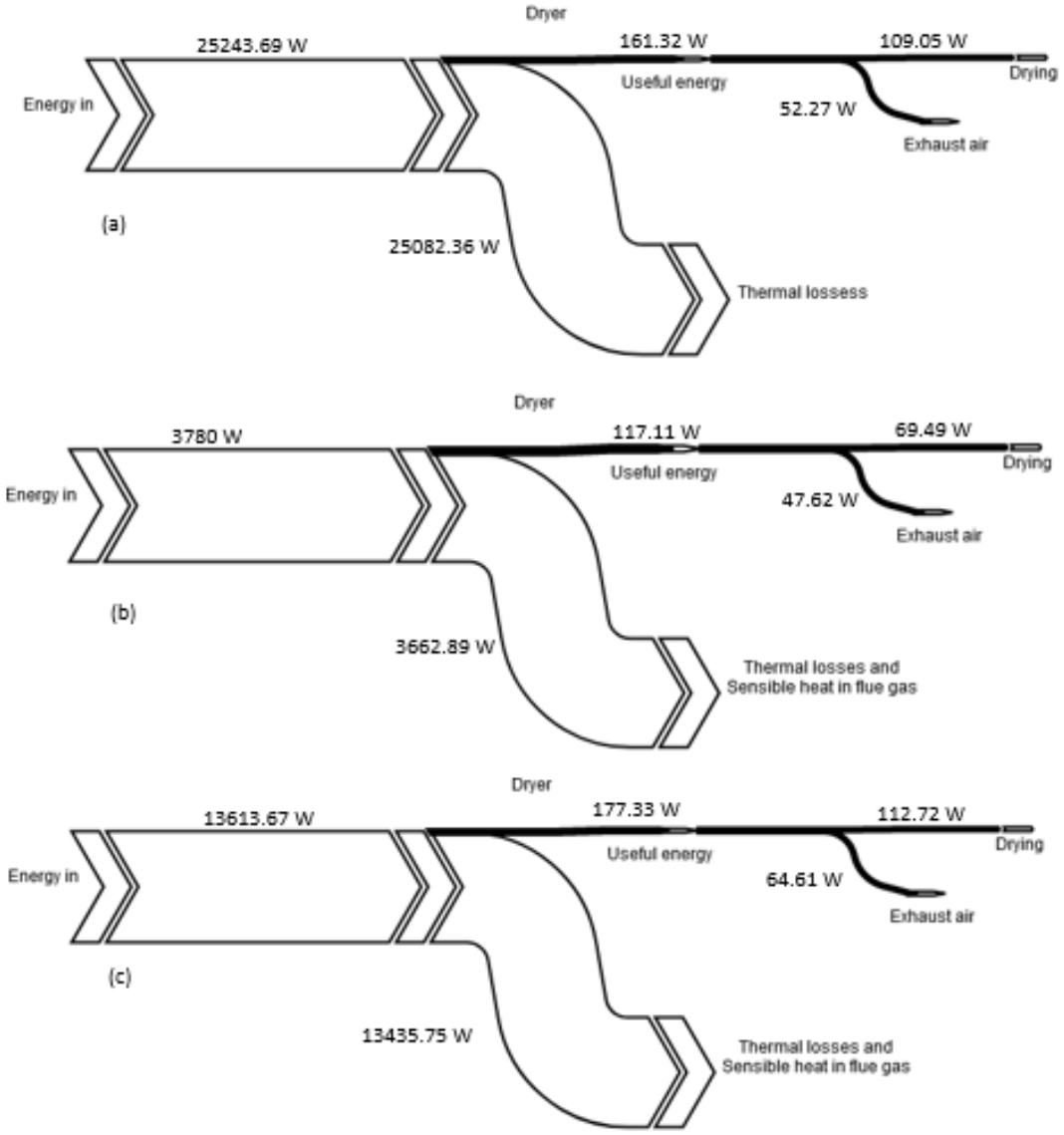

Figure 4.17: Energy flow inside the solar-biomass greenhouse dryer for (a) solar mode, (b) biomass mode and (c) solar-biomass mode.

4.3.3. Exergy analysis for the dryer

Figure 4.18 shows a graph of exergy efficiency against time for the three energy modes used in this study. From the graph, solar mode exhibited the least exergy efficiency as compared to the biomass and solar-biomass, especially during the higher solar radiation hours. The average hourly exergy efficiencies were found to be 0.63±0.81, 1.11±0.57 and 2.76±1.44% for solar, biomass and solar-biomass modes, respectively. These exergy efficiency values were lower compared to energy efficiency values due to exergy destruction occurring as a result of irreversibility in the system. This observation agrees with observations made by other researchers (Subramani *et al*. 2020).

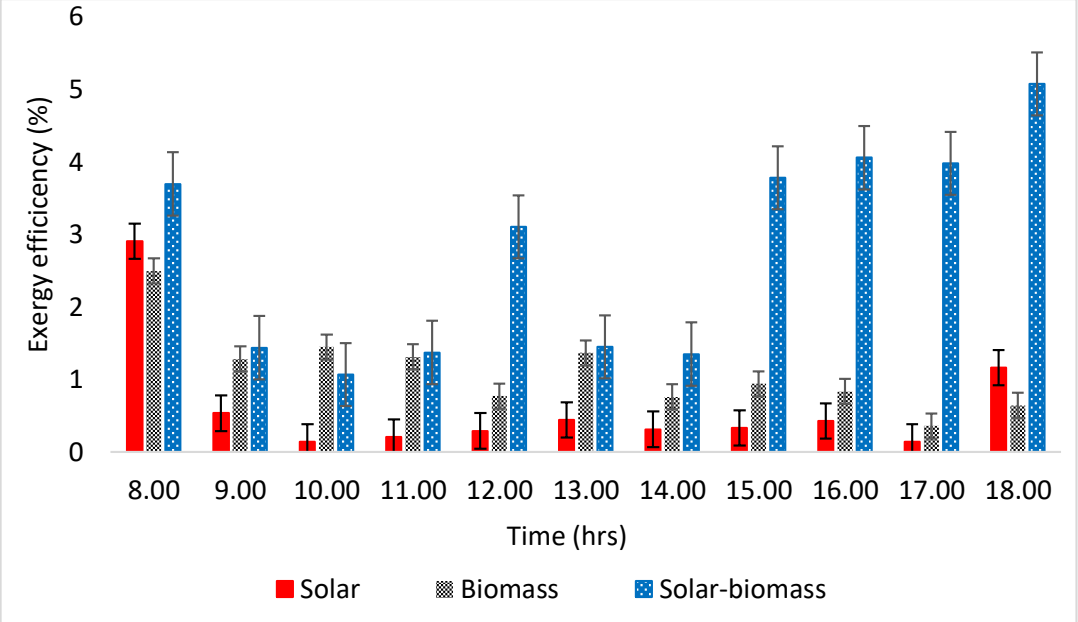

Figure 4.18: Exergy efficiency of the greenhouse dryer for the three energy modes used.

The exergy efficiencies of drying air for the solar-biomass greenhouse dryer against time for the three energy modes are shown in Figure 4.19. It was observed that exergy efficiency increased with the increase of drying time. Solar-biomass had fluctuations as earlier explained in Section 3.3. The average hourly exergy efficiency was found to be 64.60±24.78, 59.37±10.52 and 66.50±13.47% for solar, biomass and solar biomass modes, respectively. These results are within the percentage ranges reported by other scholars. Fudholi *et al*. (2016) noted an exergy efficiency of 29 to 82% while experimenting catfish drying in a greenhouse solar dryer with a heat exchanger. Ozgener and Ozgener (2009) reported average exergy efficiency of drying process as 63-73% while experimenting in a solar greenhouse dryer. The results of a one-way ANOVA confirmed there was no significant difference between the mean exergy efficiencies for the three energy modes used (F_{calc}, *= 0.50*, $F_{crit,0.95}$ *= 3.32*, $F_{crit,0.99}$ *=5.34* and p = 0.61) therefore rejecting the null hypothesis in (c). These results indicated that the energy mode used had no effect on the exergy efficiency. Specifically, the results suggested that the difference in exergy efficiency of the developed hybrid solar-biomass greenhouse dryer was due to prevailing conditions (such as solar radiation, ambient temperatures, and fuel flow rates) during the drying period.

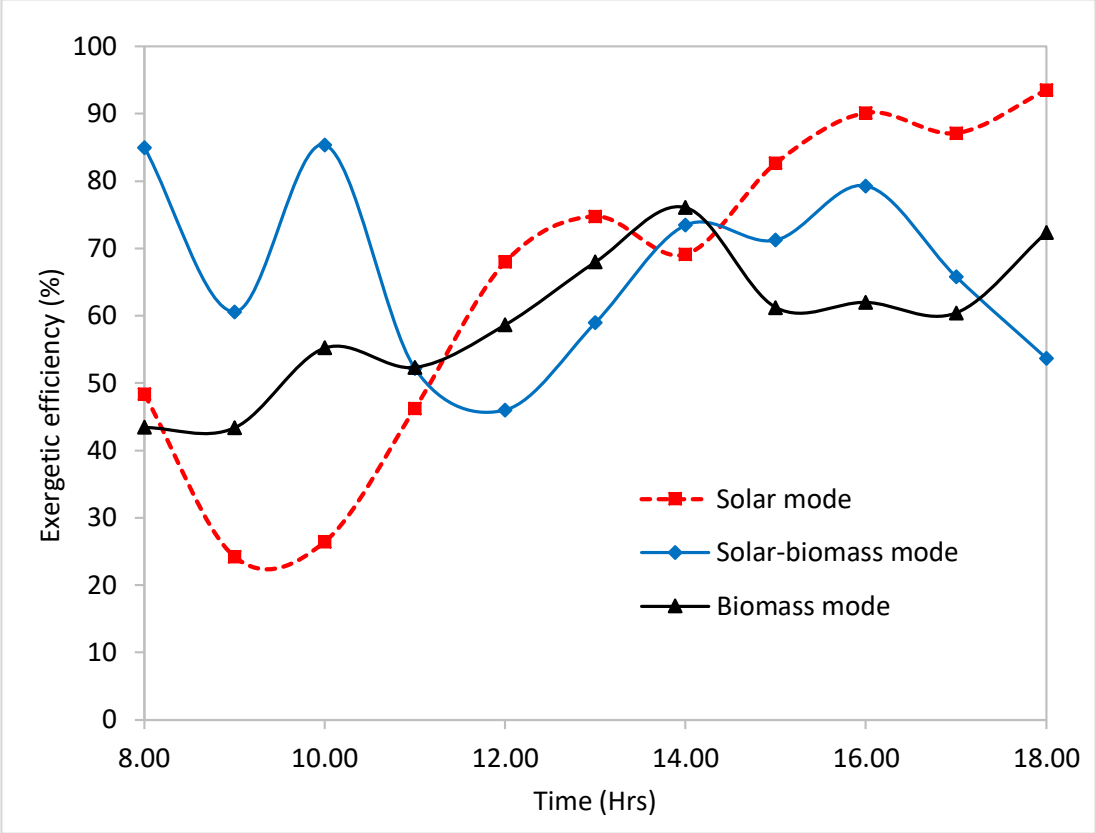

Figure 4.19: Variation of exergy efficiency of drying air against time for the three energy modes.

An exergy flow diagram is given in Figure 4.20. Again, exergy flow diagram followed a similar pattern as the energy flow diagram since the variations in exergy are computed from respective energy. The exergy losses of the greenhouse dryer were higher compared to exergy output. Ozgener and Ozgener (2013) observed high exergy loss of about 65.1% due to heat discharge of closed-loop earth-to-air heat exchanger system. Panwar *et al.* (2013) argued that the low net exergy efficiency of a tunnel dryer can be attributed to the small exergy efficiency of solar energy input raising the

temperature in a tunnel dryer. The exergy efficiencies obtained from the solar-biomass dryer developed in this study this support this argument.

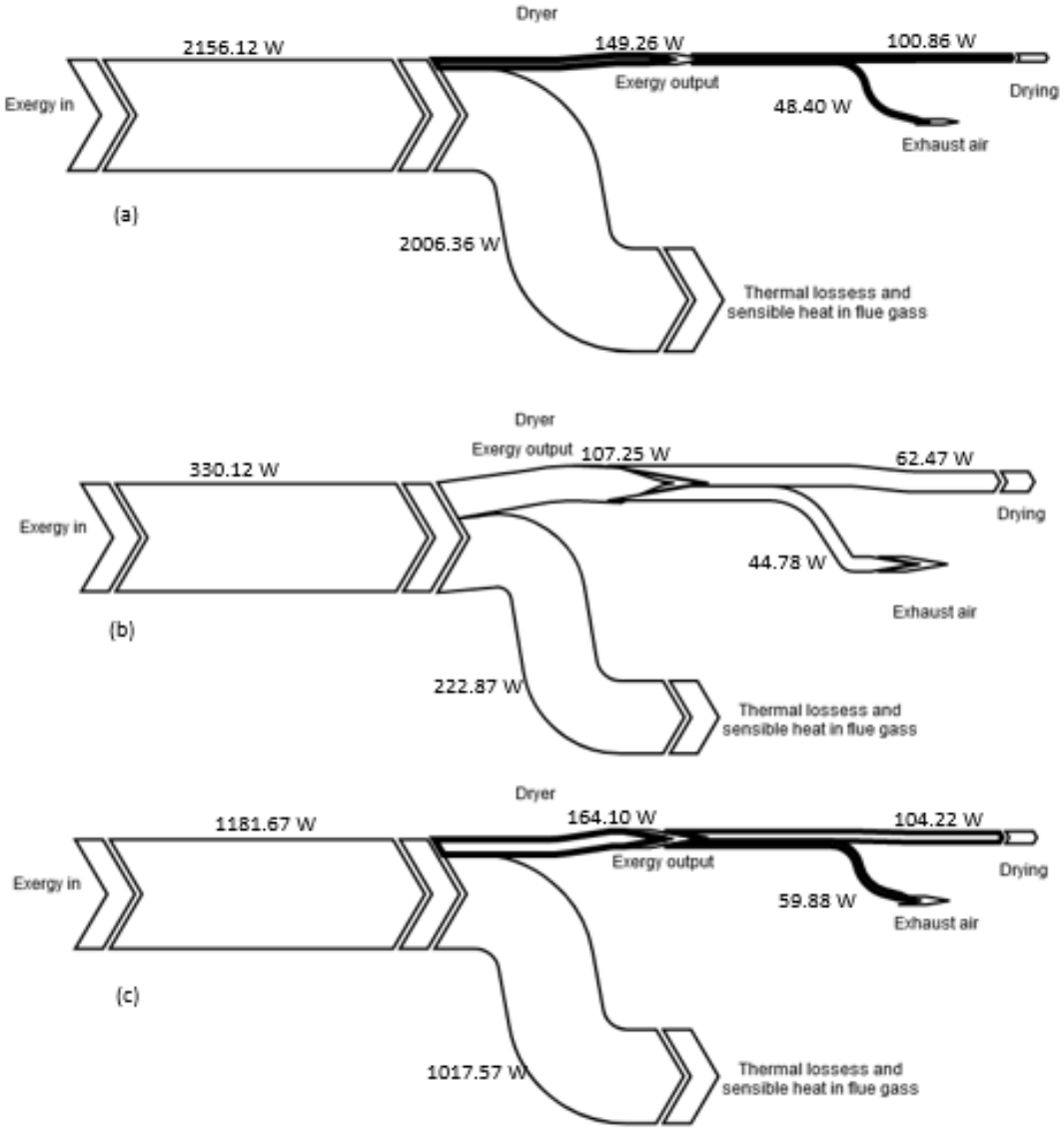

Figure 4.20: Exergy flow inside the solar-biomass greenhouse dryer for (a) solar mode, (b) biomass mode and (c) solar-biomass mode.

4.4. Optimization of the Developed Solar-Biomass Greenhouse Dryer

4.4.1. Relationship between the various linearized functions

Appendix III presents graphs for the different simplified linear functions. Graphs plotted using actual measurements obtained from Section 4.3.3 were used to develop the linear functions. Equations (4.1) and (4.2) determine the drying air temperature and exit air temperature, respectively, for solar drying mode.

$$T_{da} = 0.027I_s + 304.91, \qquad R^2 = 0.9019 \tag{4.1}$$

$$T_{ea} = 0.973T_{da} - 4.498, \qquad R^2 = 0.9409 \tag{4.2}$$

The results indicated that the linear Equation (4.1) can predict drying air temperature based on solar radiation with R^2 of 0.9019. Additionally, the developed exit air temperature equation had R^2 of 0.9409. Other researchers developed a similar simplified equation relating solar radiation to temperature (Manyumbu *et al*., 2014; Janjai et al., 2007; Condori and Saravia, 2003). Since drying air temperature is again dependent on the slope (k = 0.027) from the graph (Appendix III (I)), the larger the constant k is made, the less moisture the product will contain.

Equations (4.3) and (4.4) determine the drying air temperature and exit air temperature, respectively, for biomass drying mode. The results indicated that the linear Equation (4.3) can predict drying air temperature based on ambient air temperature with R^2 of 0.805. Additionally, the developed exit air temperature equation had R^2 of 0.8453.

$$T_{da} = T_a + 8.98, \qquad R^2 = 0.805 \tag{4.3}$$

$$T_{ea} = T_a + 5.32, \qquad R^2 = 0.8453 \tag{4.4}$$

Equations (4.5) and (4.6) determine the drying air temperature and exit air temperature, respectively, for solar-biomass drying mode. The air temperature gained in the dryer depended on variation in solar radiation as biomass heat supply was kept constant. Equation (4.7) expresses this gain. Morissette *et al*. (2011) developed a similar relationship to show temperature gain at solar collector as a function of solar radiation. The results indicated that the linear Equation (4.5) can predict drying air temperature based on solar radiation with R^2 of 0.7856. Additionally, the developed exit air temperature equation had R^2 of 0.7259.

$$T_{da} = 0.032I_s + 314.95, \qquad R^2 = 0.7856 \tag{4.5}$$

$$T_{ea} = T_a + 9.77, \qquad R^2 = 0.7259 \tag{4.6}$$

$$\Delta T = 0.029I_s + 5.563, \qquad R^2 = 0.6489 \tag{4.7}$$

4.4.2. Modifications made to the developed solar-biomass dryer

Appendix 4 shows a sample of the optimization process, while Table 4.1 presents the optimization results obtained from the GA. The result indicates that with the average ambient temperature of 306.1 K, mass air flow of 0.05 kg/s previously defined parameters the dryer can achieve an average drying air temperature of 322.8 K while drying using solar mode. Additionally, with the average ambient temperature of 295 K, mass air flow of 0.05 kg/s, mass fuel rate of 0.001 kg/s and previously defined

parameters the dryer can achieve an average drying air temperature of 333 K while drying using the solar-biomass mode. Correspondingly, with the average ambient temperature of 284 K, mass air flow of 0.01 kg/s, mass fuel flow rate of 0.001 kg/s and previously defined parameters the dryer can achieve an average drying air temperature of 333 K while drying using biomass mode. These predictions are in agreement with observations made by other scholars. Bansal *et al*. (2020) performed process parameter optimization of a flat plate solar dryer using Taguchi method. They found out that at ambient conditions of 308.5 K and solar radiation of 233.22 W/m^2 the dryer upper and lower tray temperatures were 333.1 and 320.9 K, respectively. Sethi and Dhiman (2020) developed a thermal prediction model to determine the amount of biomass heating load requirements for solar-cum-biomass hybrid greenhouse crop dryer using a flue gas heat transfer pipe network. The developed thermal model predicted greenhouse dryer temperature of 299 to 311 K equivalent to heating load of 4-6.5 kW when ambient air temperature remained between 283 and 291 K for Ludhiana climate (30°N) India.

Optimization results enabled decision-making on the improvement areas that would result in maximized drying air temperature and exergy efficiency. Modifications implemented included a change in the shape of the biomass unit from square to circular to ease the flow of flue gas into the duct heat exchanger and reduce the 'backflow' of drying air into the blower. Introduction of a blower on the shutter to accelerate flue flow and maintain a steady flow of heat along the duct. The blower was selected based on flue gas flow rate computed for a fuel flow rate of 0.001 kg/s obtained from the

optimized results. The drying air cavity volume and burning chamber volume were increased by 50% each. The modifications generated an increase in the amount of heated air and improved airflow into the ducts. The biomass stove was coupled to a double duct heat exchanger such that the inner duct conveyed the flue gases and the outer ducts had the drying air. The elbows were smooth and round to minimize turbulence in the ducts. For each energy mode used, air flow was varied as per the optimization solution of the model.

Table 4.1: Optimal solutions for each energy mode

Mode	T_a (K)	T_{da} (K)	I_s (W/m^2)	$\dot{m}_a$ (kg/s)	$\dot{m}_f$ (kg/s)	η_{ex} (%)
Solar	306.1	322.28	300	0.05	-	70.00
Biomass	284.0	333.0	-	0.01	0.001	57.71
Solar-biomass	295.0	333.0	300	0.05	0.001	57.05

T_a is ambient temperature (K), T_{da} is drying air temperature (K), I_s is outside solar radiation (W/m^2), $\dot{m}_a$ is the mass flow rate of air (kg/s), $\dot{m}_f$ is fuel flow rate (kg/s) and η_{ex} is exergy efficiency.

Figure 4.21 exemplifies the developed biomass unit. The biomass unit was fabricated using a 1.29 mm plain aluminum sheet and lagged with fibreglass of 25.4 mm thickness to minimize heat loss to the surrounding. The unit composed of two chambers: combustion chamber and drying air heating chamber. The combustion chamber had a diameter of 286 mm with the drying air chamber diameter of 568 mm, respectively and 620 mm long. The combustion compartment floor comprised a perforated grate for fuel and ash-fall in the ash pit. An auxiliary blower (Tidar, China) of 254.85 m^3/hour mounted on the shutter to supply the primary air required for complete combustion. The outer and inner cylinders tapered to a final diameter of 180 and 130 mm, respectively, at a length of 330 mm. Thus, providing coupling for the

double duct heat exchanger. The inner and outer ducts conveyed flue gases and drying air, respectively. The duct layout was as outlined in Section 3.2.2. A blower (FDA250R2/ST, China) of 2378 to 2551 m^3/hour mounted on the drying air chamber draws the ambient air through the chamber and maintained a steady supply of drying air in the greenhouse.

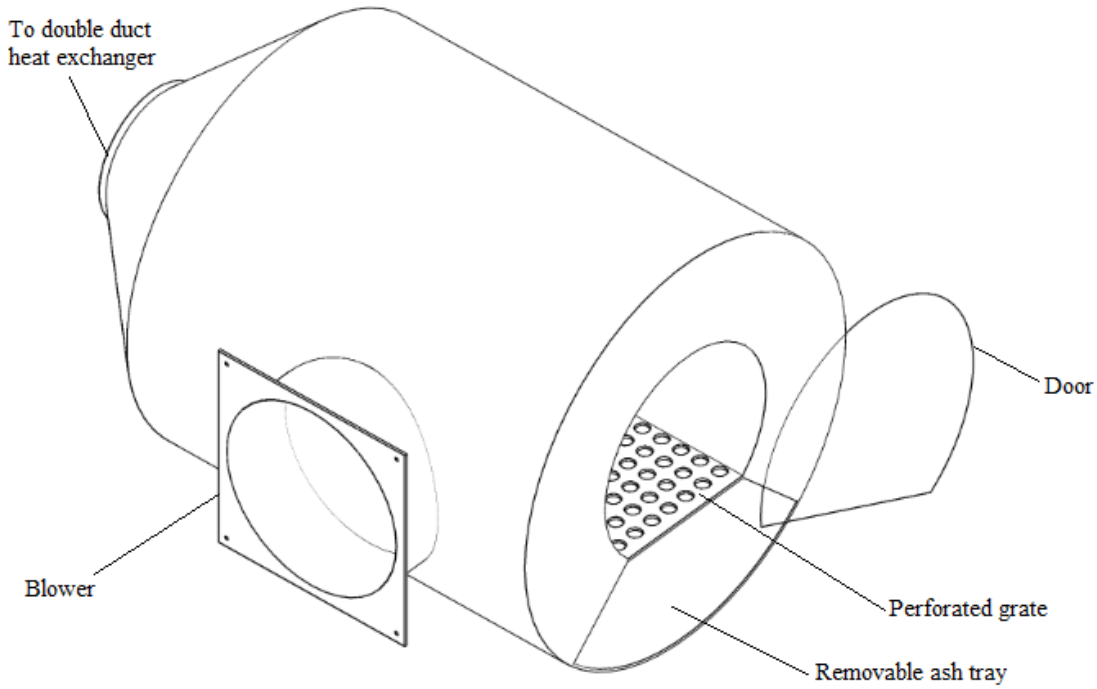

Figure 4.21: Developed biomass unit after optimization.

These improvements are in agreement with the other authors' observations. Wulandani *et al*. (2019) modified a furnace for a rack-type solar dryer from trapezoidal to cylindrical to improve the flow of combustion air into the heat exchanger pipe. Rastvorov *et al*. (2017) also studied the influence of burner form and pellet type on domestic pellet boiler performance. The authors found out that a circular burner had a

higher wood pellet firing efficiency compared to a rectangular burner. Ndindeng *et al*. (2019) compared fan-assisted gasifiers to natural draft gasifiers cook stoves in their study. The authors reported that fan-assisted gasifier cook stoves recorded better thermal indices compared with the natural draft cook stove.

4.4.3. Performance of the optimized solar-biomass greenhouse dryer

Figure 4.22 shows the variation of temperature and solar radiation with the time of the day for optimized solar-biomass mode. The drying period had an average hourly solar radiation of 306.86±166.74 W/m^2 and peak radiation of 509.5 W/m^2 recorded at noon. The corresponding average hourly inside and outside temperature was 55.45±7.19^{o}C and 30.0±3.37^{o}C, respectively. Over the drying period for the solar-biomass mode, the weather was partly cloudy with intermittent light showers during the morning hours 8.00 to 10 am and afternoon 1.00 to 2.00 pm resulting in fluctuations in solar radiation. The supply of heating energy in the greenhouse had a cumulative effect on drying air temperature and the temperatures increased from 10.00 am to 4.00 pm despite fluctuations in solar radiation. During the morning hours (8.00 am to 9.00 am) and evening hours (5.00 pm to 6.00 pm) the solar radiation was below 100 W/m^2 and the heating was yet to peak or had been withdrawn (evening) to stop the drying process hence resulted to lower drying temperature. The inside radiation was the radiation transmitted through the glazing material which is a function of outside radiation and cover optical properties thus follows same trend as outside radiation. The average ambient temperature varied with outside solar radiation (Figure 4.22).

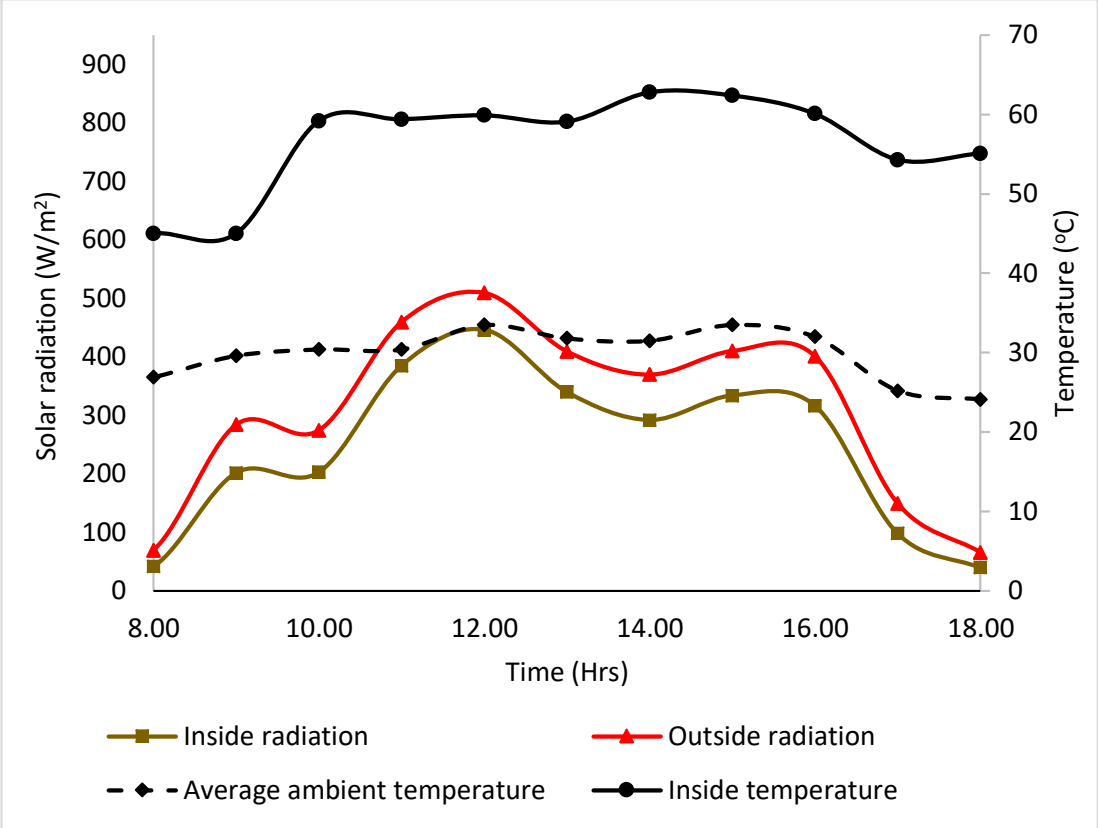

Figure 4.22: Variation of temperature and solar radiation with time of the day for optimized solar-biomass mode.

Figure 4.23 show the variation of temperature and relative humidity with daytime for the optimized biomass drying mode. Night drying had average hourly inside and outside temperature of 34.13±22.06ºC and 18.35±1.58ºC, respectively. There were rain showers throughout the night. The average ambient temperature decreased as the night progressed as the cooling effect was cumulative with least temperatures experienced at 5.00 am. The heat energy supply was kept constant (fuel flow rate of 0.001 kg/s) and the average drying air temperatures fluctuated with ambient temperatures. This is explained by the fact that the low ambient temperatures coupled

with rain water caused higher thermal losses from the glazing material. The optimized conditions resulted in moisture reduction from 73.00±4.30 and 73.09±4.14% to 16.15±4.44 and 46.68±15.31% for solar-biomass and biomass modes, respectively, after 10 hours of drying. Bananas dried using the biomass mode were further dried during the day using optimized solar mode conditions and the moisture content reduced from 46.68±15.31% to 18.02±10.80% after 4 hours. During the extended drying period, average hourly solar radiation of 360.82±265.882 W/m^2. The corresponding average hourly inside and outside temperature was 45.88±3.48^{o}C and 28.13±0.79^{o}C, respectively.

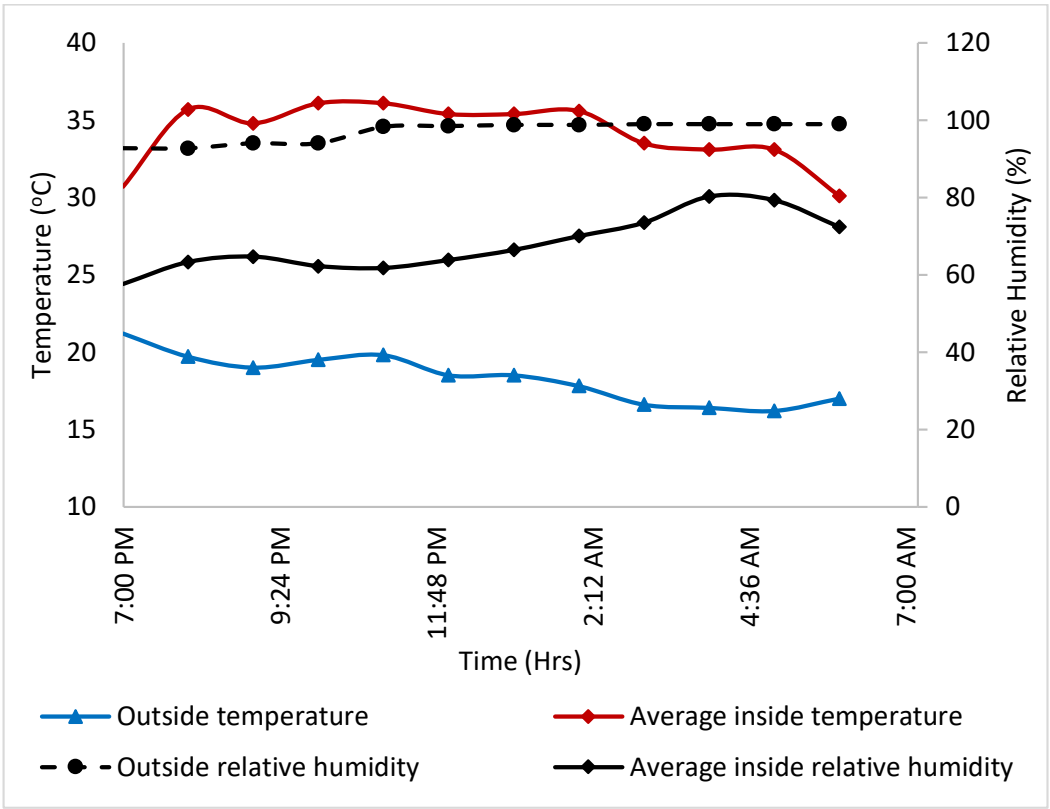

Figure 4.23: Variation of temperature and relative humidity with time of the day for optimized biomass mode.

A comparison of the dryer performance before and after optimization is as shown in Table 4.2. The results showed that there was a significant difference between ambient air temperature for the optimized and un-optimized modes ($p \leq 0.05$). The results suggested that the differences were not due to randomness but was as a result of to the difference in year seasons and prevailing weather conditions during the experiments (Rani and Tripathy, 2020; Adefemi and Ilesanmi, 2018). It was important to note that the aging of the cladding material contributes to the difference in covering material transmissivity. However, both the optimized and un-optimized experiments had similar drying durations. It was observed that the exergy efficiency recorded using the optimized system for biomass and solar-biomass modes were higher than all the exergy efficiency recorded during the un-optimized experiments. The results of a one-way ANOVA confirmed there was a significant difference between the mean exergy efficiencies for the optimized and un-optimized system (F_{calc}, = 7.50, $F_{crit,0.95}$ = 2.84, $F_{crit,0.99}$ =4.31 and p = 0.00043) therefore rejecting the null hypothesis in (d). These results indicated that the optimization had an effect on the exergy efficiency. Specifically, the results suggested that the difference in exergy efficiency for the optimized and un-optimized solar-biomass greenhouse dryer was due to improvements on the dryer after optimization. Thus, the optimized dryer exhibited better results in terms of exergy efficiency. Hence, the optimization process provided a superior system compared to the un-optimized system. Additionally, an increase in drying air temperatures achieved after optimization improved the drying rate of the product.

Table 4.2: Comparison of optimized and un-optimized drying parameters

Mode	T_a (±Std)K	T_{da} (±Std)K	I_s (±Std)W/m^2	η_{ex} (±Std)%
		Optimized		
Solar-biomass	303.00±3.37^a	328.45±7.19^a	306.9±166.74^a	80.21±14.26^a
Biomass	291.40±1.6^c	307.10±2.1^b	-	79.28±10.38^a
		Un-optimized		
Solar-biomass	294.76±1.99^b	307.97±6.59^b	192.42±168.80^a	66.50±13.47^b
Biomass	290.26±2.67^c	299.22±4.09^c	-	59.37±10.52^b
LSD	1.71	3.96	164.25	9.74

T_a is ambient temperature (K), T_{da} is drying air temperature (K), I_s is outside solar radiation (W/m^2) and η_{ex} is exergy efficiency (%). Mean values within columns with different superscripts are significantly different ($p \leq 0.05$; one-way ANOVA, *LSD* post hoc test).

Table 4.3 shows a comparison between optimized parameters obtained from the GA and experimental. Both ambient and drying air temperatures were higher than the model output for solar-biomass and biomass modes. However, they were within the ranges acknowledged for drying for each mode as earlier defined in Section 3.4.2. Ambient and drying air temperatures were lower than the model output for the solar drying mode. The exergy efficiency of the optimized system was higher than the model prediction since a slight change in temperature causes a variation in exergy. There was no variation observed between the experimental and model air and the fuel flow rates. Results obtained from the GA simulation showed a good agreement with the experimental results.

Table 4.3: Comparison of optimized and experimental results

Mode	Parameters	From GA	Experimental (±Std)	% error (PE)
Solar-biomass	T_a (K)	295.00	303.00±3.37	2.71
	T_{da} (K)	333.00	328.00±7.19	1.38
	I_s (W/m^2)	300.00	306.90±166.74	2.30
	$\dot{m}_a$ (kg/s)	0.05	0.05	0
	$\dot{m}_f$ (kg/s)	0.001	0.001	0
	η_{ex} (%)	57.05	80.21±14.26	40.60
Biomass	T_a (K)	284.00	291.40±1.6	2.46
	T_{da} (K)	333.00	307.10±2.1	7.78
	$\dot{m}_a$ (kg/s)	0.01	0.01	0
	$\dot{m}_f$ (kg/s)	0.001	0.001	0
	η_{ex} (%)	57.71	79.28±10.38	37.50
Solar (Extended biomass drying)	T_a (K)	306.10	301.13±0.79	1.62
	T_{da} (K)	322.28	318.88±3.48	1.06
	I_s (W/m^2)	300.00	360.82±265.882	20.27
	$\dot{m}_a$ (kg/s)	0.05	0.05	0
	η_{ex} (%)	70.00	78.08±5.38	11.54

T_a is ambient temperature (K), T_{da} is drying air temperature (K), I_s is outside solar radiation (W/m^2), $\dot{m}_a$ is the mass flow rate of air (kg/s), $\dot{m}_f$ is fuel flow rate (kg/s) and η_{ex} is exergy efficiency (%).

In conclusion, maintaining an air mass flow rate of 0.05 kg/s for solar and solar-biomass modes helps in achieving maximum exergy efficiency from the developed solar-biomass dryer. Biomass mode requires a lower air mass flow rate of 0.01 kg/s. Further, both solar-biomass and biomass modes must maintain a fuel feed rate of 0.001 kg/s. Products dried using biomass mode can be further dried using solar drying to achieve safe moisture levels for storage. This combination shortens the solar hours required for drying and will ensure continuity of drying during peak demand. The use of biomass energy to complement solar for radiations below 300 W/m^2 can help shorten the drying period to less than a day. The test under optimized solar mode should be performed during the summer season when the solar radiation is above 300 W/m^2 for most hours of the day.

4.5. Effect of Drying on Nutritive and Organoleptic Properties of Bananas

4.5.1. Colour changes in banana slices during drying

The results for colour measurements for both fresh and dried banana slices dried using solar, biomass, solar-biomass and open sun are presented in Tables 4.4 to 4.7, respectively. The results obtained show that the values of L^* and b^* for the dried slices were lower than those for fresh ones for all the drying methods considered. On the other hand, the values of a^* for dried slices were higher than those for fresh slices for all banana varieties and each drying method used. Further, it was observed that the peeled samples were lighter than corresponding unpeeled samples as they had higher values of L^* and b^* and lower values of a^*. The variation in colour of fresh banana slices between varieties was attributed to the different genotypes among them. It also showed that the varieties had varying amounts of carotenoids responsible for yellowness in fruits (Kumar *et al*., 2019). In addition, as a result of the green colour in the peel, the unpeeled samples resulted in more darkened samples as compared to peeled samples. As reported by Kumar *et al*. (2019), such observations can be useful in guiding the selection of banana variety, whether to use peeled or unpeeled bananas depending on the end-use of the dried product.

Table 4.4: Colour parameters for both fresh and dried banana slices for solar mode

Banana variety	*L**(±Std)	*a**(±Std)	*b**(±Std)
	Peeled fresh sample		
Apple banana	87.22±0.03 [a]	4.72±0.08 [c]	20.95±4.07 [c]
Gros Michel AAA	87.13±0.16 [a]	8.34±0.27 [a]	31.28±0.4 [a]
Kiganda AAA	86.16±2.98 [a]	7.11±0.18 [b]	29.68±1.41 [ab]
Muraru AAA	87.94±1.15 [a]	3.27±1.12 [d]	25.52±1.98 [b]
LSD	-	1.00	4.43
	Unpeeled fresh sample		
Apple banana	82.72±8.46 [a]	0.40±2.98 [a]	19.30±4.86 [b]
Gros Michel AAA	74.12±4.71 [a]	0.86±8.05 [a]	27.80±2.35 [a]
Kiganda AAA	75.89±10.06 [a]	2.35±8.42 [a]	29.88±4.47 [a]
Muraru AAA	75.89±18.34 [a]	-0.61±3.80 [a]	25.65±2.26 [a]
LSD	-	-	8.65
	Peeled dry sample		
Apple banana	86.19±0.29 [a]	10.61±1.27 [b]	17.60±2.21 [a]
Gros Michel AAA	84.00±0.30 [b]	15.00±0.04 [a]	13.77±0.33 [b]
Kiganda AAA	80.74±0.00 [c]	14.63±1.28 [a]	15.71±0.76 [ab]
Muraru AAA	80.97±2.13 [c]	13.74±1.25 [a]	14.72±0.57 [b]
LSD	1.93	2.07	2.59
	Unpeeled dry sample		
Apple banana	77.64±12.61 [a]	10.17±5.71 [a]	17.12±7.54 [a]
Gros Michel AAA	68.49±1.57 [a]	11.98±4.94 [a]	17.22±4.92 [a]
Kiganda AAA	65.64±1.73 [a]	15.25±2.57 [a]	16.81±1.80 [a]
Muraru AAA	70.18±15.18 [a]	9.02±3.03 [a]	20.16±7.54 [a]
LSD	-	-	-

*L** (Lightness/ darkness), *a** (redness/greenness) and *b** (yellowness/blueness). Mean values with different superscripts in the same column for each treatment (peeled or un-peeled) are significantly different ($p \leq 0.05$; one-way ANOVA, *LSD* post hoc test).

Table 4.5: Colour parameters for both fresh and dried banana slices for biomass mode

Banana variety	*L**(±Std)	*a**(±Std)	*b**(±Std)
	Peeled fresh sample		
Apple banana	86.53±1.41 [b]	8.05±1.42 [a]	24.06±0.00 [a]
Gros Michel AAA	89.67±0.00 [a]	7.49±1.63 [a]	21.45±1.30 [b]
Kiganda AAA	89.47±1.20 [a]	7.16±0.76 [a]	25.42±1.27 [a]
Muraru AAA	90.12±1.61 [a]	6.53±1.51 [a]	21.84±0.42 [b]
LSD	2.61	-	1.74
	Unpeeled fresh sample		
Apple banana	70.87±24.32 [a]	0.34±6.50 [a]	28.68±11.94 [a]
Gros Michel AAA	73.69±17.47 [a]	0.47±6.87 [a]	25.56±8.30 [a]
Kiganda AAA	75.59±22.49 [a]	0.56±4.14 [a]	22.60±0.75 [a]
Muraru AAA	70.31±22.14 [a]	0.48±8.23 [a]	29.70±6.22 [a]
LSD	-	-	-
	Peeled dry sample		
Apple banana	82.12±1.10 [a]	8.64±0.45 [a]	16.05±2.83 [b]
Gros Michel AAA	86.54±2.55 [a]	9.22±0.62 [a]	19.61±1.55 [ab]
Kiganda AAA	84.82±3.13 [a]	8.23±1.41 [a]	23.93±1.42 [a]
Muraru AAA	86.59±1.56 [a]	8.46±0.00 [a]	20.38±2.93 [a]
LSD	-	-	4.88
	Unpeeled dry sample		
Apple banana	65.64±22.85 [a]	0.88±8.21 [a]	26.13±10.49 [a]
Gros Michel AAA	62.15±35.36 [a]	2.09±3.90 [a]	18.11±8.34 [a]
Kiganda AAA	64.03±35.50 [a]	2.71±4.36 [a]	17.49±1.27 [a]
Muraru AAA	62.65±25.67 [a]	2.23±7.81 [a]	21.36±5.06 [a]
LSD	-	-	-

*L** (Lightness/ darkness), *a** (redness/greenness) and *b** (yellowness/blueness). Mean values with different superscripts in the same column for each treatment (peeled or un-peeled) are significantly different ($p \leq 0.05$; one-way ANOVA, *LSD* post hoc test).

Table 4.6: Colour parameters for both fresh and dried banana slices for solar-biomass mode

Banana variety	*L**(±Std)	*a**(±Std)	*b**(±Std)
	Peeled fresh sample		
Apple banana	82.30±1.41 [a]	-0.88±1.56 [b]	19.69±1.70 [c]
Gros Michel AAA	78.40±0.95 [b]	1.10±0.58 [a]	30.50±1.42 [a]
Kiganda AAA	83.80±0.00 [a]	-4.40±0.76 [c]	26.90±2.36 [b]
Muraru AAA	83.50±1.50 [a]	-2.20±0.31 [b]	22.40±0.00 [c]
LSD	2.05	1.65	2.82
	Unpeeled fresh sample		
Apple banana	76.70±4.10 [ab]	1.05±1.34 [a]	24.80±0.28 [a]
Gros Michel AAA	74.75±0.35 [b]	0.80±0.99 [a]	28.90±1.98 [a]
Kiganda AAA	80.00±1.41 [a]	-2.65±0.21 [b]	26.10±7.64 [a]
Muraru AAA	80.95±1.77 [a]	-1.70±0.28 [b]	24.65±0.49 [a]
LSD	5.52	1.56	-
	Peeled dry sample		
Apple banana	75.60±1.41 [b]	0.30±0.10 [ab]	17.10±0.14 [b]
Gros Michel AAA	66.20±0.00 [c]	2.20±1.44 [a]	16.80±0.32 [b]
Kiganda AAA	64.20±0.14 [d]	0.10±1.54 [ab]	21.00±1.12 [a]
Muraru AAA	83.10±1.13 [a]	-1.10±0.00 [b]	16.50±0.06 [b]
LSD	1.50	2.48	1.00
	Unpeeled dry sample		
Apple banana	77.40±0.07 [a]	1.05±0.64 [a]	17.75±1.48 [a]
Gros Michel AAA	66.55±1.34 [b]	1.05±0.35 [a]	16.65±0.07 [a]
Kiganda AAA	61.05±0.49 [c]	1.80±0.85 [a]	18.10±0.14 [a]
Muraru AAA	76.15±2.62 [a]	0.95±1.20 [a]	16.45±0.49 [a]
LSD	2.49	-	-

*L** (Lightness/ darkness), *a** (redness/greenness) and *b** (yellowness/blueness). Mean values with different superscripts in the same column for each treatment (peeled or un-peeled) are significantly different ($p \leq 0.05$; one-way ANOVA, *LSD* post hoc test).

Table 4.7: Colour parameters for both fresh and dried banana slices for open sun

Banana variety	*L**(±Std)	*a**(±Std)	*b**(±Std)
	Peeled fresh sample		
Apple banana	87.22±0.03 [a]	4.57±0.30 [c]	25.75±3.79 [a]
Gros Michel AAA	78.63±0.54 [b]	8.24±0.13 [a]	30.56±1.41 [a]
Kiganda AAA	86.16±4.40 [a]	6.76±0.68 [b]	29.63±1.34 [a]
Muraru AAA	88.16±1.03 [a]	3.28±1.11 [d]	25.42±1.98 [a]
LSD	4.30	1.15	-
	Unpeeled fresh sample		
Apple banana	83.21±7.73 [a]	0.35±3.05 [a]	23.10±10.80 [a]
Gros Michel AAA	76.95±0.71 [a]	0.60±7.64 [a]	28.15±1.85 [a]
Kiganda AAA	66.39±23.49 [a]	2.25±8.56 [a]	30.03±4.68 [a]
Muraru AAA	75.80±18.35 [a]	-0.48±4.60 [a]	25.65±1.97 [a]
LSD	-	-	-
	Peeled dry sample		
Apple banana	68.20±2.08 [a]	35.88±7.44 [a]	12.05±1.17 [b]
Gros Michel AAA	70.15±0.11 [a]	15.58±0.40 [b]	11.60±1.44 [b]
Kiganda AAA	71.67±6.04 [a]	16.62±1.46 [b]	13.25±1.68 [b]
Muraru AAA	71.93±0.90 [a]	18.55±1.78 [b]	17.90±1.53 [a]
LSD	-	6.94	2.73
	Unpeeled dry sample		
Apple banana	65.45±6.83 [a]	25.63±11.16 [a]	12.87±1.54 [a]
Gros Michel AAA	64.19±0.31 [a]	15.18±10.70 [a]	13.46±2.43 [a]
Kiganda AAA	60.54±1.61 [a]	18.40±1.58 [a]	15.40±0.96 [a]
Muraru AAA	64.68±6.13 [a]	18.48±0.57 [a]	15.36±3.01 [a]
LSD	-	-	-

*L** (Lightness/ darkness), *a** (redness/greenness) and *b** (yellowness/blueness). Mean values with different superscripts in the same column for each treatment (peeled or un-peeled) are significantly different ($p \leq 0.05$; one-way ANOVA, *LSD* post hoc test).

The total colour difference (ΔE^*) was found to be in the range of 7.04±0.29 to 24.27±2.52, 4.86±0.93 to 16.53±12.81, 6.02±0.02 to 21.71±2.28 and 22.06±2.44 to 39.14±7.63, for solar, biomass, solar-biomass and open sun dried banana slices, respectively (Table 4.8). The final product had a darker colour compared to the corresponding fresh product. It was noted that there was colour change for all the modes used with open sun drying having the highest value of colour difference indicating that drying under open sun resulted in least preservation of colour. The colour change during drying was attributed to enzymatic browning as a result of

differences in phenolic compounds (Amankwah *et al*., 2019), which are associated with oxidative browning of the banana slices. Barroca and Guiné (2013) made similar observations while drying two banana varieties, namely *Musa nana* and *Musa cavendishii*, in a convective dryer.

Table 4.8: Total colour difference of banana slices dried using various drying methods

Banana variety	Total colour difference (ΔE^*) (±Std) for each drying method				
	Solar mode	Biomass mode	Solar-biomass mode	Open sun	*LSD*
			Peeled		
Apple banana	7.04±0.29 ^{b}	9.26±2.36 ^{b}	7.48±0.37 ^{b}	39.14±7.63 ^{a}	6.80
Gros Michel AAA	19.00±0.10 ^{b}	4.86±0.93 ^{c}	18.39±1.98 ^{b}	22.06±2.44 ^{a}	2.76
Kiganda AAA	16.91±0.91 ^{c}	5.03±1.89 ^{d}	21.16±0.61 ^{b}	25.13±3.21 ^{a}	3.25
Muraru AAA	16.65±2.00 ^{b}	4.88±1.56 ^{c}	6.02±0.02 ^{c}	23.58±4.32 ^{a}	4.28
			Unpeeled		
Apple banana	11.84±8.45 ^{b}	6.12±0.80 ^{b}	7.63±1.51 ^{b}	33.43±13.10 ^{a}	15.84
Gros Michel AAA	19.49±2.56 ^{a}	16.53±12.81 ^{a}	14.83±1.05 ^{a}	27.28±7.01 ^{a}	-
Kiganda AAA	24.27±2.52 ^{a}	13.67±11.16 ^{a}	21.71±2.28 ^{a}	28.54±1.64 ^{a}	-
Muraru AAA	14.03±1.33 ^{b}	11.53±3.25 ^{bc}	9.87±1.48 ^{c}	26.15±0.31 ^{a}	3.25

Mean values within rows with different superscripts are significantly different ($p \leq 0.05$; one-way ANOVA, *LSD* post hoc test).

The average hue angle values for fresh and dried banana slices were found to be 79.54±3.40 and 51.26±5.99, 76.26±4.31 and 67.57±4.13, 92.69±4.37 and 88.47±3.54 and 7.89±3.03 and 36.89±9.79, for solar, biomass, solar-biomass and open sun dried banana slices, respectively. There was significance difference in the average hue angle of fresh and dried banana slices t (14) = 11.61, p = 0.00000001; t (14) = 4.11, p = 0.001, t (14) = 2.13, p = 0.05 and t (14) = 11.86, p = 0.00000001 for solar, biomass, solar-biomass and open sun drying, respectively and hence rejecting the null

hypothesis in (e) on basis of colour. These results indicated that each energy mode had an effect on the hue angle of the dried product. Precisely, the results suggested that after drying the hue angle of the banana slices decreased indicating a change of colour from yellow to red. It also shows that colour saturation intensified during drying due to enzymatic browning as earlier cited.

4.5.2. Changes in firmness during drying

The firmness of the banana slices before and after drying using different drying methods appears in Figure 4.24. The average firmness values for fresh and dried banana slices were 2.1±0.44 and 7.33±1.75 N, 2.35±0.62 and 5.23±1.43 N, 2.38±0.38 and 6.36±1.62 N and 2.21±0.44 and 6.28±1.28 N for solar, biomass, solar-biomass and open sun-dried banana slices, respectively. The percentage increase in firmness was in the range of 151.28±56.04% to 317.50±8.92%, 98.08±14.96% to 153.19±60.54%, 91.30±61.49% to 233.33±26.07% and 125.64±36.26% to 262.50±12.62% for solar, biomass, solar-biomass and open sun-dried banana slices, respectively (Table 4.9). The results indicated that the firmness values of dried banana slices were higher than those of fresh banana slices for all the treatments. The increase in firmness was attributed to reduction in moisture content of the banana slices responsible for collapse of the cell structure during drying. Furthermore, the results showed that banana slices dried using solar mode had the highest increase in firmness value compared to other modes indicating there was rapid removal of surface moisture content leading to increased case hardening of the slices (Omolola *et al.,* 2018). The results suggested that the samples dried using solar mode would require more energy in grinding compared to

other drying modes. The drying of agricultural products has exhibited similar behaviour. Rodriguez *et al*. (2019) observed that dried raspberries had higher firmness than fresh raspberries. The values of firmness are in the range of values reported by Omoloa *et al*, (2018). The authors reported hardness values of 1.15 to 14.62 N and 1.28 to 14.29 N of dried ripe banana slices (*Musa spp*., AAA group, *cv* '*Luvhele*' and '*Mabonde*'). In addition, Swasdisevi *et al*. (2007) reported hardness values of 3 mm Cavendish banana slices dried at a pressure of 5 kPa and temperatures of 50, 55 and 60^{o}C in the range of 6.23±0.17 and 6.29±0.12 N.

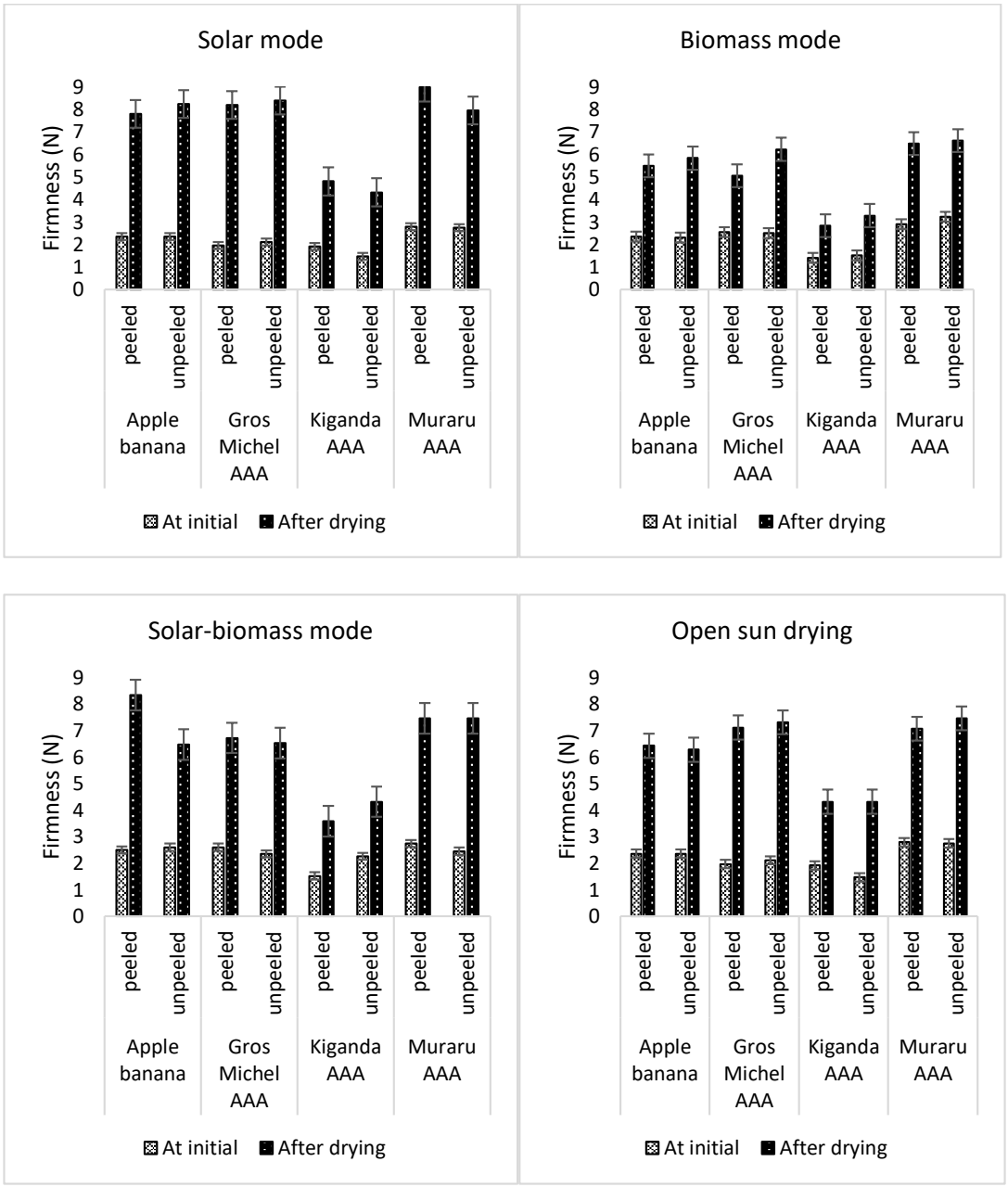

Figure 4.24: Comparison of banana slice firmness before and after drying using different drying methods.

Table 4.9: Percentage increase in firmness of banana slices dried using different drying methods

Banana variety	Increase in firmness (±Std) % for each drying method				
	Solar mode	Biomass mode	Solar-biomass mode	Open sun	*LSD*
			Peeled		
Apple banana	231.25±61.87 ^{ab}	133.33±18.13 ^{c}	233.33±26.07 ^{a}	172.92±23.26 ^{abc}	86.17
Gros Michel AAA	317.50±8.92 ^{a}	98.08±14.96 ^{d}	158.49±22.89 ^{c}	262.50±12.62 ^{b}	26.07
Kiganda AAA	151.28±56.04 ^{a}	100.00±37.71 ^{a}	135.48±33.01 ^{a}	125.64±36.26 ^{a}	-
Muraru AAA	221.05±48.01 ^{a}	123.73±29.00 ^{b}	171.43±21.49 ^{ab}	152.63±9.15 ^{b}	64.71
			Unpeeled		
Apple banana	250.00±58.93 ^{a}	153.19±60.54 ^{a}	149.06±28.97 ^{a}	166.67±58.93 ^{a}	-
Gros Michel AAA	297.67±3.30 ^{a}	149.01±23.27 ^{c}	177.08±35.36 ^{c}	246.51±27.27 ^{b}	44.38
Kiganda AAA	193.33±34.75 ^{a}	116.13±10.46 ^{ab}	91.30±61.49 ^{b}	193.33±39.74 ^{a}	96.01
Muraru AAA	189.29±12.06 ^{a}	104.55±25.54 ^{b}	204.00±0.24 ^{a}	171.43±58.59 ^{ab}	69.27

Mean values within rows with different superscripts are significantly different ($p \leq 0.05$; one-way ANOVA, *LSD* post hoc test).

There was significance difference in the average firmness values of fresh and dried banana slices t (14) = 8.02, p = 0.000001; t (14) = 5.21, p = 0.0001, t (14) = 6.76, p = 0.00001 and t (14) = 8.50, p = 0.0000007 for solar, biomass, solar-biomass and open sun drying, respectively and hence rejecting the null hypothesis in (e) on basis of firmness. These results suggested that drying had an effect on the firmness value of the dried product. Explicitly, the results suggested that the firmness value of the banana slices increased during drying due to fusing of cell structure during drying. This phenomenon was attributed to reduction in banana slices moisture content as earlier cited.

4.5.3. Changes in vitamin C during drying

The average amount of initial vitamin C content was found to be 53.25, 38.92, 38.39 and 38.27 mg/100g for Apple banana, Kiganda AAA, Gros Michel AAA and Muraru AAA, respectively. These amounts reduced to 43.18, 33.11, 34.27 and 35.50 mg/100g after drying, respectively. The percentage retention was found to be in the range of 72.44±3.96% to 85.87±2.64%, 69.23±14.14% to 86.90±2.84%, 63.85±3.19% to 87.19±13.97% and 62.32±4.82% to 77.14±6.38% for solar, biomass, solar-biomass and open sun drying respectively. The values of the percentage retention of vitamin C for dried banana slices are presented in Table 4.10. The percentage retention was a comparison of the amount of vitamin C content in the dried banana slices to the amount that was present in fresh banana slices and thus the values were less than 100% indicating a decrease in the amounts after drying. The decrease in vitamin C after drying was attributed to various factors which led to its destruction during drying such as exposure of the product to oxygen, light, temperature and relative humidity (Şahin *et al*., 2010). In addition, the reduction in vitamin C during drying has been observed by Amankwah *et al*. (2019) and Şahin *et al.* (2010). The percentage retention values are of similar magnitude to those reported by Ndayambaje *et al.* (2019). The authors reported a percentage retention of vitamin C of 74.54% for unripe sun-dried plantain (*Musa paradisiaca*).

Table 4.10: Percentage retention of vitamin C for banana slices dried using different drying methods

Banana variety	Retention of vitamin C (±Std)% for each drying method				
	Solar mode	Biomass mode	Solar-biomass mode	Open sun	*LSD*
			Peeled		
Apple banana	77.84±11.88 [ab]	86.90±2.84 [a]	82.08±7.85 [a]	68.86±7.14 [b]	15.52
Gros Michel AAA	78.40±1.96 [a]	69.23±14.14 [a]	87.19±13.97 [a]	72.60±1.48 [a]	-
Kiganda AAA	79.19±8.41 [a]	79.20±5.96 [a]	77.10±7.32 [a]	77.14±6.38 [a]	-
Muraru AAA	72.44±3.96 [b]	84.98±4.14 [a]	63.85±3.19 [c]	62.32±4.82 [c]	5.43
			Unpeeled		
Apple banana	80.30±10.41 [a]	73.44±5.27 [a]	73.74±1.27 [a]	66.38±14.78 [a]	-
Gros Michel AAA	77.89±7.13 [a]	85.19±11.18 [a]	80.19±5.92 [a]	71.43±7.49 [a]	-
Kiganda AAA	85.87±2.64 [a]	85.19±4.12 [a]	80.53±16.31 [a]	72.36±2.53 [a]	-
Muraru AAA	76.53±6.06 [ab]	80.02±2.32 [a]	86.33±3.46 [a]	66.07±10.52 [b]	10.59

Mean values within rows with different superscripts are significantly different ($p \leq 0.05$; one-way ANOVA, *LSD* post hoc test).

It was noted that the amount of vitamin C for fresh and dried sample varied for the different banana cultivars and peeled samples had higher vitamin C content as compared to unpeeled samples with exception of Kiganda AAA under open sun (Figure 4.25). The amount of vitamin C present in any given variety was attributed greatly to the genotype of the fruit as the samples were obtained from matching locations sharing similar agro-climatic zone (UM2) and cultural practices as earlier specified. Similarly, Hapsari and Lestari (2016) reported different vitamin C content for four Indonesian banana cultivars ranging from 16.45 to 30.27 mg/100 g of the edible portion with an average of 22.84 mg/100 g of the edible portion. It was noted that though the samples had lower vitamin C content compared to recommended daily intake of 70mg, unripe bananas contain high amounts of resistance starch which improves digestion as it is not digested in the small intestine but ferments in the large

intestine causing proliferation of beneficial bacteria in the body as reported in literature (Bezerra *et al.*, 2013; Kumar *et al*., 2012). Additionally, to achieve the recommended daily intake amounts of vitamins and minerals the products require further fortification. These results can be used in selection of the banana variety to be used depending on the intended use of the dried product.

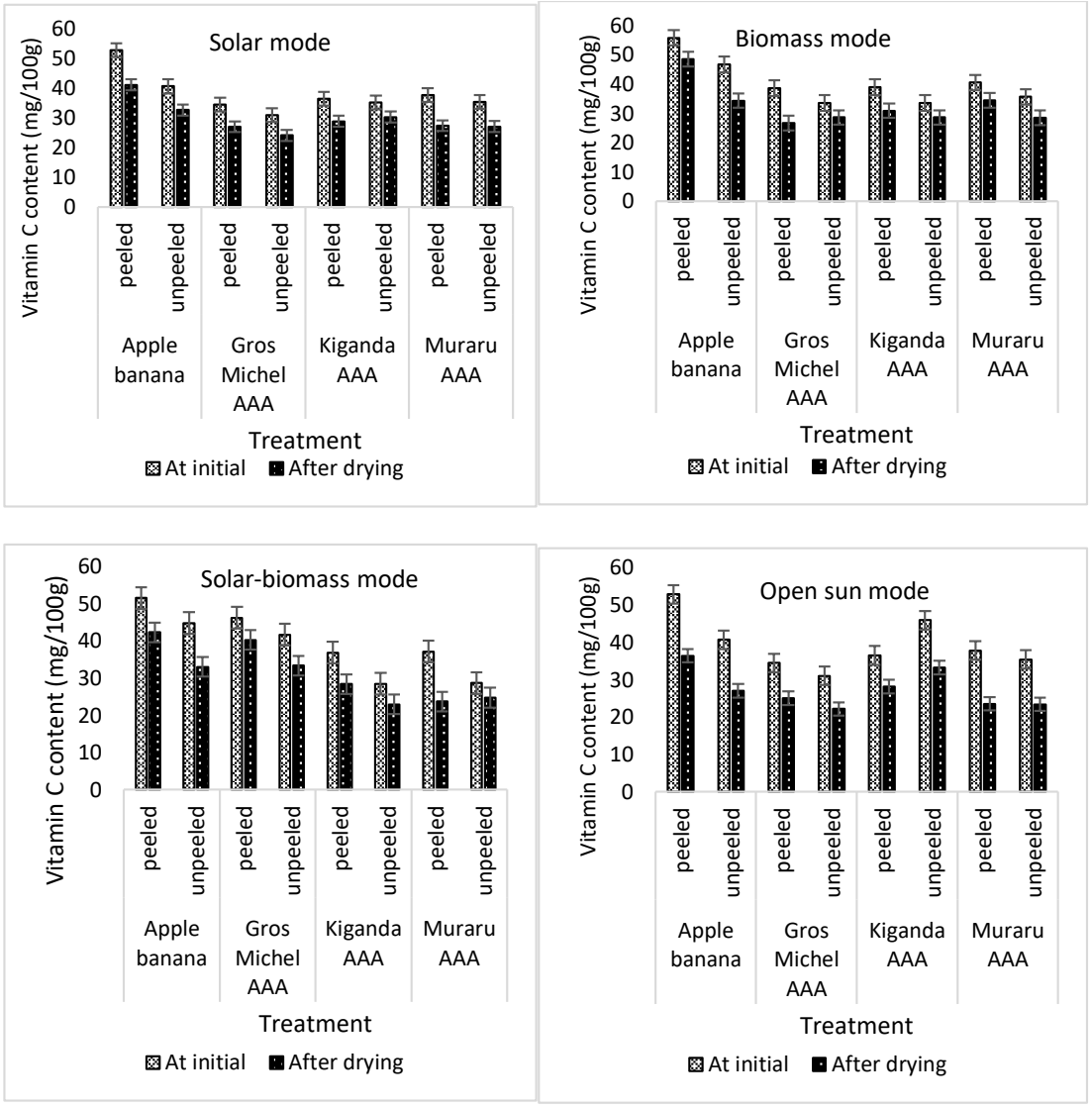

Figure 4.25: Comparison of vitamin C content before and after drying using different drying methods.

The average amount of vitamin C for fresh and dried banana slices were found to be 37.98±6.61 and 29.82±5.22, 40.38±7.56 and 32.52±7.03, 39.37±8.22 and 31.07±7.43 and 39.31±7.04 and 27.35±5.07, for solar, biomass, solar-biomass and open sun dried banana slices, respectively. There was significance difference in the average amount of vitamin C of fresh and dried banana slices t (14) = 2.74, p = 0.016; t (14) = 2.15, p = 0.05, t (14) = 2.12, p = 0.05 and t (14) = 3.90, p = 0.002 for solar, biomass, solar-biomass and open sun drying, respectively and hence rejecting the null hypothesis in (e) on basis of vitamin C. These results showed that each energy mode had an effect on the amount of Vitamin C of the dried product. Precisely, the results suggested that after drying the amount of vitamin C of the banana slices decreased as it is thermo-sensitive as earlier cited.

4.5.4. Quality of dried banana slices after optimization of the dryer

The overall means and standard deviation of the colour difference for optimized biomass and solar-biomass mode appear in Table 4.11. The total colour difference was in the range of 6.24±1.83 to 15.47±7.64 and 6.46 ±0.38 to 14.39±0.38 for biomass and solar-biomass mode, respectively. These values of colour change are lower than colour change values reported in the un-optimized system. Figures 4.26 and 4.27 show the comparison of banana slice firmness before and after drying using optimized modes. The overall percentage increase in firmness for biomass and solar biomass mode was 172.51±22.31 and 200.39±56.66%, respectively. The values showed higher firmness in the dried product in the optimized dryer compared to un-optimized dryer. Figures 4.28 and 4.29 show the comparison of vitamin C content before and after drying using

the optimized modes. The optimized drying resulted in percentage retention of vitamin C of 92.27±2.95% and 87.92±6.03% for biomass and solar-biomass modes, respectively. These percentages are higher than the percentage retention obtained in the un-optimized dryer. Therefore, by optimizing the dryer exergy efficiency, there was improvement in the quality of the dried product as it had less colour change, higher percentage increase in firmness and higher retention of vitamin C as compared to previous un-optimized values presented in Sections 4.5.1 to 4.5.3.

Table 4.11: Total colour difference of banana slices dried using optimized dryer

Variety	Total colour difference (ΔE^*) (±Std) for each drying method	
	Biomass mode	Solar-biomass mode
	Peeled	
Apple banana	9.01 ±0.34	6.75 ±1.66
Gros Michel AAA	9.37 ±2.24	6.46 ±0.38
Kiganda AAA	6.24±1.83	8.45±3.11
Muraru AAA	9.11±1.24	8.36±2.73
	Unpeeled	
Apple banana	10.89±5.33	7.51±0.32
Gros Michel AAA	15.47±7.64	14.39±0.38
Kiganda AAA	6.84±3.69	13.42±3.11
Muraru AAA	9.48±2.07	9.33±5.80

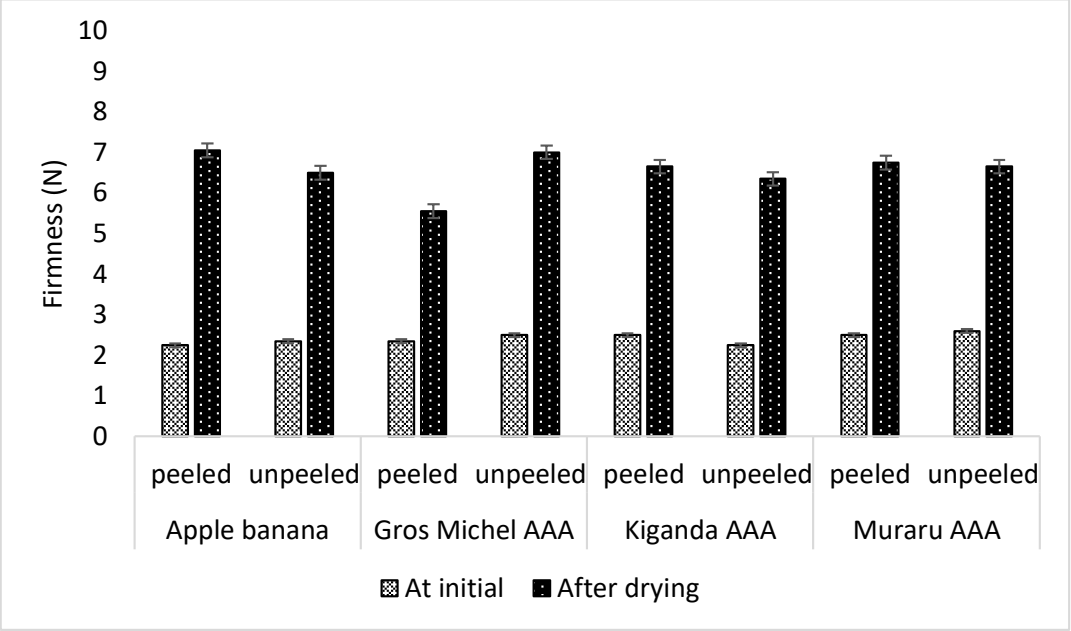

Figure 4.26: Comparison of banana slice firmness before and after drying using optimized biomass mode.

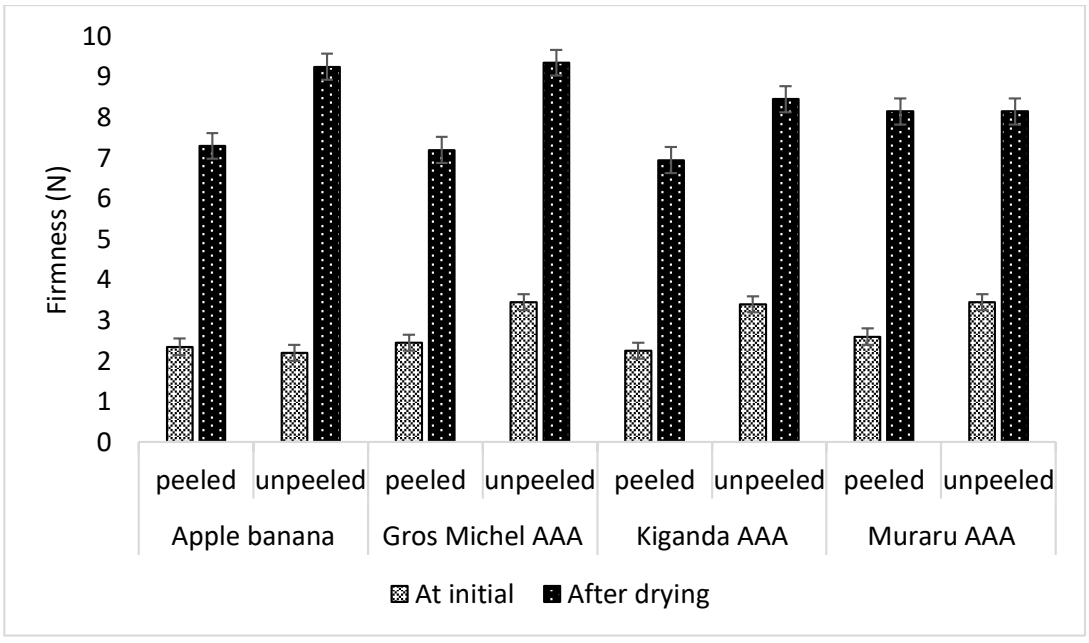

Figure 4.27: Comparison of banana slice firmness before and after drying using optimized solar-biomass mode.

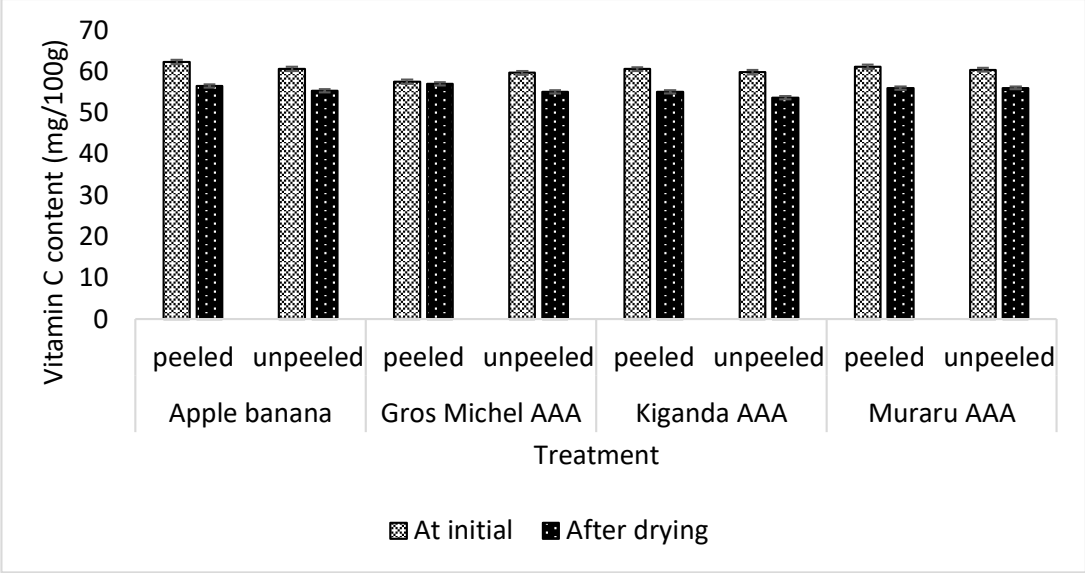

Figure 4.28: Comparison of vitamin C content before and after drying using optimized biomass mode.

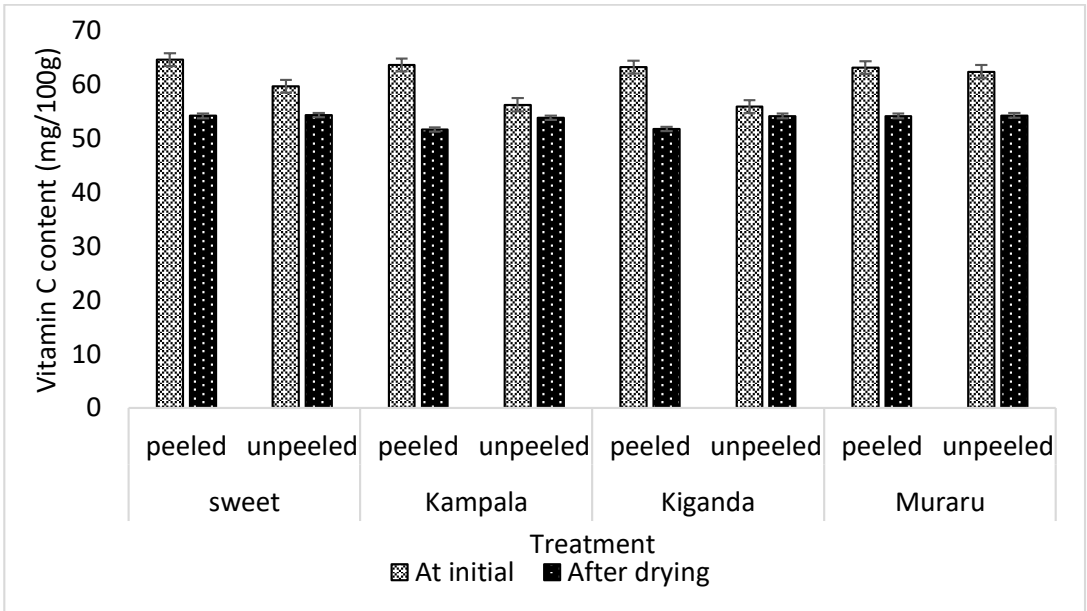

Figure 4.29: Comparison of vitamin C content before and after drying using optimized solar-biomass mode.

CHAPTER FIVE

CONCLUSIONS AND RECOMMENDATIONS

5.1. Conclusions

The specific conclusions drawn from this study are as follows:

1. The developed computer models for simulating drying time for banana slices using a solar-biomass hybrid greenhouse dryer gave reasonable estimates of drying time (R^2 values of 0.8099, 0.5393 and 0.8845 for solar, biomass and solar-biomass modes, respectively). These models can be used for providing design data for solar-biomass greenhouse dryer and also for optimization of this type of a solar dryer.
2. The no load experiments of the developed solar-biomass greenhouse dryer exhibited high temperature gains in the drying air and lower relative humidity of 16.61±6.81^{o}C and 9.77±17.89%, 8.20±1.42^{o}C and 20.60±7.44% and 16.77±5.77^{o}C and 21.48±13.94% for solar, biomass and solar-biomass modes, respectively, compared to ambient air. These conditions in the dryer indicated the potential of the drying air in holding more moisture as compared to ambient air. Thus, the dryer has a greater drying potential compared to open sun drying.
3. The results showed that using biomass as a supplemental heat source to solar energy during drying yields comparable drying rates to solar energy drying on a clear sky day. The average hourly exergy efficiency of drying air was found to be 64.60±24.78, 59.37±10.52 and 66.50±13.47%, for solar, biomass and solar-biomass modes, respectively. Energy and exergy efficiency for the solar mode drying was lower than that of biomass and solar-biomass modes. However, the analysis showed no statistical difference between the means for drying air exergy

efficiency for the three energy modes used in drying. Moreover, exergy analysis enabled identification of magnitudes and locations of energy losses and it provided useful information in choosing the most suitable parameters for optimization.

4. The optimization results showed that solar and solar-biomass modes required the same airflow rate (0.05 kg/s) indicating that at these combinations the dryer received almost equal energy input. Biomass mode trade-offs indicated that a lower flow rate (0.01 kg/s) was required for drying. Further, both solar-biomass and biomass modes must maintain a fuel feed rate of 0.001 kg/s for maximum exergy efficiency (solar-biomass: 80.21±14.26%; biomass: 79.28±10.38%) and drying air temperature of 333 K. Performance evaluation of the optimized dryer showed that the optimized dryer provided a superior system compared to the un-optimized one ($p \leq 0.05$).
5. Regardless of the drying method, results obtained showed that the dried products were darker, firmer and had lower vitamin C content than the corresponding fresh products. Resulting total colour difference ranged from 7.04±0.29 to 24.27±2.52, 4.86±0.93 to 16.53±12.81, 6.02±0.02 to 21.71±2.28 and 22.06±2.44 to 39.14±7.63 for solar, biomass, solar-biomass and open sun drying, respectively. The percentage increase in firmness of banana slices after drying ranged between 151.28±56.04% to 317.50±8.92%, 98.08±14.96% to 153.19±60.54%, 91.30±61.49% to 233.33±26.07% and 125.64±36.26% to 262.50±12.62% for solar, biomass, solar-biomass and open sun drying, respectively. The reduction in vitamin C content ranged from 72.44±3.96% to 85.87±2.64%, 69.23±14.14% to 86.90±2.84%, 63.85±3.19% to 87.19±13.97% and 62.32±4.82% to 77.14±6.38%

for solar, biomass, solar-biomass and open sun drying respectively. However, drying of banana slices in the greenhouse dryer resulted in better conservation of quality compared to open sun drying.

5.2. Recommendations

5.2.1. Recommendations from this study

The recommendations drawn from this study are as follows:

a) The developed model should be used in estimation of drying time for the developed solar-biomass dryer to help in management of time during batch drying.

b) The optimized dryer and process parameters for each mode determined from this study should be adopted by users of the dryer to maximize exergy efficiency and drying air temperature.

c) It is recommended to dry produce in the solar-biomass greenhouse dryer as opposed to open sun drying as one achieves shorter drying period and better retention of colour and vitamin C. This is because using solar mode in the solar-biomass greenhouse dryer, the moisture content reduced from74.1±4.9% to 16.2±3.6% while open sun drying reduced to 32.81±3.6% after 11 hours.

d) It is recommended that during low solar radiation (radiations below 300 W/m^2), use of biomass energy to complement solar energy is important so as to achieve drying rates comparable to using solar mode. Moreover, products dried using biomass mode (night time) can be further dried using solar mode to achieve safe moisture levels for storage. This combination shortens the solar hours required for drying and will ensure continuity of drying during peak demand.

e) It was observed that among the four banana varieties, Apple banana had the highest amounts of vitamin C (53.25 and 43.18 mg/100g) while Muraru AAA had the least (38.27 and 35.50 mg/100g) for fresh and dried samples, respectively. These results can be used in guiding the selection of the banana variety to be used depending on the intended use of the dried product.

f) The dried banana slices can be milled into flour, fortified and used alone or used to formulate composite flours for producing low gluten products.

5.2.2. Recommendations for further research

The following are recommendations for further studies:

a) The developed model used average hourly measured data in the prediction of drying time. The possibility of using real-time data together with equations obtained in Appendix III in estimating the drying time should be explored.

b) A decision support system to manage product drying in the developed dryer by incorporating drying time models into a software module to manage the drying process should be considered in future studies.

c) The development of the designed solar-biomass dryer was for 200 µ polythene film glazing material. The possibility of using other polythene film thicknesses as a glazing material in the development of the dryer should be investigated.

d) The optimization performed in this study was based on maximizing exergy efficiency and drying air temperature. Further optimization based on other extensive thermodynamic properties of the system should be explored.

e) Evaluation of the optimized solar mode drying was not effectively performed due to season conditions. The performance of the optimized solar mode during the summer season when the solar radiation is above 300 W/m^2 for most hours of the day should be investigated.

f) The analysis of the dried product detailed in this work focused on colour, vitamin C content and firmness. Other dried food properties such as aroma, taste and acceptance of the dried product should be investigated.

REFERENCES

Abano, E. E. (2010). Assessments of drying characteristics and physio-organoleptic properties of dried pineapple slices under different pre-treatments. *Asian Journal of Agricultural Research, 4*(3), 155-161.

Abano, E. E., and Sam-Amoah, L. K. (2011). Effects of different pre -treatments on drying characteristics of banana slices. *ARPN Journal of Engineering and Applied Sciences 6*(3), 121-129.

Abhay, B. L., Chandramohan, V. P., and Raju V. R. K. (2019). Energy and exergy analysis on drying of banana using indirect type natural convection solar dryer. *Heat Transfer Engineering, 1*(1), 1-11.

Adefemi, A. O., and Ilesanmi, D. A. (2018). Development and optimisation of drying parameters for low-cost hybrid solar dryer using response surface method. *Journal of Sustainable Bioenergy Systems, 8*(2), 23-35.

Adeniji, T. A., Tenkouano, A., Ezurike, J. N., Ariyo, C. O., and Vroh-Bi, I. (2010). Value-adding postharvest processing of cooking bananas (*Musa spp*. AAB and ABB genome groups): A Review. *African Journal of Biotechnology, 9*(54), 9135-9141.

Aduewa, T. O., Ogunlowo, A. S., and Ojo, S. T. (2014). Development of hot-air supplemented solar dryer for white yam (*Dioscorea rotundata*) Slices. *Journal of Agriculture and Veterinary Science, 7*(12), 114-123.

Agriculture and Food Authority (AFA). (2017). Creating wage employment in horticulture sector in Kenya. Agriculture and Food Authority. Retrieved from *https://agricultureauthority.go.ke*.

Ahamed, J. U., Saidur, R., and Masjuki, H. H. (2011). A review on exergy analysis of vapour compression refrigeration system. *Renewable and Sustainable Energy Reviews, 15*(3), 1593-600.

Akpinar, E. K. (2011). Drying of parsley leaves in a solar dryer and under open sun: modeling, energy and exergy aspects. *Journal of Food Process Engineering, 34*(1), 27-48.

Alagbe, E. E., Amlabu, Y. S., Daniel, E. O., and Ojewumi, M. (2020). Effect of varying drying temperature on the soluble sugar and nutritional content of banana. *The Open Chemical Engineering Journal, 14*(1), 11-16.

Almuhanna, E. A. (2012). Utilization of a solar greenhouse as a solar dryer for drying dates under the climatic conditions of Eastern Province of Saudi Arabia. Part 1: Thermal performance analysis of a solar dryer. *Journal of Agricultural Science, 4*(3), 237-246.

Amankwah, E., Kyere, G., Kyeremateng, H., and van Boxtel, A. (2019). Experimental verification of yam (*Dioscorea rotundata*) drying with solar adsorption drying. *Applied Science, 9*(18), 1-15.

Amer, B. M., Hossain, M. A., and Gottschalk, K. (2009). Design and performance evaluation of a new hybrid solar dryer for banana. *Energy Conversion and Management, 51*(4), 813-820.

Anand, C., Vivek, V., Arun, M., and Bhaskar, T. (2020). Natural convection and direct type (NCDT) solar dryers: a review. *Drying Technology, 38*(7), 1-22.

Arun, S., Velmurugan, K., and Kumar, V. K. (2014). Optimization and comparison studies of solar tunnel greenhouse dryer coupled with and without biomass

back-up heater. *International Journal of Innovative Science and Modern Engineering, 2*(11), 41-47.

Association of Official Analytical Chemists. (2010). Official methods of analysis of AOAC International, 18th Edition, Washington DC, USA.

Aurore, G., Parfait, B., and Fahrasmane, L. (2009). Bananas, raw materials for making processed food products. *Trends in Food Science and Technology,20*(2),78-91.

Ayyappan, S. (2018). Performance and CO_2 mitigation analysis of a solar greenhouse dryer for coconut drying. *Energy and environment, 29*(8), 1482-1494.

Bala, B. K., and Janjai, S. (2013). Solar drying of agricultural products. *Stewart postharvest review, 2*(4), 1-8.

Bansal, A. Gupta, U., and Singh, S. (2020). Optimization of Flat Plate Solar Dryer using Taguchi Method. *International Journal of Engineering and Advanced Technology, 9*(4), 815-821.

Barki, E., Ukwenya, J., and Idoko, F. (2019). Exergy analysis of solar dryer with a back-up incinerator. *International Journal of Engineering Technologies and Management Research, 6*(8) 12-20.

Barnwal, P., and Tiwari, A. (2008). Design, Construction and Testing of Hybrid Photovoltaic Integrated Greenhouse Dryer. *International Journal of Agricultural Research, 3*(2), 110-120.

Barroca, M. J., and Guiné, R. (2013). Variation of physical properties of banana along drying for cvs. *Musa nana* and *Musa cavendishii*. Conference paper. Conference: VII Congreso Ibérico de Agroingeniería y Ciencias Hortícolas, At Madrid, Espanha.

Bennamoun, L. (2012). An overview on application of exergy and energy for determination of solar drying efficiency. *International Journal of Energy Engineering, 2*(5), 184-194.

Bezerra, C. R., Antônio, A. E., and Silva, L. (2013). Nutritional potential of green banana flour obtained by drying in spouted bed. *Revista Brasileira de Fruticultura, 35*(4), 1140-1146.

Bradley, N. (2007). The response surface methodology. Master of Science in Applied Mathematics and Computer Science, Indiana University of South Bend, USA.

Brat, P., Bugaud, C., Guillermet, C., and Salmon, F. (2019). Review of banana green life throughout the food chain: From auto-catalytic induction to the optimisation of shipping and storage conditions. *Scientia Horticulturae, 262*(1), 1-13.

Buditjahjanto, A., Hariadi, M., and Purnomo, M. H. (2011). A hybrid intelligent system for decision making. *Journal of Applied Sciences Research, 7*(3), 274-285.

Butts, C. L., Davidson, Jr. J. I., Lamb, M. C., Kandala, C. V., and Troeger, J. M. (2004). Estimating drying time for a stock peanut curing decision support system. *Transactions of the ASAE, 47*(3), 925-932.

Condori, M., and Saravia, L. (2003). Analytical model for the performance of the tunnel-type greenhouse drier. *Renewable Energy, 28*(3), 467-485.

Delphine, A., Angeline, B., Allan, B., Penelope, P., Rony, S., and Maryke, L. (2019). Recent advances in banana (*Musa spp*.) bio-fortification to alleviate vitamin A

deficiency. *Critical Reviews in Food Science and Nutrition, 59*(21), 3498-3510.

Dependra, U., and Jagrit, B. (2014). Development of heat exchangers for water pasteurization in improved cooking stove. *International Journal of Engineering Research and General Science, 2*(1), 6-14.

Dhumne L. R., Bipte, V. H., and Jibhkate, Y. M. (2016). Optimization of solar tunnel dryer using genetic algorithm. *International Research Journal of Engineering and Technology, 3*(4), 1297-1300.

Dincer, I. (2002). On energetic, exergetic and environmental aspects of drying systems. *International Journal of Energy Research, 26*(8), 717-727.

Dragicevic, S. M. (2011). Determining the optimum orientation of a greenhouse on the basis of the total solar radiation availability. *Thermal science, 15*(1), 215-221.

Dronachari, M., and Shriramulu. (2019). Application of different types solar dryers in agriculture crops- a review. *International Journal of Pure and Applied Biosciences, 7*(2), 303-326.

Durillo, J. J., and Nebro, A. J. (2011). jMetal: A Java framework for multi-objective optimization. *Advances in Engineering Software, 42*, 760-771.

Efomah, A. N., and Gbabo, A. (2015). The physical, proximate and ultimate analysis of rice husk briquettes produced from a vibratory block mould briquetting machine. *International Journal of Innovative Science, Engineering and Technology, 2*(5), 814-822.

Ehiem, J. C., Irtwange, S. V., and Obetta, S. E. (2009). Design and development of an industrial fruit and vegetable dryer. *Research Journal of Applied Sciences, Engineering and Technology, 1*(2), 44-53.

Erbay, Z., and Hepbasli A. (2013). Advanced Exergy Analysis of a Heat Pump Drying System Used in Food Drying. *Drying Technology, 31*(7), 802-810.

Erbay, Z., and Icier, F. (2010). A review of thin layer drying of foods: Theory, Modelling, and Experimental Results. *Critical Reviews in Food Science and Nutrition, 50*(5), 441-464.

Fadhel, M. I., Abdo, R. A., Yousif, B. F., Zaharim, A., and Sopian, K. (2011). Thin-layer drying characteristics of banana slices in a force convection indirect solar drying. In: 6th IASME/WSEAS International Conference on Energy and Environment: Recent Researches in Energy and Environment, Cambridge, United Kingdom: 310-315.

Feng, H., Yin, Y., and Tang, J. (2012). Microwave drying of food and agricultural materials: Basics and heat and mass transfer modelling. *Food Engineering Reviews, 4*(2), 89-106.

Florea, A., Cofaru, I., Roman, L., and Cofaru, N. (2016). Applying the multi-objective optimization techniques in the design of suspension systems. *Journal of Digital Information Management, 14*(6), 351-367.

Food Agricultural Organization (FAO). (2014). Global initiative on food loss and waste reduction-save food. Food Loss Assessments: Causes and solutions. Case studies in small-scale agriculture and fisheries subsectors. Rome, Italy. Retrieved from *http://www.fao.org.*

Fudholi, A., Yendra, R., Basri, D. F., Ruslan, M. H., and Sopian, K. (2016). Energy and exergy analysis of hybrid solar drying system. *Contemporary Engineering Sciences, 9*(5), 215-223.

Fuentes-Zaragoza, E., Riquelme-Navarrete, M. J., Sánchez-Zapata, E., and Pérez-Álvarez, J. A. (2010). Resistant starch as functional ingredient: A review. *Food Research International, 43*(4), 931-942.

Genobiagon Jr., P. G., and Alagao, F. B. (2019). Performance of low-cost dual circuit solar assisted cabinet dryer for green banana. *Journal of Mechanical Engineering Research and Developments, 42*(1), 42-45.

Ghani, J. A., Choudhury, I. A., and Hassan, H. H. (2004). Application of Taguchi method in the optimization of end milling parameters. *Journal of Materials Processing Technology, 145*(1), 84-92.

Habwe, F. O., Walingo, K. M., and Onyango, M. O. A. (2008). Chapter 13 Using Food Science and Technology to Improve Nutrition and Promote National Development, Robertson, G.L. & Lupien, J.R. (Eds), © International Union of Food Science and Technology.

Hapsari, L., and Lestari, D. A. (2016). Fruit characteristic and nutrient values of four Indonesian banana cultivars (*Musa spp*.) at different genomic groups. *AGRIVITA Journal of Agricultural Science, 38*(3), 303-311.

Hegde, V. N., Hosur, V. S., Rathod, S. K., Harsoor, P., and Narayana, B. K. (2015). Design, fabrication and performance evaluation of solar dryer for banana. *Energy, Sustainability and Society, 5*(1), 1-12.

Hepbasli, A., Colak, N., Hancioglu, E., Icier, F., and Erbay, Z. (2010). Exergo-economic analysis of plum drying in a heat pump conveyor dryer. *Drying Technology, 28*(12), 1385-1395.

Horticultural Crops Directorate (2018). Nairobi Horticultural Centre, Kenya: Horticulture validated report 2017-2018.

Hrovatin, J., Prekrat, S., Oblak, L., and Ravnik, D. (2015). Ergonomic suitability of kitchen furniture. *Coll. Antropol, 39*(1), 185-191.

Intawee, P., and Janjai, S. (2011). Performance evaluation of a large-scale polyethylene covered greenhouse solar dryer. *International Energy Journal, 12*(1), 39-52.

International Institute of Tropical Agriculture. (2010). Annual Report 2010.

Islam, M. S., Haque, M. A., and Islam, M. N. (2012). Effects of drying parameters on dehydration of green banana (*Musa sepientum*) and its use in potato (*Solanum tuberosum*) chips formulation. *The Agriculturists, 10*(1), 87-97.

Janjai, S. (2012). A greenhouse type solar dryer for small-scale dried food industries: Development and dissemination. *International Journal of Energy and Environment, 3(*3), 383-398.

Janjai, S., Khamvongsa, V., and Bala, B. K. (2007). Development, design, and performance of a PV-ventilated greenhouse dryer. *International Energy Journal, 8*(4), 249-258.

Joshi, M., Kumar, N., and Baredar, P. (2019). Optimization of solar dryer using Taguchi Method. *International Journal of Recent Technology and Engineering, 8*(3), 3320-3326.

Kabubo, J., and Mulwa, R. (2019). Adaptation to climate change and climate variability and its implications for household food security in Kenya. *Food Security, 11*(6), 1289-1304.

Kadam, S. U., Tiwari, B. K., and O'Donnell, C. P. (2015). Improved thermal processing for food texture modification. *Modifying Food Texture, 1*(1), 115-131.

Kaddumukasa, P. Kyamuhangire, W., Muyonga, J., and Muranga, F. I. (2005). The effect of drying methods on the quality of green banana flour. *African Crop Science Conference Proceedings, 7*, 1267-1271.

Kassem, A. M., Habib, Y. A., Harb, S. K., and Kallil, K. S. (2011). Effect of architectural form of greenhouse solar dryer system on drying of onion flakes. *Egyptian Journal Agricultural Research, 89*(2), 627-638.

Kasyoka, M. R., Mwangi, M., Kori, N., Mbaka, J., and Gitonga, N. (2011). Banana distribution and their seed systems in central and eastern Kenya. *African Crop Science Conference Proceedings, 10*, 457-459.

Kasyoka, M. R., Mwangi, M., Mbaka, J., Kori, N., Gitonga, N., and Muasya, R. (2010). Preferred banana varieties and their seed systems in Eastern and Central provinces of Kenya. 2nd RUFORUM Biennial Meeting Entebbe, Uganda: 897-900.

Kazanci, B. O., Shukuya, M., and Olesen, B. W. (2016). Exergy performance of different space heating systems: A theoretical study. *Building and Environment, 99*, 119-129.

Kiburi, F. G., Kanali, C. L., and Mbuge. D. O. (2014). Evaluating the performance of super absorbent hydrogel in drying of seed maize under hermetic conditions. *Proceedings of 2014 International Conference on Sustainable Research and Innovation, 5*, 104-107.

Kiburi, F. G., Kanali, C. L., Kituu, G. M., Ajwang, P. O., and Ronoh, E. K. (2020). Performance evaluation and economic feasibility of a solar-biomass hybrid greenhouse dryer for drying banana slices. *Renewable Energy Focus, 34*(00), 60-68.

Kilalo, D., Olubayo, F., Obukosia, S. and Shibairo, S.I. (2009). Farmer management practices of citrus insect pests in Kenya [short communication]. *African Journal of Horticultural Science, 2*, 168-176.

Kituu, G. M., Shitanda, D., Kanali, C. L., Mailutha, J. T., Njoroge C. K., Wainaina, J. K., and Bongyereire, J. S. (2010). A simulation model for solar energy harnessing by the tunnel section of a solar tunnel dryer. *Agricultural Engineering International: the CIGR Ejournal. Manuscript 1553*, 12, 1-13.

Kituu, G. M., Shitanda, D., Kanali, C., Mailutha, T. T., and Wainaina, J. (2012). Artificial breeding of an optimized solar tunnel dryer using genetic algorithms. *International Journal of Sustainable Energy, 31*(5), 313-325.

Kivevele, T., and Huan, Z. (2014). A review on opportunities for the development of heat pump drying systems in South Africa. *South African Journal of Science, 110*(5/6), 1-11.

Kocer, A. A., Yuksel, Y. E., and Ozturk, M. (2014). Investigation of a biomass gasification system based on energy and exergy analysis. *Proceedings of the 5th International Symposium on Sustainable Development,* 187-196.

Koyuncu, T. (2006). An Investigation on the performance improvement of greenhouse type agricultural dryers. *Renewable Energy, 31*(7), 1055-1071.

Krishnan, S., and Sivaraman, B. (2017). Effect of slice thickness on quality of dried products in a solar cabinet dryer. *American-Eurasian Journal of Sustainable Agriculture, 11*(2), 1-7.

Kumar, P. S., Saravanana, A., Sheeba, N., and Uma, S. (2019). Structural, functional characterization and physicochemical properties of green banana flour from dessert and plantain bananas (*Musa spp.*). *LWT- Food Science and Technology, 116*, 1-12.

Kumar., S. K. P., Bhowmik, D., Duraivel, S., and Umadevi, M. (2012). Traditional and medicinal uses of banana. *Journal of Pharmacognosy and Phytochemistry, 1*(3), 51-63.

Lapczynska-Kordon, T., Fraczek, B., Slipek, J., and Ivanowa, Z. (2013). Genetic algorithms in optimization of dried fruits and vegetables quality. Engineering for Rural Development. 12th International Scientific Conference, Jelgava, Latvia, 628-632.

Lingayat, A., Chandramohan, V. P., and Raju, V. R. K. (2019). Energy and exergy analysis on drying of banana using indirect type natural convection solar dryer. *Heat Transfer Engineering, 41*(6-7), 551-561.

Lokeswaran, S., and Eswaramoorthy, M. (2013). Experimental studies on a solar drier system with a biomass back-up heater. *Energy Sources, Part A: Recovery, Utilization, and Environmental Effects*, *35*(5), 467-475.

Lukas, S., and Josef, R. (2014). Maize cobs for energetic use properties and challenges as fuel for small-scale combustion. *Proceedings of 2014 International Conference of Agricultural Engineering*, C0257.

Maina, B., Ambuko, J., Hutchinson, M. J., and Owino, W. O. (2019). The effect of waxing options on shelf life and postharvest quality of "ngowe" mango fruits under different storage conditions. *Advances in Agriculture, 2019*, 1-9.

Majdi, H., and Esfahani, J. (2018). Energy and drying time optimization of convective drying: Taguchi and LBM methods. *Drying Technology*, *37*(6), 722-734.

Manyumbu, E., Martin, V., and Fransson, T. (2014). Simple mathematical modelling and simulation to estimate solar-regeneration of a silica gel bed in a naturally ventilated vertical channel for Harare, Zimbabwe. *Energy Procedia*, *57*(1), 1733-1742.

Mathew, A. A., and Venugopal, T. (2018). Solar power drying system: a comprehensive assessment on types, trends, performance and economic evaluation. *International Journal of Ambient Energy*, *8*(1), 1-67.

Medeiros, L., and Remley, D. (2009). Drying fruits and vegetables. Ohio State University Extension; and, Extension. Ohio State, USA.

Menges, H. O., and Ertekin, C. (2006). Thin layer drying model for treated and untreated Stanley plums. *Energy Conversion and Management*, *47*(15), 2337-2348.

Mesmoudi, K., Soudani, A., and Bournet, P. (2010). Determination of the inside air temperature of a greenhouse with tomato crop under hot and arid climates. *Journal of Applied Sciences and Environmental Management, 5*(2), 117-129.

Michel, P. (2019). Exergy analysis and process optimization with variable environment temperature. *Energies, 12*(24), 3-19.

Mondru, M., Kumar, S., Rao, B., Smith, D. D., Venkata, H., Kumar, H., and Kumar, S. (2017). Performance evaluation of photovoltaic ventilated hybrid greenhouse dryer under no-load condition. *Agricultural Engineering International: CIGR Journal, 19*(2), 93-101.

Moreira, A., de Castro, C., and Fageria, N. K. (2010). Efficiency of boron application in an Oxisol cultivated with banana in the Central Amazon. *An Acad Bras Cienc, 82*(4), 1137-1145.

Morissette, R., Savoie, P., and Lizotte, P. (2011). Drying baled hay with combined solar and biomass heat sources. CSBE/SCGAB 2011 Annual Conference, Inn at the Forks, Winnipeg, Mb. Paper No. CSBE11-203.

Mortaza, A., Soleiman H., and Arun, S. M. (2015). Application of artificial neural networks (ANNs) in drying technology: A Comprehensive Review. *Drying Technology, 33*(12), 1-189.

Muchoki, C. N., Imungi, J. K., and Lamuka, P. O. (2007). Changes in beta-carotene, ascorbic acid and sensory properties in fermented, solar-dried and stored Cowpea leaf vegetables. *African Journal of Food, Agriculture, Nutrition and Development, 7*(3), 16-26.

Mugo, F., and Gathui, T. (2010). Biomass energy use in Kenya. A background paper prepared for the International Institute for Environment and Development for an international ESPA workshop on biomass energy, 19-21 October 2010, Parliament House Hotel, Edinburgh. Practical Action, Nairobi, Kenya.

Narayana, C. K., Jeyabaskaran, K. J., and Mustaffa, M. M. (2017). Chemical and mineral composition of four cultivars of banana (*Musa sp*.) belonging to different genomic groups grown in India. *International Journal of Current Microbiology and Applied Sciences, 6*(9), 2862-2867.

Ndayambaje, J. P., Dusengemungu, L., and Bahati, P. (2019). Nutritional composition of plantain flour of (*Musa paradisiaca*): the effect of various drying methods in Rwanda. *American Journal of Food Science and Technology, 7*(3), 99-103.

Ndindeng, S. A., Wopereis, M., Sanyang, S., Futakuchi, K., Atanga, N.S., Marco, W., Sidi, S., and Koichi, F. (2019). Evaluation of fan-assisted rice husk fuelled gasifier cook stoves for application in sub-Sahara Africa. *Renewable Energy, 139*, 924–935.

Ndirangu, S. N., Kanali, C. L., Mutwiwa, U. N., Kituu, G. M., and Ronoh, E. K. (2018). Analysis of designs and performance of existing greenhouse solar dryers in Kenya. *Journal of Postharvest Technology, 6*(1), 27-35.

Nguyen, M., and Price, W. E. (2007). Air drying of banana: influence of experimental parameters slab thickness, banana maturity and harvesting season. *Journal of Food Engineering, 79*(1), 200-207.

Njuguna, J., Nguthi, F., Wepukhulu, S., Wambugu, F., Gitau, D. Karuoya, M., and Karamura, D. (2008). Introduction and evaluation of improved banana

cultivars for agronomic and yield characteristics in Kenya. *African Crop Science Journal, 16(*1), 35-40.

Nwakuba, N. R., Asoegwu, S. N., and Nwaigwe, K. N. (2016). Energy requirements for drying of sliced agricultural products: A review. *Agricultural Engineering International: The CIGR Journal*, *18*(2), 144-154.

Nwakuba, N. R., Chukwuezie, O. C., Asoegwu, S. N., Nwandikom, G. I., and Okereke, N. A. A. (2018). A prediction model of energy requirements for drying of okra slices in a hybrid solar electric dryer. *Umudike Journal of Engineering and Technology, 4*(1), 155-163.

Okoroigwe, E. C., Eke, M. N., and Ugwu, H. U. (2013). Design and evaluation of combined solar and biomass dryer for small and medium enterprises for developing countries. *International Journal of Physical Sciences, 8*(25), 1341-1349.

Olutoye, P. A., and Uthamalingam, B. (2012). Mass-heater supplemented greenhouse dryer for post-harvest preservation in developing countries. *Journal of Sustainable Development*, *5*(10), 40-49.

Omiti J., Otieno, D., McCullogh, E., and Nyanamba, T. (2007). Strategies to promote market–oriented smallholder agriculture in developing countries: A case study of Kenya. *Proceedings of the Second International African Association of Agricultural Economics*, August 20–22, 2007, Accra, Ghana.

Omolola, A. O, Jideani A. I. O., and Kapila, P. F. (2015). Modelling of thin layer drying characteristics of banana cv. Luvhele. *Bulgarian Journal of Agriculctural Science, 21*(2), 342-348.

Omolola, A. O., Jideani A. I. O., Kapila, P. F., and Jideani, V. A. (2018). Optimization of oven drying conditions of banana (*Musa spp*., AAA Group, *cv* '*Luvhele*' and '*Mabonde*') using response surface methodology. *Agrociencia, 52* (4), 539-551.

Oyero J. O., Sadiku, S.O.E., Ajisegiri, E. S. A. and Eyo, A. A. (2007). Biochemical evaluation of enclosed solar dried and salted Oreochromis niloticus. *Research Journal of Animal Sciences, 1*(3), 97–101.

Ozgener, O., and Ozgener, L. (2009). Exergy analysis of drying process: An experimental study in solar greenhouse. *Drying Technology, 27*(4), 580–586.

Ozgener, O., and Ozgener, L. (2013). Three cooling seasons monitoring of exergetic performance analysis of an EAHE assisted solar greenhouse building. *Journal of Solar Energy Engineering, 135*(2), 1-7.

Panwar, N. L., Kaushik, S. C., and Kothari, S. (2013). Thermal modelling and experimental validation of solar tunnel dryer: a clean energy option for drying surgical cotton. *International Journal of Low-Carbon Technologies, 1*(0), 1-13.

Pekke, M. A., Pan, Z. L., Atungulu, G. G., Smith, G., and Thompson, J. F. (2013). Drying characteristics and quality of bananas under infrared radiation heating. *International Journal of Agriculture and Biological Engineering, 6*(3), 58-70.

Piotr, P. L., and Grzegorz, P. (2003). Effect of drying on microstructure of plant tissue. *Drying Technology, 21*(4), 657-683.

Poświata, A., and Szwast, Z. (2012). Discrete Hamiltonians for minimum of available Energy in bubble fluidized drying operations. *Proceedings of the World Congress on Engineering*, London, UK.

Prakash, O. M., and Kumar, A. (2014). Solar greenhouse drying: a review. *Renewable and Sustainable Energy Reviews, 29*(1), 905-910.

Querikiol, E. M., and Taboada, E. B. (2018). Drying kinetics of mango by-products in a greenhouse-type solar dryer using a wireless weighing scale. *International Journal of Applied Engineering Research, 13*(22), 15933-15943.

Rani, P., and Tripathy, P. P. (2020). Drying characteristics, energetic and exergetic investigation during mixed-mode solar drying of pineapple slices at varied air mass flow rates. *Renewable Energy, 167,* 508-519.

Rastvorov, D., Osintsev, K.V., and Toropov, E.V. (2017). Influence of burner form and pellet type on domestic pellet boiler performance. *IOP Conference Series: Earth and Environmental Science, 87*(032034), 1-6.

Rodriguez, A., Bruno, E., Paola, C., Campañone, L., Mascheroni, R. H. (2019). Experimental study of dehydration processes of raspberries (*Rubus idaeus*) with microwave and solar drying. *Food Science and Technology, 39*(2), 336-343.

Ronoh, E. K., Kanali, C. L., Mailutha, J. T., and Shitanda, D. (2010). Thin layer drying kinetics of amaranth (*Amaranthus cruentus*) grains in a natural convection solar tent dryer. *African Journal of Food, Agriculture, Nutrition and Development, 10*(3), 2218-2233.

Rosen, M. A., and Dincer, I. (2001). Exergy as the confluence of energy, environment and sustainability development. *Exergy International Journal, 1*(1), 3-13.

Sahdev, R. K., Kumar, M., and Dhingra, A. K. (2016). A review on applications of greenhouse drying and its performance. *Agricultural Engineering International: CIGR Journal, 18*(2), 395-412.

Şahin, F. H., Ülger, P., Aktas, T., and Orak, H. (2010). Effects of different drying techniques on some nutritional components of tomato (*Lycopersicon esculentum*). *Journal of Agricultural Machinery Science, 6*(1), 71-78.

Sangamithra, A., Gabriela, J. S., Prema, S. R., Priyavarshini, R., Chandrasekar, V., and Sasikala, S. (2014). An overview of a polyhouse dryer. *Sustainable Energy Reviews, 40*(1), 902-910.

Sangpradit, K. (2014). Study of the solar transmissivity of plastic cladding materials and influence of dust and dirt on greenhouse cultivations. *Energy Procedia, 56*, 566-573.

Santos, P. H. S., and Silva, M. A. (2008). Retention of vitamin C in drying processes of fruits and vegetables. A review. *Drying Technology, 26*(12), 1421-1437.

Sanusi, R. A., Odukoya, G. M., and Ejoh, S. I. (2018). Cooked yield and true nutrient retention values of selected commonly consumed staple foods in South-west Nigeria. *Africa Journal Biomedical Research, 21*(2), 147-151.

Sawant, S. G., and Gawai, D. U. (2011). Biochemical changes in banana fruits due to postharvest fungal pathogens. *Current Botany, 2*(1), 41-42.

Sethi, V. P. and Dhiman, M. (2020). Design, space optimization and modelling of solar-cum-biomass hybrid greenhouse crop dryer using flue gas heat transfer pipe network. *Solar Energy, 206*, 120-135.

Seveda, M.S. (2012). Design and development of walk-in type hemi-cylindrical solar tunnel dryer for industrial use. *International Scholarly Research Network Renewable Energy, 2012*(3), 1-9.

Shiundu, K. M., and Oniang'o, R. (2007). Marketing African leafy vegetables, challenges and opportunities in the Kenyan context. *African Journal of Food, Agriculture, Nutrition and Development, 7*(4), 1-17.

Singh, R. P., and Medina, A. G. (2012). Food Properties and Computer-Aided Engineering of Food Processing Systems. Nato Science Series E: Springer Netherlands.

Subramani, S., Sekar, S. D., Valarmathi, T. N., and Lionus, G. M. (2020). Energy and exergy analysis of greenhouse drying of ivy gourd and Turkey berry. *Thermal Science, 24*(1), 645-656.

Sunil, S., Sharma, N., Garg, A., and Kumar, S. (2013). An overview of optimization techniques used in solar drying. *Asian Journal of Science and Applied Technology, 1*(1), 5-11.

Swasdisevi, T., Devahastin, S., Ngamchum, R., and Soponronnarit, S. (2007). Optimization of a drying process using infrared-vacuum drying of Cavendish banana slices. *Journal of Science and Technology, 29*(3), 809-816.

Taiwo, K. A., and Adeyemi, O. (2009). Influence of blanching on the drying and rehydration of banana slices. *African Journal of Food Science, 3*(10), 307-315.

Tastan, M., and Gökozan, H. (2019). Real-time monitoring of indoor air quality with internet of things-based e-nose. *Applied Sciences, 9*(16), 1-13.

Tiwari, G. N., Das, T., Chen, C. R., and Barnwal, P. (2009). Energy and exergy analyses of greenhouse fish drying. *International Journal of Exergy*, *6*(5), 620-636.

Tonui, S. K, Mutai, E. B. K., Mutuli, D. A., Mbuge, D. O., and Too, K. V. (2014). Design and evaluation of solar grain dryer with a back-up heater. *Research Journal of Applied Sciences, Engineering and Technology*, *7*(15), 3036-3043.

Tsatsaronis, G., and Cziesla, F. (2009). Strengths and limitations of exergy analysis. In: Frangopoulos C, editor. Encyclopedia of life support systems (EOLSS), theme: exergy, energy systems analysis and optimization. Oxford, UK: Eolss Publishers, *1*, 121-146.

Türker, B., Savlak, N., and Kaşikci, B. M. (2016). Effect of green banana peel flour substitution on physical characteristics of gluten-free cakes. *Current Research in Nutrition Food Science*, *4*(2), 197-204.

Wakjira, M., Adugna, D., and Berecha, G. (2011). Determining slice thickness of banana (*musa spp*.) for enclosed solar drying using solar cabinet dryer under Ethiopian condition. *American Journal of Food Technology*, *6*(7), 568-580.

Wall, G. (2010). On exergy and sustainable development in environmental engineering. *The Open Environmental Engineering Journal*, *3*(1), 21-32.

Winiczenko, R., Górnicki, K., Kaleta, A., Martynenko, A., Janaszek-Mańkowska, M., and Trajer, J. (2018). Multi-objective optimization of convective drying of apple cubes. *Computers and Electronics in Agriculture*, *145*, 341-348.

Wrolstad, R. E, and Smith, D. E. (2017). Color analysis. *Food Analysis, Food Science Text Series*, S. S. Nielson, Ed., Springer International Publishing AG, Berlin, Germany.

Wulandani, D., Agustina, S. E., Yulianto, M., Nelwan, L. O., and Rahman, L. M. (2019). Design modification of greenhouse effect solar-hybrid rack type dryer. *IOP Conf. Series: Materials Science and Engineering*, *557*(012054), 1-5.

Yassen, T. A., Al-Kayiem, H. H., and Habib, K. (2014). Evaluation of hybrid solar-biomass dryer with no load. *MATEC Web of Conferences*, *13*(06007), 1-4.

Yuwana, Y., and Sidebang, B. (2017). Performative improvement of solar-biomass hybrid dryer for fish drying. *International Journal on Advanced Science Engineering Information technology*, *7*(6), 2251-2257.

Zaineb, A, Sami, K., Ilhem, H., Wissem, E., and Amen, A. G. (2020). Experimental study of a new mixed mode solar greenhouse drying system with and without thermal energy storage for pepper. *Renewable Energy*, *145*, 1972-1984.

Zoukit, A., El Ferouali, H., Salhi, I., Doubabi, S., and Abdenouri, N. (2018). Mathematical modelling of an innovative hybrid solar-gas dryer. *Journal of Energy Systems*, *2*(4), 260-276.

Mouser, (2018). DHT11-Technical-Data-Sheet. Retrieved from *https://www.mouser.com/datasheet/2/758/DHT11-Technical-Data-Sheet-Translated-Version-1143054.pdf.*

APPENDICES

Appendix I (I): Code for the simulation models

```
/*
```

Consider the following Parameters where;

W_p = Weight of bananas (kg)

M_{w1} = Initial moisture content (%w.b.)

M_{w2} = Final moisture content (%w.b.)

C_d = Specific heat of banana (kJ/kg^{o}C)

T_{da} = Drier temperature (^{o}C)

T_a = Ambient temperature (^{o}C)

C_p = Specific heat of water (kJ/kg^{o}C)

h_{fg} = Latent heat of water (kJ/kg)

A = Surface Area (m^2)

I_s = Solar radiation flux incident (W/m^2)

t = Number of hours (hrs)

τ = Cover transmittance

W_w = Moisture removed

W_d = Dry weight of bananas

ΔT = Change in temperature

M_i = Initial moisture content (% d.b.)

Q_t = Total heat required

Q_{in} = Solar energy available

```
*/
import java.io.*;
import java.text.AttributedString;
import java.awt.*;
import java.util.Scanner;
import javax.swing.JFrame;
import java.awt.event.*;
import java.awt.font.TextAttribute;
public class Combination extends Frame implements ActionListener {
        private static final long serialVersionUID = 1L;
        // Declare and initiate some Global variables within the class
```

double M_{w1} = 80;

double M_{w2} = 15;

double C_d = 3.45;

double T_{da} = 60;

double T_a = 25;

double C_p = 4.2;

double h_{fg} = 2264.76;

double η_{stove} = 0.35;

double H_{v1} = 18000;

double A = 102.18;

double I = 500;

double τ = 0.5;

double time, M_1, W_w, W_d, ΔT, M_i, Q_t, Q_{in}, Q_b, Q_{avail};

// Create textFields to display data on the form

TextField textfieldW_p = new TextField();

TextField textfieldW_w = new TextField();

TextField textfieldW_d = new TextField();

TextField textfieldΔT = new TextField();

TextField textfieldM_i = new TextField();

TextField textfieldQ_t = new TextField();

TextField textfieldQ_b = new TextField();

TextField textfieldM_1 = new TextField();

TextField textfieldQ_{in} = new TextField();

TextField textfiel$t$ = new TextField();

TextField textfieldQ_{avail} = new TextField();

TextField textfieldM_{w1} = new TextField("80");

TextField textfieldM_{w2} = new TextField("15");

TextField textfieldC_d = new TextField("3.45");

TextField textfieldT_a = new TextField("25");

TextField textfieldT_{da} = new TextField("60");

TextField textfieldC_p = new TextField("4.2");

TextField textfield h_{fg} = new TextField("2264.76");

TextField textfield η_{stove} = new TextField("0.35");

```
TextField textfield$H_{v1}$ = new TextField("18000");
TextField textfield$I_s$ = new TextField("500");
TextField textfield$A$ = new TextField("102.18");
TextField textfieldτ = new TextField("0.5");
//changing font style of labels
Font font = new Font("Verdana",Font.BOLD,12);
// Create button to help perform computations
Button buttonCompute = new Button("Compute");
public void combinedChecked() {
        textfield $\eta_{stove}$.setText("0.35");
        textfield$H_{v1}$.setText("18000");
        textfield$I_s$.setText("500");
        textfield$A$.setText("102.18");
        textfieldτ.setText("0.5");
}
public void computeAll(){
        double $W_p$;
        $W_p$ = Double.parseDouble( textfield$W_p$.getText() );
        $M_{w1}$ = Double.parseDouble( textfield$M_{w1}$.getText() );
        $M_{w2}$ = Double.parseDouble( textfield$M_{w2}$.getText() );
        $C_d$ = Double.parseDouble( textfieldCd.getText() );
        $T_a$ = Double.parseDouble( textfield$T_a$.getText() );
        $T_{da}$ = Double.parseDouble( textfield$T_{da}$.getText() );
        $C_p$ = Double.parseDouble( textfield$C_p$.getText() );
        $h_{fg}$ = Double.parseDouble( textfield $h_{fg}$.getText() );
        textfield $\eta_{stove}$.setText(textfield $\eta_{stove}$.getText());
        $\eta_{stove}$ = Double.parseDouble( textfield $\eta_{stove}$.getText() );
        textfield$H_{v1}$.setText(textfield$H_{v1}$.getText());
        $H_{v1}$ = Double.parseDouble( textfield$H_{v1}$.getText() );
        textfield$I_s$.setText(textfield$I_s$.getText());
        $I_s$ = Double.parseDouble( textfieldI.getText() );
        textfield$A$.setText(textfield$A$.getText());
        $A$ = Double.parseDouble( textfield$A$.getText() );
```

```
        τ = Double.parseDouble(textfieldτ.getText());
        // Compute Moisture removed Ww
        Ww = (Wp*(Mw1-Mw2)/(100-Mw2));
        // Compute dry weight
        Wd = Wp - Ww;
        // Compute Change in temperature
        ΔT = Tda – Ta;
        // Compute initial moisture content d.b.
        Mi = (Mw1/(100-Mw1)) *100;
        // Compute Total heat required
        Qt = Wd*Cd* ΔT + Mi*Cp* ΔT + Ww*hfg;
        // Qt should be equal to Qin = Qb
        Qb = Qt;
        Qin = Qt;
        // Compute all heat supply
        Qavail = 0.5*(Qb + Qin);
        M1 = 0.5*(Qb/(ηstove*Hv1));
        // Compute time for solar-biomass mode
        ts-b = 0.5*(Qin/(A*I*T));
        textfieldWp.setText(String.valueOf(new Double(Wp)));
        textfieldWw.setText(String.valueOf(new Double(Ww)));
        textfieldWd.setText(String.valueOf(new Double(Wd)));
        textfieldΔT.setText(String.valueOf(new Double(ΔT)));
        textfieldMi.setText(String.valueOf(new Double(Mi)));
        textfieldQt.setText(String.valueOf(new Double(Qt)));
        textfieldQb.setText(String.valueOf(new Double(Qb)));
        textfieldM1.setText(String.valueOf(new Double(M1)));
        textfieldQin.setText(String.valueOf(new Double(Qin)));
        textfieldts-b.setText(String.valueOf(new Double(ts-b)));
        textfieldQavail.setText(String.valueOf(new Double(Qavail)));
}
public void biomassChecked() {
        textfield ηstove.setText("0.35");
```

```
            textfield$H_{v1}$.setText("18000");
            textfield$A$.setText("---");
            textfield$I_s$.setText("---");
            textfieldτ.setText("---");
}
public void computeBiomass(){
            double $W_p$;
            $W_p$ = Double.parseDouble(textfield$W_p$.getText());
            $M_{w1}$ = Double.parseDouble(textfield$M_{w1}$.getText());
            $M_{w2}$ = Double.parseDouble(textfield$M_{w2}$.getText());
            $C_d$ = Double.parseDouble(textfield$C_d$.getText());
            $T_a$ = Double.parseDouble(textfield$T_a$.getText());
            $T_{da}$ = Double.parseDouble(textfield$T_{da}$.getText());
            $C_p$ = Double.parseDouble(textfield$C_p$.getText());
            $h_{fg}$ = Double.parseDouble(textfield$h_{fg}$.getText());
            $\eta_{stove}$ = Double.parseDouble(textfield $\eta_{stove}$.getText());
            $H_{v1}$ = Double.parseDouble(textfield$H_{v1}$.getText());
            // Compute Moisture removed $W_w$
            $W_w$ = ($W_p$*($M_{w1}$-$M_{w2}$)/(100-$M_{w2}$));
            // Compute dry weight
            $W_d$ = $W_p$ - $W_w$;
            // Compute Change in temperature
            $\Delta T$ = $T_{da}$ – $T_a$;
            // Compute initial moisture content d.b.
            $M_i$ = ($M_{w1}$/(100-$M_{w1}$)) *100;
            // Compute Total heat required
            $Q_t$ = $W_d$*$C_d$*$\Delta T$ + $M_i$*$C_p$* $\Delta T$ + $W_w$*$h_{fg}$;
            // $Q_t$ should be equal to $Q_{in}$
            $Q_b$ = $Q_t$;
                        // Compute Biomass heat supply
            $M_1$ = $Q_b$/( $\eta_{stove}$*$H_{v1}$);
            $t_b$ = ($M_1$/2) -1;
            textfield$Q_{in}$.setText("---");
```

```
        textfield$t_b$.setText(String.valueOf(new Double($t_b$)));
        textfield$Q_{avail}$.setText("---");
        textfield$W_p$.setText(String.valueOf(new Double($W_p$)));
        textfield$W_w$.setText(String.valueOf(new Double($W_w$)));
        textfield$W_d$.setText(String.valueOf(new Double($W_d$)));
        textfield $\Delta T$.setText(String.valueOf(new Double($\Delta T$)));
        textfield$M_i$.setText(String.valueOf(new Double($M_i$)));
        textfield$Q_t$.setText(String.valueOf(new Double($Q_t$)));
        textfield$Q_b$.setText(String.valueOf(new Double($Q_b$)));
        textfield$M_1$.setText(String.valueOf(new Double($M_1$)));
}
public void solarChecked() {
        textfield$I_s$.setText("500");
        textfield$A$.setText("102.18");
        textfieldτ.setText("0.5");
        textfield $\eta_{stove}$.setText("---");
        textfield$H_{v1}$.setText("---");
}
public void computeSolar(){
        double $W_p$;
        $W_p$ = Double.parseDouble(textfield$W_p$.getText());
        $M_{w1}$ = Double.parseDouble(textfield$M_{w1}$.getText());
        $M_{w2}$ = Double.parseDouble(textfield$M_{w2}$.getText());
        $C_d$ = Double.parseDouble(textfield$C_d$.getText());
        $T_a$ = Double.parseDouble(textfield$T_a$.getText());
        $T_{da}$ = Double.parseDouble(textfield$T_{da}$.getText());
        $C_p$ = Double.parseDouble(textfield$C_p$.getText());
        $h_{fg}$ = Double.parseDouble(textfield$h_{fg}$.getText());
        $A$ = Double.parseDouble(textfield$A$.getText());
        $I_s$ = Double.parseDouble(textfield$I_s$.getText());
        $\tau$ = Double.parseDouble(textfieldτ.getText());
        // Compute Moisture removed $W_w$
        $W_w$ = ($W_p$*($M_{w1}$-$M_{w2}$)/(100-$M_{w2}$));
```

```
        // Compute dry weight
        Wd = Wp - Ww;
                // Compute Change in temperature
        ΔT = Tda – Ta;
        // Compute initial moisture content d.b.
        Mi = (Mw1/(100-Mw1)) *100;
        // Compute Total heat required
        Qt = Wd*Cd* ΔT + Mi*Cp* ΔT + Ww*hfg;
        // Qt should be equal to Qin
        Qin = Qt;
        // Compute time
        ts = Qin/(A*Is*τ);
        textfieldWw.setText(String.valueOf(new Double(Ww)));
        textfieldWd.setText(String.valueOf(new Double(Wd)));
        textfield ΔT.setText(String.valueOf(new Double(ΔT)));
        textfieldMi.setText(String.valueOf(new Double(Mi)));
        textfieldQt.setText(String.valueOf(new Double(Qt)));
        textfieldQin.setText(String.valueOf(new Double(Qin)));
        textfield ts.setText(String.valueOf(new Double(ts)));
        textfieldQb.setText("---");
        textfieldM1.setText("---");
        textfieldQavail.setText("---");
}
public void addYellowLine(Frame frame) {
        for(int i=0; i<3; i++) {
        Label label = new Label();
        label.setBackground(Colour.yellow);
        frame.add(label);
        }
}
public void addHeading(Frame frame, String heading) {
        Label yellolabel1 = new Label();
        yellolabel1.setBackground(Colour.yellow);
        frame.add(yellolabel1);
```

```
        Label labelLheader = new Label(heading);
        labelLheader.setAlignment(Label.CENTER);
        labelLheader.setFont(font);
        labelLheader.setBackground(Colour.yellow);
        frame.add(labelLheader);
        Label yellolabel2 = new Label();
        yellolabel2.setBackground(Colour.yellow);
        frame.add(yellolabel2);
}
        public void addRow(Frame frame,String rowTitle, TextField textfield, String
        rowUnit) {
        Label labela = new Label(rowTitle);
        labela.setFont(font);
        frame.add(labela);
        frame.add(textfield);
        Label labelb = new Label(rowUnit);
        labelb.setFont(font);
        frame.add(labelb);
}
//This function creates the graphical user Interface(Form)
public void GraphicalUserInterface()throws IOException{
        final Frame frame = new Frame("All Modes");
        frame.setBackground(Colour.gray);
        frame.setSize(new Dimension(700, 700));
        addYellowLine(frame);
        addHeading(frame, "INPUT");
        Label labelBananWeight = new Label("Weight of the bananas (Wp)");
        labelBananWeight.setBackground(Colour.yellow);
        labelBananWeight.setFont(font);
        frame.add(labelBananWeight);
        textfieldWp.setBackground(Colour.white);
        textfieldWp.setForeground(Colour.darkGray);
        frame.setLayout (new GridLayout(34,3));
        frame.add(textfieldWp);
```

```
Label labelBananWeightUnit = new Label("kg");
labelBananWeightUnit.setBackground(Colour.yellow);
labelBananWeightUnit.setFont(font);
frame.add(labelBananWeightUnit);
CheckboxGroup modeGroup = new CheckboxGroup();
final Checkbox chkSolar = new Checkbox("Solar"modeGroup,false);
chkSolar.setBackground(Colour.white);
final Checkbox chkBiomass = new Checkbox("Biomass"modeGroup,false);
chkBiomass.setBackground(Colour.white);
finalCheckboxchkCombined=new heckbox("Combined",modeGroup,false);
chkCombined.setBackground(Colour.white);
//Where to change checkbox items
chkBiomass.addItemListener(new ItemListener() {
        public void itemStateChanged(ItemEvent arg0) {
                // TODO Auto-generated method stub
                biomassChecked();
        }
});
chkSolar.addItemListener(new ItemListener() {
        public void itemStateChanged(ItemEvent arg0) {
                // TODO Auto-generated method stub
                solarChecked();
        }
});
chkCombined.addItemListener(new ItemListener() {
        public void itemStateChanged(ItemEvent arg0) {
                // TODO Auto-generated method stub
                combinedChecked();
        }
});
addHeading(frame, "Choose mode:");
frame.add(chkSolar);
frame.add(chkBiomass);
frame.add(chkCombined);
```

```
addYellowLine(frame);
addYellowLine(frame);
addRow(frame, "Initial moisture content (Mw1)", textfieldMw1, "%w.b.");
addRow(frame, "Final moisture content (Mw2)", textfieldMw2, "%w.b.");
addRow(frame, "Specific heat of banana (Cd)", textfieldCd, "kJ/kg\u00b0C");
addRow(frame, "Ambient temperature (Ta)", textfieldTa, "\u00b0C");
addRow(frame, "Drier temperature (Tda)", textfieldTda, "\u00b0C");
addRow(frame, "Specific heat of water (Cp)", textfieldCp, "kJ/kg\u00b0C");
addRow(frame, "Latent heat of water (hfg)", textfieldhfg, "kJ/kg");
addRow(frame, "Biomass stove efficiency (ηstove)", textfield ηstove, " ");
addRow(frame, "Heating value of biomass (Hv1)", textfieldHv1, "kJ/kg");
addRow(frame, "solar radiation flux incident (Is)", textfieldIs, "w/m\u00b2");
addRow(frame, "Surface Area (A)", textfieldA, "m\u00b2");
addRow(frame, "Cover transmittance (τ)", textfieldτ, " ");
addHeading(frame, "OUTPUT");
textfieldWw.setText(String.valueOf(new Double(Ww)));
textfieldWd.setText(String.valueOf(new Double(Wd)));
textfield ΔT.setText(String.valueOf(new Double(ΔT)));
textfieldMi.setText(String.valueOf(new Double(Mi)));
textfieldQt.setText(String.valueOf(new Double(Qt)));
textfieldQb.setText(String.valueOf(new Double(Qb)));
textfieldM1.setText(String.valueOf(new Double(M1)));
textfieldQin.setText(String.valueOf(new Double(M1)));
textfieldt.setText(String.valueOf(new Double(time)));
textfieldQavail.setText(String.valueOf(new Double(Qavail)));
addRow(frame, "Moisture Removed(Ww)", textfieldWw, "kg");
addRow(frame, "Dry Weight (Wd)", textfieldWd, "kg");
addRow(frame, "Temperature Change (ΔT)", textfield ΔT, "\u00b0C");
addRow(frame, "Initial Moisture d.b (Mi)", textfieldMi, "%d.b.");
addRow(frame, "Total heat required (Qt)", textfieldQt, "kJ");
addRow(frame, "Biomass heat supply (Qb)", textfieldQb, "kJ");
addRow(frame, "Biomass weight (M1)", textfieldM1, "kg");
addRow(frame, "solar energy available (Qin)", textfieldQin, "kJ");
```

```
addRow(frame, "Time (t)", textfieldt, "Hrs");
addRow(frame, "Total energy available (Qavail)", textfieldQavail, "kJ");
addYellowLine(frame);
Label label = new Label();
label.setBackground(Colour.yellow);
frame.add(label);
buttonCompute.setBackground(Colour.WHITE);
buttonCompute.addActionListener(this);
buttonCompute.setFont(font);
buttonCompute.addActionListener(new ActionListener() {
        public void actionPerformed(ActionEvent arg0) {
                // TODO Auto-generated method stub
                if(chkSolar.getState() == true){
                        computeSolar();
                }else if(chkBiomass.getState() == true ){
                        computeBiomass();
                }else if(chkCombined.getState() == true){
                        computeAll();
                }
        }
});
frame.add(buttonCompute);
Label label1 = new Label();
label1.setBackground(Colour.yellow);
frame.add(label1);
addYellowLine(frame);
addYellowLine(frame);
frame.pack();
frame.setVisible(true);
frame.addWindowListener(new WindowListener() {
        public void windowOpened(WindowEvent arg0) {
                // TODO Auto-generated method stub
        }
        public void windowIconified(WindowEvent arg0) {
```

```
                        // TODO Auto-generated method stub
                    }
                    public void windowDeiconified(WindowEvent arg0) {
                        // TODO Auto-generated method stub
                    }
                    public void windowDeactivated(WindowEvent arg0) {
                        // TODO Auto-generated method stub
                    }
                    public void windowClosing(WindowEvent arg0) {
                        // TODO Auto-generated method stub
                        frame.dispose();
                    }
                    public void windowClosed(WindowEvent arg0) {
                        // TODO Auto-generated method stub
                    }
                    public void windowActivated(WindowEvent arg0) {
                        // TODO Auto-generated method stub
                    }
                    });
        }
        public static void main(String[] args) throws IOException {
            Combination combination = new Combination();
            combination.GraphicalUserInterface();
        }
        public void actionPerformed(ActionEvent arg0) {
            // TODO Auto-generated method stub
        }
}
```

Appendix I (II): Summary of variable input data used in model validation

Mode	Time (Hrs)	T_a (°C)	T_{da} (°C)	I_s (W/m^2)	MC (% w.b)
Solar	0	25.5±5.6	35.6±2.2	183.2±44.2	74.1±4.9
	4	34.3±1.5	55.2±0.6	892.8±30.4	54.1±9.4
	7	38.0±1.3	54.3±2.4	565.2±91.6	34.4±10.4
	11	34.0±1.5	45.4±1.3	595.7±87.5	16.2±3.6
Biomass	0	20.8±0.4	30.7±1.2	-	78.3±3.9
	5	19.5±0.5	27.5±0.4	-	70.9±5.7
	8	15.8±0.4	24.6±0.5	-	67.5±7.0
	11	14.7±0.5	24.6±0.6	-	62.4±6.2
Solar-biomass	0	21.0±2.7	35.5±4.4	401.0±93.3	73.0±5.3
	3	21.3±3.5	34.2±4.0	266.0±141.0	58.5±7.8
	6	21.3±2.3	36.5±1.6	28.3±22.0	49.4±9.2
	9	20.7±2.2	33.3±3.7	133.5±49.4	26.3±11.1
	13	25.4±1.2	54.2±3.4	312.6±121.4	11.4±5.5

Appendix II (I): A photograph of the developed solar-biomass dryer.

Appendix II (II): A photograph of the developed thermally insulated biomass unit.

Appendix II (III): A photograph showing sample preparation before drying.

Appendix II (IV): A photograph showing the inside of the dryer with product loaded.

Appendix III (I): Variation of drying air temperature with solar radiation for solar mode.

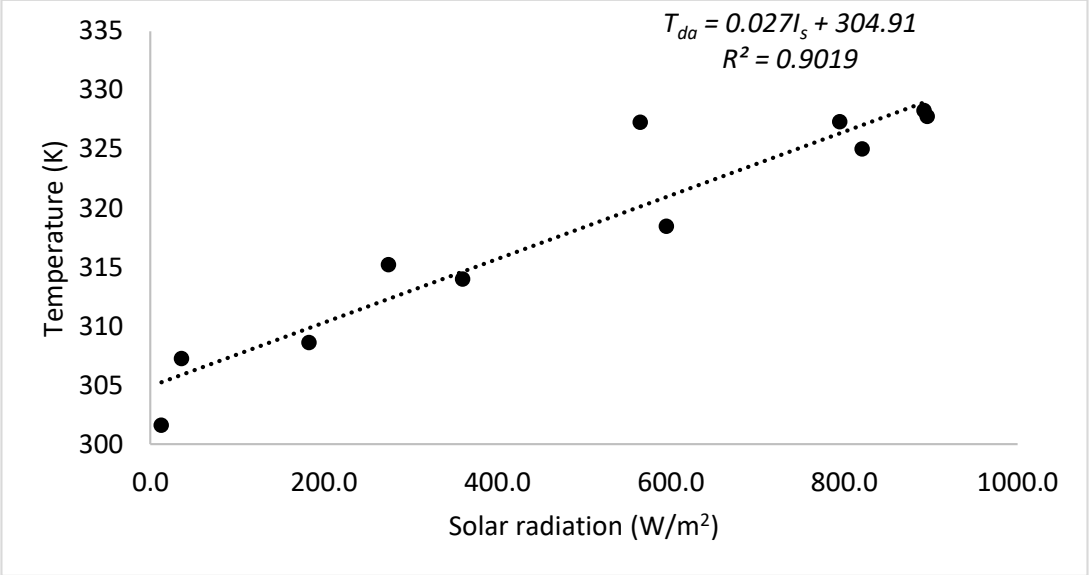

Appendix III (II): Variation of exit air temperature with drying air temperature for solar mode.

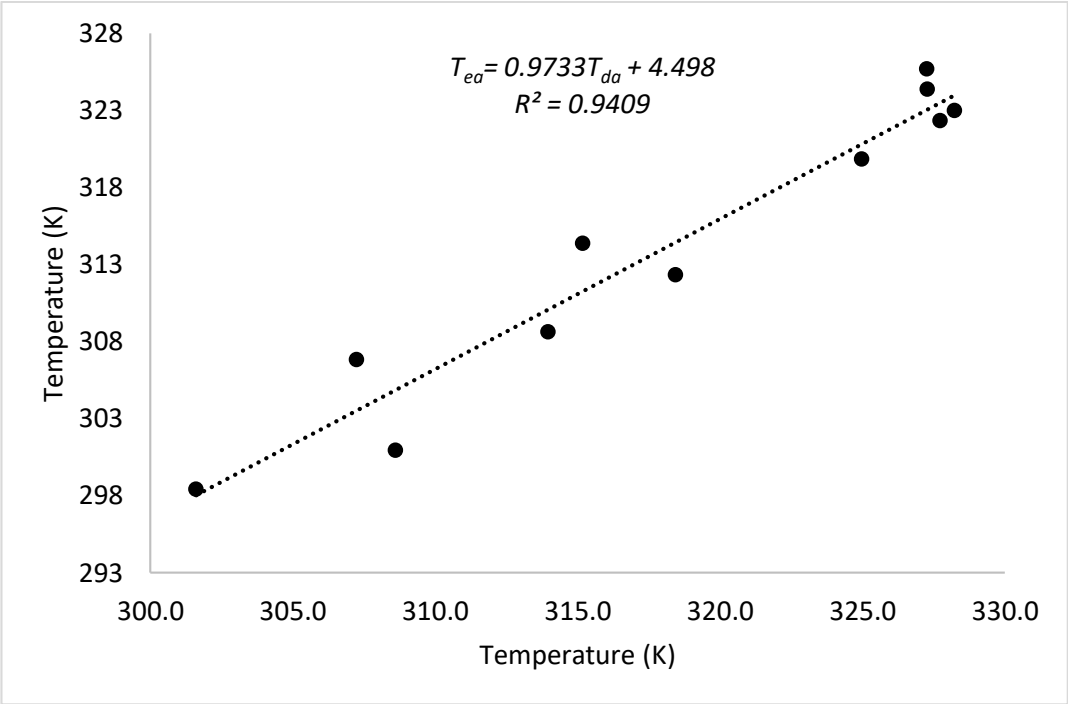

Appendix III (III): Variation of drying air temperature with ambient air temperature for biomass mode.

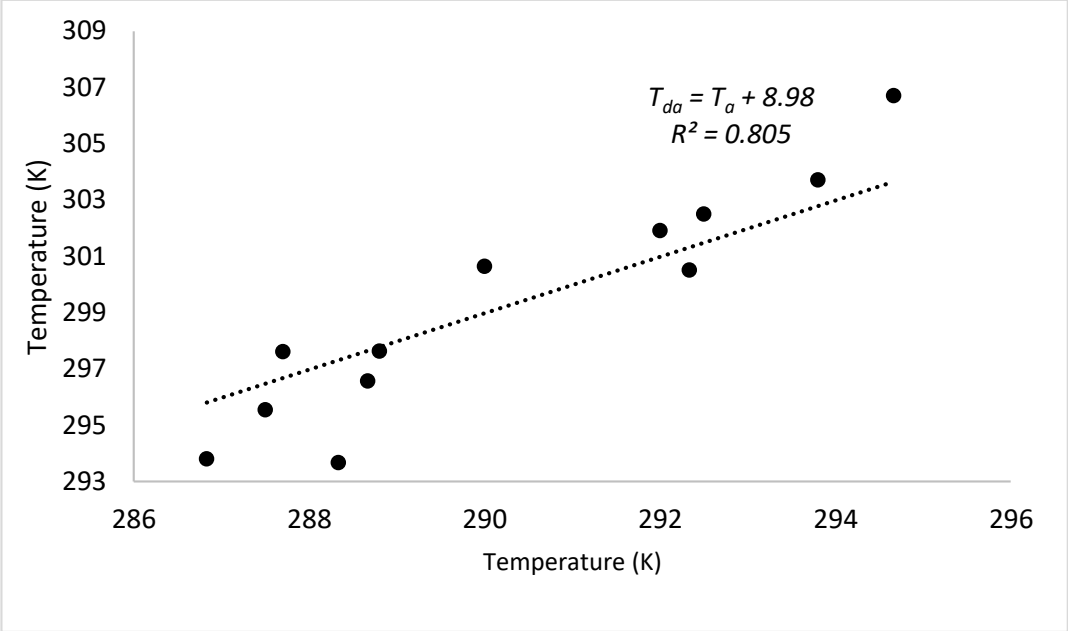

Appendix III (IV): Variation of exit air temperature with drying air temperature for biomass mode.

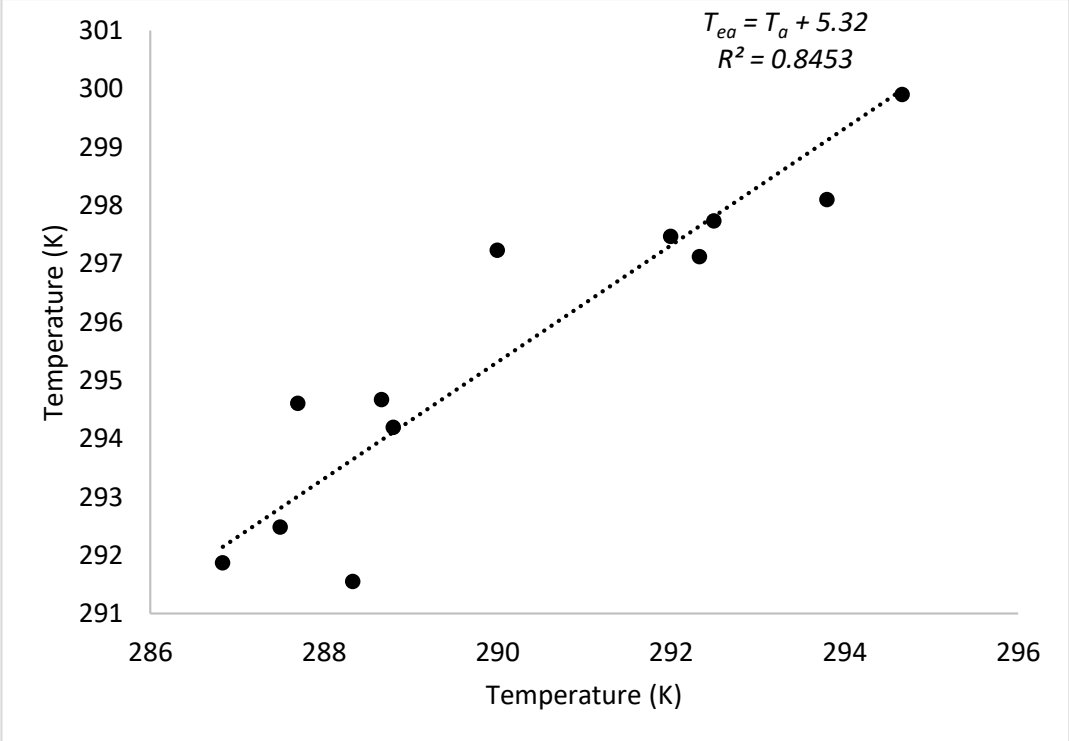

Appendix III (V): Variation of drying air temperature with solar radiation for solar-biomass mode.

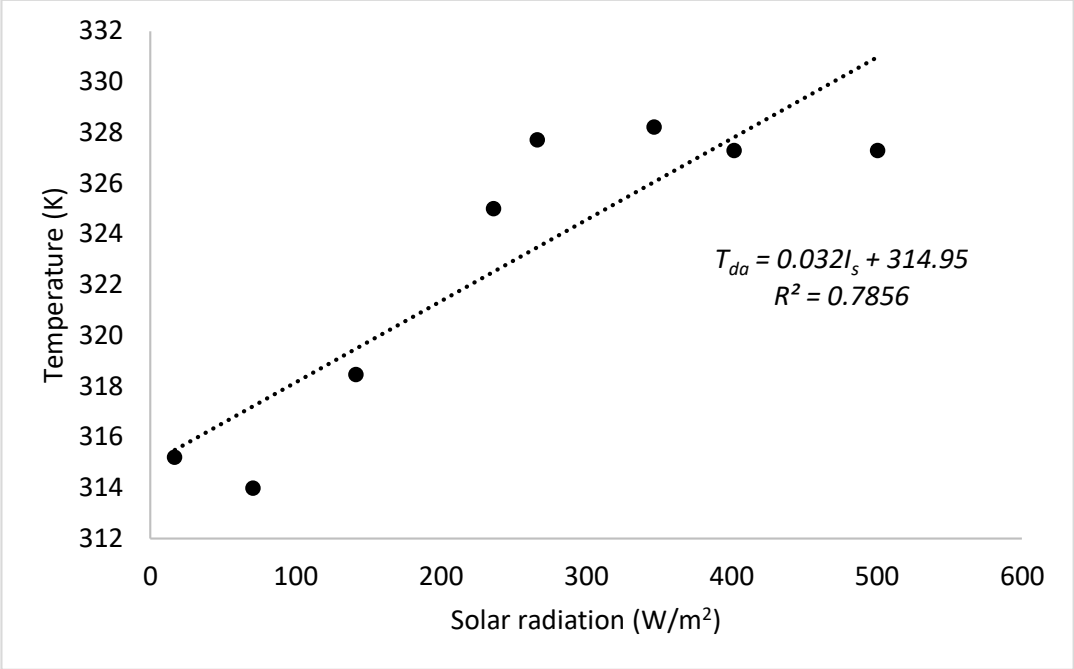

Appendix III (VI): Variation of temperature change against solar radiation for solar-biomass mode.

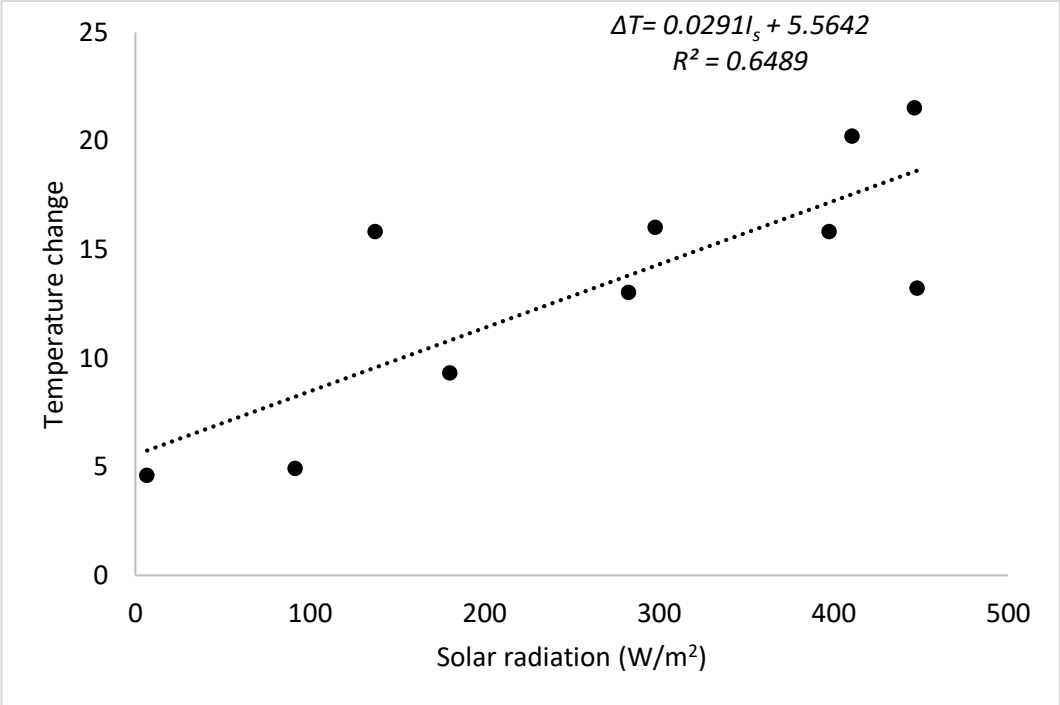

Appendix III (VII): Variation of exit air temperature with ambient air temperature for solar biomass mode.

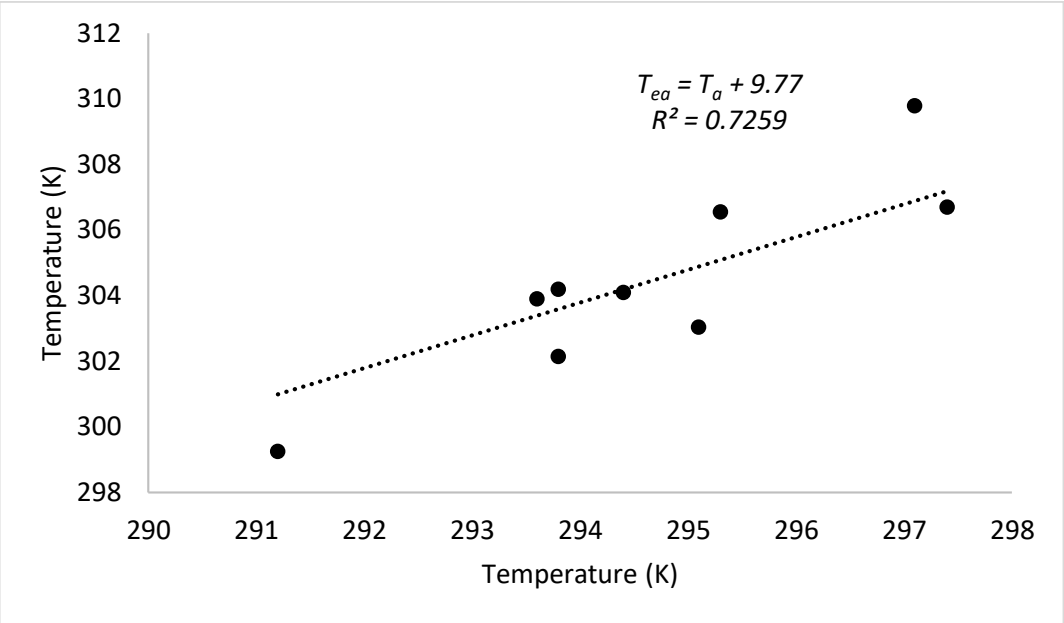

Appendix IV (I): A sample of optimization console screen.

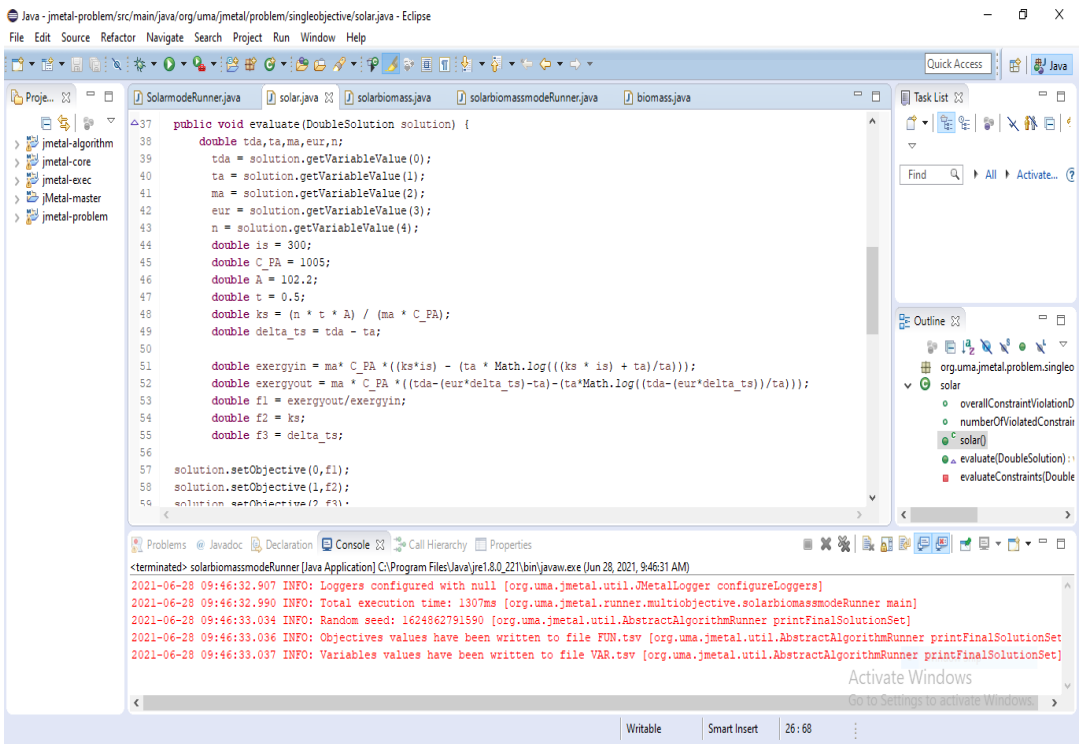

Appendix IV (II): A sample of optimization results for variables values.

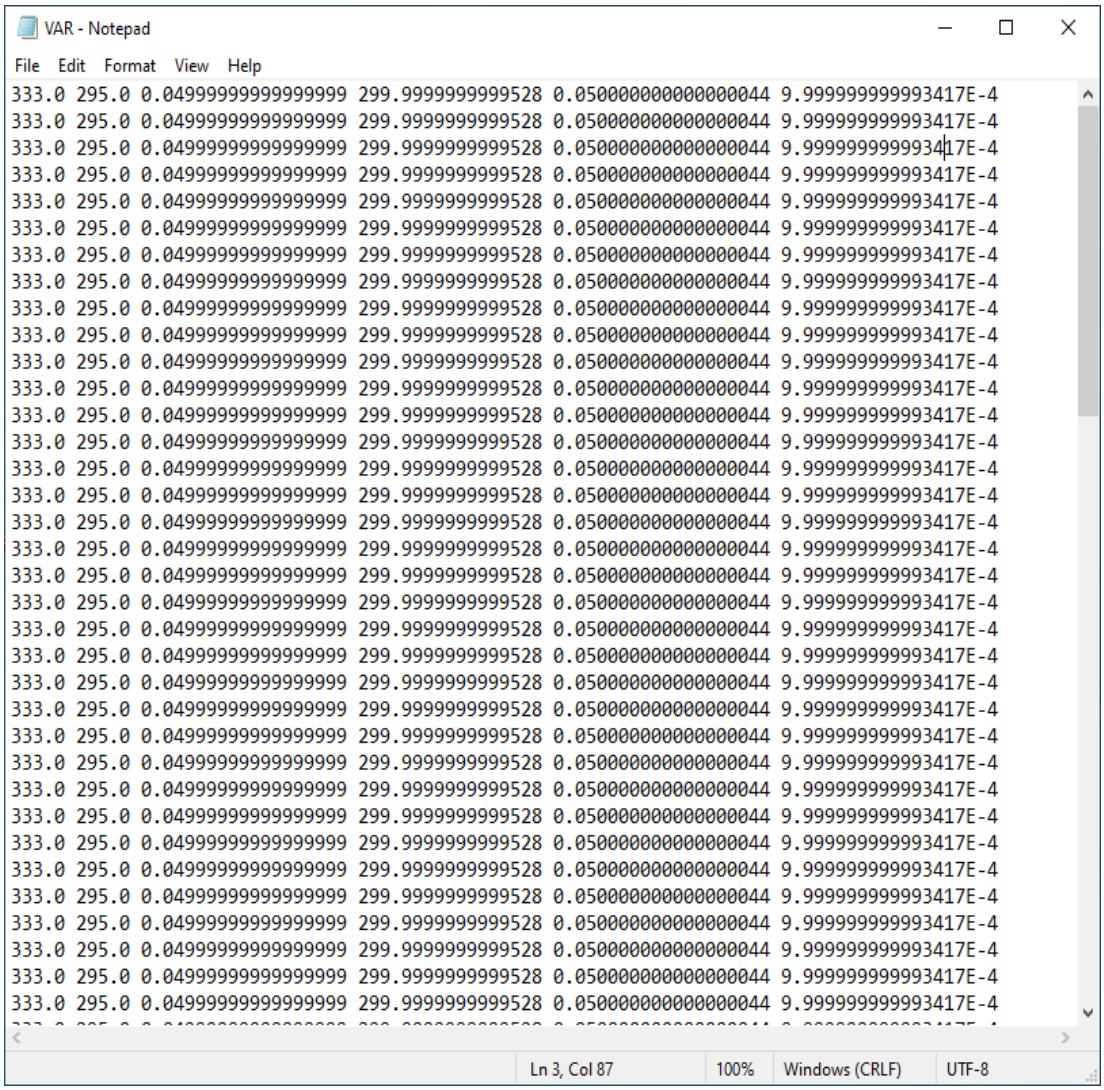

Appendix IV (III): A sample of optimization results for function values.